



**CÁTIA DANIELA
ISAÍAS PEREIRA**

**Populações linfocitárias em doentes com
Mucopolissacaridose**

**Lymphocyte populations in Mucopolysaccharidosis
patients**

Dissertação apresentada à Universidade de Aveiro para cumprimento dos requisitos necessários à obtenção do grau de Mestre em Biomedicina Molecular, realizada sob a orientação científica da Doutora Maria de Fátima Matos Almeida Henriques de Macedo, Professora Auxiliar Convidada da Secção Autónoma de Ciências da Saúde da Universidade de Aveiro.

o júri

presidente

Professora Doutora Odete Abreu Beirão da Cruz e Silva
Professora Auxiliar com Agregação da Universidade de Aveiro

arguente

Doutora Luzia Manuela Lima Teixeira Ranginha
Investigadora da Universidade do Porto – Instituto de Ciências Biomédicas de Abel Salazar

orientador

Doutora Maria de Fátima Matos Almeida Henriques de Macedo
Professora Auxiliar Convidada da Universidade de Aveiro

agradecimentos

À minha orientadora, Doutora Fátima Macedo, por tudo aquilo que me ensinou no decurso de um longo ano de trabalho, por ter criado um bom ambiente para a minha aprendizagem, assim como pela preciosa orientação que prestou na revisão deste trabalho.

À Doutora Clara Sá Miranda, pela oportunidade única que me foi concedida de desenvolver este trabalho na UniLiPe.

À minha colega de laboratório, Cátia Pereira, pela disponibilidade constante para me ensinar as técnicas indispensáveis à realização deste trabalho, bem como para esclarecer quaisquer dúvidas.

À Luz Maia e ao Nuno Lopes, por terem contribuído com alguns dos resultados experimentais apresentados neste trabalho.

A todas as instituições hospitalares envolvidas neste projeto, pelo apoio prestado na colheita e envio de amostras sanguíneas de pacientes.

À Enfermeira Graça Melo, pela colaboração na colheita de amostras de sangue de dadores voluntários.

Aos membros da UniLiPe e OBF, pela simpatia com que me receberam no IBMC.

À minha família, por ter acreditado em mim em todos os momentos da minha vida, e especialmente aos meus pais e avós, que sempre se esforçaram para me proporcionar todos os meios para que conseguisse seguir os meus sonhos.

Ao meu irmão, por ter estado sempre presente para me orientar e apoiar nas transições difíceis do meu percurso académico.

Ao meu namorado, por todos os momentos especiais proporcionados ao longo deste último ano, que tanto me reconfortaram e ajudaram a superar as imensas dificuldades até então encontradas.

Aos meus amigos, pela inesgotável paciência e compreensão pelos (já muitos) períodos de ausência prolongada a favor dos estudos.

À Patrícia Ferreira, por tantas vezes nos termos unido para enfrentar os inúmeros obstáculos destes cinco longos anos universitários.

palavras-chave

doenças de sobrecarga lisossomal, mucopolissacaridoses tipo II e tipo VI, células do sistema imunitário, linhas de células B transformadas pelo vírus Epstein–Barr

resumo

As doenças de sobrecarga lisossomal (DSLs) constituem um grupo de distúrbios metabólicos raros maioritariamente causados por mutações em hidrolases lisossomais, que conduzem à acumulação anormal de diferentes substratos macromoleculares no interior do lisossoma. Este trabalho é focado nas mucopolissacaridoses (MPSs), um grupo de DSLs resultantes da atividade deficiente de enzimas envolvidas no catabolismo dos glicosaminoglicanos. A MPS II é caracterizada pela perda de atividade da enzima iduronato-2-sulfatase, levando ao armazenamento intralisossomal de sulfato de dermatano e sulfato de heparano. A MPS VI é definida pela acumulação de sulfato de dermatano dentro do lisossoma, devido a uma deficiência na atividade enzimática de arilsulfatase B. O lisossoma é um compartimento celular importante para o funcionamento normal do sistema imunitário. Em diversos modelos de DSLs, foram anteriormente descritas alterações nas células do sistema imunitário. Os principais objetivos do presente trabalho eram: (i) estudar as várias populações leucocitárias – incluindo células T e seus subconjuntos, células *natural killer* (NK), células B e suas subpopulações, e monócitos – no sangue periférico de doentes com MPS II e MPS VI; (ii) produzir linhas de células B transformadas pelo vírus Epstein–Barr (EBV) destes pacientes, assim como avaliar a eficácia na sua produção e determinar o seu fenótipo. A caracterização do sistema imunitário nas doenças MPS II e MPS VI revelou um decréscimo significativo na frequência de células NK e monócitos em doentes com MPS VI, mas não em doentes com MPS II, em comparação com indivíduos controle. Em contraste, não foram identificadas alterações na percentagem de células T, células *natural killer* T invariantes (iNKT) e células B nos grupos de doentes com MPS II e MPS VI, comparando com o grupo controle. A análise detalhada do estado de memória de células T auxiliares e células T citotóxicas revelou desequilíbrios nos fenótipos *naïve* e de memória em ambos os compartimentos de células T em doentes com MPS VI, mas não em doentes com MPS II, em comparação com indivíduos controle. As linhas de células B transformadas pelo EBV foram produzidas com sucesso nos dois grupos de doentes com MPS, mas a eficácia na sua produção foi superior no caso dos doentes com MPS VI, comparando com os indivíduos controle e doentes com MPS II. O fenótipo predominante das linhas de células B transformadas pelo EBV era similar entre ambos os grupos de doentes com MPS e o grupo controle, o qual foi avaliado como sendo correspondente à subpopulação de células B de memória duplamente negativas. Em conclusão, este trabalho permitiu caracterizar melhor o sistema imunitário nestas duas doenças raras.

keywords

lysosomal storage diseases, mucopolysaccharidoses type II and type VI, immune system cells, Epstein–Barr virus-transformed B cell lines

abstract

Lysosomal storage diseases (LSDs) constitute a group of rare metabolic disorders mostly caused by mutations in lysosomal hydrolases, which conduce to abnormal accumulation of different macromolecular substrates inside the lysosome. This work is focused on the mucopolysaccharidoses (MPSs), a group of LSDs arising from the deficient activity of enzymes involved in the catabolism of glycosaminoglycans. The MPS II is characterized by loss of activity of the enzyme iduronate-2-sulfatase, leading to the intralysosomal storage of dermatan sulfate and heparan sulfate. The MPS VI is defined by the accumulation of dermatan sulfate within the lysosome, owing to a deficiency in the enzymatic activity of arylsulfatase B. The lysosome is an important cellular compartment for the normal functioning of the immune system. In several models of LSDs, alterations in the immune system cells were previously described. The main aims of the present work were: (i) to study the various leukocyte populations – including T cells and their subsets, natural killer (NK) cells, B cells and their subpopulations, and monocytes – in the peripheral blood of MPS II and MPS VI patients; (ii) to produce Epstein–Barr virus (EBV)-transformed B cell lines from these patients, as well as to evaluate the efficacy in their generation and determine their phenotype. The characterization of the immune system in MPS II and MPS VI diseases revealed a significant decrease in the frequency of NK cells and monocytes in MPS VI patients, but not in MPS II patients, in comparison with control subjects. In contrast, no alterations were identified in the percentage of T cells, invariant natural killer T (iNKT) cells, and B cells in the groups of MPS II and MPS VI patients comparing with the control group. The detailed analysis of the memory state of helper T cells and cytotoxic T cells revealed imbalances in the naïve and memory phenotypes in both T cell compartments in MPS VI patients, but not in MPS II patients, as compared with control subjects. The EBV-transformed B cell lines were successfully produced in the two MPS patient groups, but the efficacy in their generation was higher in the case of MPS VI patients when comparing with control subjects and MPS II patients. The predominant phenotype of EBV-transformed B cell lines was similar between both groups of MPS patients and the control group, which was assessed as corresponding to the double-negative memory B cell subpopulation. In conclusion, this work allowed to better characterize the immune system in these two rare diseases.

CONTENTS

1. Introduction.....	1
1.1. Lysosomal storage diseases.....	1
1.1.1. Mucopolysaccharidoses	2
1.1.1.1. Mucopolysaccharidosis type II.....	4
1.1.1.2. Mucopolysaccharidosis type VI	9
1.1.2. Immunological alterations in lysosomal storage diseases.....	14
1.2. Invariant natural killer T cells.....	15
1.3. B lymphocytes	18
1.3.1. Development of B cell subpopulations	19
1.3.1.1. B-1 cells.....	20
1.3.1.2. Transitional B cells.....	21
1.3.1.3. Follicular B cells	22
1.3.1.4. Plasmablasts and plasma B cells	24
1.3.1.5. Memory B cells.....	25
1.3.1.6. Marginal zone B cells.....	26
1.3.1.7. Regulatory B cells	27
1.3.2. Transformation of peripheral B cells by Epstein–Barr virus.....	28
2. Aims.....	31
3. Materials and Methods	33
3.1. Subject selection and blood sample collection.....	34
3.2. Isolation of peripheral blood mononuclear cells.....	36
3.3. Production of EBV infectious virions.....	37
3.4. Transformation of B cells by EBV	37
3.5. Culture of EBV-transformed B cells	37
3.6. Flow cytometry	38
3.7. Cryopreservation of EBV-transformed B cell lines.....	40
3.8. Thawing of EBV-transformed B cell lines.....	40
3.9. Statistical analysis.....	40
Chapter I: Characterization of the Immune System in MPS II and MPS VI Patients – Manuscript in Preparation.....	43
4. Chapter I – Results.....	45
4.1. MPS patients and control subject characteristics	45
4.2. T cell and T cell subset frequency in MPS II and MPS VI patients.....	45

4.3. NK cell frequency in MPS II and MPS VI patients.....	49
4.4. iNKT cell and iNKT cell subset frequency in MPS II and MPS VI patients.....	50
4.5. B cell frequency in MPS II and MPS VI patients.....	52
4.6. Monocyte frequency in MPS II and MPS VI patients.....	53
4.7. Longitudinal study in MPS VI patients.....	54
5. Chapter I – Discussion.....	57
5.1. T cell, B cell, NK cell, and monocyte frequency in MPS II and MPS VI patients.....	58
5.2. T cell subset frequency in MPS II and MPS VI patients.....	59
5.3. iNKT cell and iNKT cell subset frequency in MPS II and MPS VI patients.....	60
5.4. Longitudinal study in MPS VI patients.....	61
Chapter II: Production and Characterization of EBV-transformed B Cell Lines from MPS II and MPS VI Patients.....	65
6. Chapter II – Results.....	67
6.1. MPS patients and control subject characteristics.....	67
6.2. Efficacy in the production of EBV-transformed B cell lines from MPS II and MPS VI patients.....	67
6.3. Phenotype of EBV-transformed B cell lines from MPS II and MPS VI patients.....	75
7. Chapter II – Discussion.....	81
7.1. Production of EBV-transformed B cell lines from MPS II and MPS VI patients.....	81
7.2. Phenotype of EBV-transformed B cell lines from MPS II and MPS VI patients.....	85
8. Conclusion and Future Perspectives.....	89
9. Literature.....	93
Appendix.....	103

LIST OF FIGURES AND TABLES

Table 1.1. General classification of MPS disorders.....	4
Figure 1.1. Deficiencies in GAG catabolism in MPS II disease	5
Table 1.2. Clinical symptoms characteristic of MPS II disease.....	7
Figure 1.2. Typical features of MPS II patients	8
Figure 1.3. Deficiency in GAG catabolism in MPS VI disease	10
Table 1.3. Clinical symptoms characteristic of MPS VI disease	11
Figure 1.4. Typical features of MPS VI patients.....	12
Figure 1.5. TCR- and cytokine-mediated activation of iNKT cells	17
Figure 1.6. Basic structure of an antibody and of BCR	18
Figure 1.7. Differentiation of follicular B cells in secondary lymphoid tissues	23
Figure 1.8. Developmental stages of the B-2 cell lineage	27
Figure 3.1. Experimental design of the study.....	33
Table 3.1. Characterization of the MPS II and MPS VI patients included in the analysis of the immune system in MPS II and MPS VI diseases, as well as in the production of EBV-transformed B cell lines.....	35
Figure 3.2. PBMC isolation by density gradient centrifugation with Histopaque®-1077 medium..	36
Table 3.2. Antibodies and tetramer used in flow cytometry to identify and characterize phenotypically the T cell, iNKT cell, NK cell, and B cell populations	39
Table 3.3. Antibodies used in flow cytometry to characterize phenotypically the EBV-transformed B cell lines	39
Figure 4.1. Flow cytometry analysis of T cells and T cell subsets.....	46
Figure 4.2. T cell and T cell subset frequency in MPS II and MPS VI patients	47
Figure 4.3. Naïve, effector memory, and central memory T cell subset frequency in MPS II and MPS VI patients	48
Figure 4.4. Flow cytometry analysis of NK cells.....	49
Figure 4.5. NK cell frequency in MPS II and MPS VI patients	49
Figure 4.6. Flow cytometry analysis of iNKT cells and iNKT cell subsets	50
Figure 4.7. iNKT cell and iNKT cell subset frequency in MPS II and MPS VI patients.....	51
Figure 4.8. CD161-expressing iNKT cell frequency in MPS II and MPS VI patients	52
Figure 4.9. Flow cytometry analysis of B cells	52
Figure 4.10. B cell frequency in MPS II and MPS VI patients	53
Figure 4.11. Flow cytometry analysis of monocytes	53
Figure 4.12. Monocyte frequency in MPS II and MPS VI patients.....	54

Figure 4.13. Longitudinal study of the frequency of B cells, T cells, T cell subsets, and iNKT cells in MPS VI patients	55
Table 5.1. Results of the analysis of the immune system in MPS II and MPS VI diseases	57
Figure 6.1. EBV-infected B cell clusters	68
Figure 6.2. Growth progression of EBV-transformed B cell lines from two control subjects	69
Figure 6.3. Growth progression of EBV-transformed B cell lines from two MPS II patients	70
Figure 6.4. Growth progression of EBV-transformed B cell lines from two MPS VI patients	71
Figure 6.5. B cell frequency before and after EBV-induced transformation of B cells in MPS II and MPS VI patients	73
Figure 6.6. Evolution of B cell frequency before and after EBV-induced transformation of B cells in MPS II and MPS VI patients	74
Figure 6.7. B cell expansion after EBV-induced transformation of B cells in MPS II and MPS VI patients	75
Figure 6.8. Flow cytometry analysis of B cell subsets	76
Figure 6.9. B cell subset frequency in EBV-transformed B cell lines from MPS II and MPS VI patients	77
Figure 6.10. B cell subset frequency before EBV-induced transformation of B cells in MPS II and MPS VI patients	78
Figure 6.11. B cell subset frequency before and after EBV-induced transformation of B cells in MPS II and MPS VI patients	79

LIST OF ABBREVIATIONS

α -GalCer	α -Galactosylceramide
ACK	Ammonium-chloride-potassium
APC	Antigen presenting cell
ARSB	Arylsulfatase B
BAFF	B-cell activating factor
Bcl-2	B-cell lymphoma 2
BCR	B cell receptor
BSA	Bovine serum albumin
CD	Cluster of differentiation
CR2	Complement receptor type 2
CS	Chondroitin sulfate
DC	Dendritic cell
DS	Dermatan sulfate
EBNA	Epstein-Barr nuclear antigen
EBV	Epstein-Barr virus
EDTA	Ethylenediamine tetraacetic acid
ERT	Enzyme replacement therapy
FACS	Fluorescence-activated cell sorting
GAG	Glycosaminoglycan
GC	Germinal center
HLA	Human leukocyte antigen
HS	Heparan sulfate
HSC	Hematopoietic stem cell
HSCT	Hematopoietic stem cell transplantation
IBMC	<i>Instituto de Biologia Molecular e Celular</i>
IDS	Iduronate-2-sulfatase
iFBS	Inactivated fetal bovine serum
IFN	Interferon
Ig	Immunoglobulin
IL	Interleukin
iNKT	Invariant natural killer T
KS	Keratan sulfate
LMP	Latent membrane protein
LSD	Lysosomal storage disease
MHC	Major histocompatibility complex

MPS	Mucopolysaccharidosis
NK	Natural killer
NKT	Natural killer T
PBMC	Peripheral blood mononuclear cell
PBS	Phosphate buffered saline
TCR	T cell receptor
TGF	Transforming growth factor
Th	T helper

1. INTRODUCTION

1.1. *Lysosomal storage diseases*

The lysosome, an organelle containing more than sixty types of acid hydrolases, is the major intracellular site for enzymatic degradation of most macromolecules [1–7]. By fusing with late endosomes/phagosomes or autophagosomes, macromolecular substrates are delivered to the lysosome to be digested by soluble lysosomal hydrolytic enzymes [1–6]. The resulting breakdown products are transported back to the cytosol by membrane-bound lysosomal transporter proteins or via vesicular membrane trafficking [1,3,4,6]. Hence, lysosomal catabolites become available for being subsequently used in energy homeostasis or reutilized in new biosynthetic processes by other cell organelles [1,4].

Additional functions of the lysosome include antigen presentation, innate immunity, phagocytosis, autophagy, signal transduction, receptor recycling and regulation, cell membrane repair, tissue remodeling, neurotransmission, and apoptosis [2,4,7].

Lysosomal storage diseases (LSDs) constitute a heterogeneous group comprising over fifty rare, genetically distinct metabolic disorders, which arise mostly from recessively inherited, loss-of-function mutations that impair the intralysosomal catabolic pathways [1–7]. The genetic alterations typically affect a soluble lysosomal hydrolase, but mutations in genes coding a non-enzymatic lysosomal protein or a non-lysosomal protein implicated in the biogenesis or vesicular trafficking of lysosomal proteins may also be associated with LSD phenotypes [1–4,6,7]. In consequence of the deficiency of a protein critical for lysosome function or regulation, the intralysosomal accumulation of non-degraded macromolecules or monomeric catabolic products progressively occurs, especially in cells, tissues, and organs where substrate turnover is high [1–4, 6,7]. Owing to this primary storage leading to enlarged dysfunctional lysosomes, many other enzymatic processes are eventually inhibited, which results in the accumulation of secondary undigested compounds [2,3,6]. Thus, not only the lysosomal activity is impaired but also the functions of other organelles (e.g. Golgi complex, mitochondria, endoplasmic reticulum) may be compromised, causing a multisystemic dysfunction of numerous cell activities [2,3,6,7].

According to the nature of the major materials that accumulate within the lysosome, LSDs are typically categorized in mucopolysaccharidoses (MPSs), sphingolipidoses, other lipidoses, glycoproteinoses, and glycogenosis [4,5]. Moreover, some LSDs are grouped depending on the

lysosomal protein defects, being classified as multiple lysosomal enzyme deficiencies and lysosomal transport deficiencies [5].

Although being considered individually rare, the overall combined prevalence of LSDs is around 12.5 per 100,000 live births [3], but it may be as high as 20 per 100,000 live births if undiagnosed or misdiagnosed cases are accounted for [6]. Epidemiological studies conducted in different countries reported a collective prevalence of LSDs of approximately 8 in British Columbia [8], 12.08 in Italy [9], 12.25 in the Czech Republic [10], 12.99 in Australia [11], and 14 per 100,000 live births in The Netherlands [12]. Considering the Portuguese population, this group of inborn errors of metabolism occurs with a higher combined prevalence, which is estimated to be 25 per 100,000 live births, with the sphingolipidoses as the most prevalent subclass, followed by the MPSs [13].

Within the LSDs, the subgroup of MPSs is the focus of this thesis, which is discussed hereinafter.

1.1.1. Mucopolysaccharidoses

MPSs constitute a family of rare, inherited metabolic disorders resulting from a deficiency in the activity of specific lysosomal enzymes implicated in the catabolism of glycosaminoglycans (GAGs) [4,7,14–19]. The global prevalence of MPSs is around 1.9 in British Columbia [8], 2.4 in Italy [9], 3.7 in the Czech Republic [10], 4.4 in Australia [11], and 4.5 per 100,000 live births in The Netherlands [12]. More particularly, the prevalence of this type of LSD in Portugal is approximately 4.8 per 100,000 live births [13].

GAGs are unbranched polymeric chains of carbohydrates consisting of specific repeating disaccharide units, being divided in four main groups: (i) dermatan sulfate (DS) and chondroitin sulfate (CS); (ii) hyaluronan; (iii) heparan sulfate (HS); and (iv) keratan sulfate (KS) [4,7,14,15, 17–20]. With the exception of hyaluronan, all other GAGs occur naturally as components of proteoglycans by binding to secreted or cell surface-attached glycoproteins [7,14,15,18–20]. Proteoglycans, along with hyaluronan, are important constituents of many extracellular matrices, participating in cell adhesion and neuritogenesis (e.g. DS, CS), activation of growth factors and composition of cellular membranes (e.g. HS), cell motility and neuronal regeneration (e.g. KS), as well as tissue hydration and resistance to compression (e.g. hyaluronan) [7,17,18,20]. During

proteolytic removal of the core protein, proteoglycans are metabolized into DS, CS, HS, or KS outside the cell [14,15]. Along with hyaluronan, these GAGs are delivered by endocytosis and autophagy to the lysosome to undergo intracellular digestion, a process involving five sulfatases, four exoglycosidases, one non-hydrolytic transferase, and one endoglycosidase [14,15,17,18].

Any deficiency of one of these lysosomal enzymes conduces to blockade of the stepwise degradation of DS, CS, HS, KS, or hyaluronan and may affect one or several GAG breakdown pathways simultaneously [14,15,17,18]. Because presentation of these substrates to cells for intralysosomal catabolism continues to occur normally, there is a persistent accumulation of undigested or partially degraded GAGs inside lysosomes and in the extracellular matrix of a variety of tissues, leading to alteration of cell homeostasis [7,14–19]. In addition, MPSs are biochemically defined by an increase of GAG fragments in urine, blood, and/or cerebrospinal fluid of affected patients [14–19].

As GAGs are a crucial structural element of the extracellular matrix of all animal tissues, the impairment of their catabolism potentiates a diversity of alterations that extend to virtually all organ systems [7,15,16,19]. The various MPS disorders share a multisystemic clinical picture that typically consists of dysostosis multiplex, growth retardation, abnormal facies, and organomegaly, as well as variable cardiovascular, respiratory, auditory, and visual involvement, accompanied by neurocognitive dysfunction in some cases [4,7,14–17,19]. Even though MPS patients may have a normal appearance at birth, soon their childhood is marked by the onset of symptomatic disease, characterized by a chronic, progressive course and different degrees of severity [14–17].

Early and accurate diagnosis is of paramount importance due to the multisystemic and progressive nature of MPSs, and also because it can frankly improve treatment outcomes in those types for which enzyme replacement therapy (ERT) or hematopoietic stem cell transplantation (HSCT) are currently available [16,19]. Nonetheless, given that clinical symptoms are highly heterogeneous, diagnosis is often difficult to perform and inevitably delayed, which may potentiate the occurrence of irreversible organ damage [16,19].

The general characterization of the MPSs, including the deficient lysosomal enzyme, the genetic inheritance and mutated gene locus, as well as the major GAG storage materials accumulated intralysosomally, is summarized in Table 1.1.

Table 1.1. General classification of MPS disorders [4,14–16]

Disease	Enzymatic deficiency	Genetic heritage (gene locus)	Increased GAGs
MPS I Hurler Hurler-Scheie Scheie	α -L-iduronidase	Autosomal recessive (<i>IDUA</i> : 4p16.3)	DS, HS
MPS II (Hunter)	Iduronate-2-sulfatase	X-linked recessive (<i>IDS</i> : Xq28)	DS, HS
MPS III Sanfilippo A Sanfilippo B Sanfilippo C Sanfilippo D	Heparan- <i>N</i> -sulfatase α - <i>N</i> -acetyl-glucosaminidase Acetyl-CoA: α -glucosaminide <i>N</i> -acetyltransferase <i>N</i> -acetylglucosamine-6-sulfatase	Autosomal recessive (<i>SGSH</i> : 17q25.3) (<i>NAGLU</i> : 17q21) (<i>HGSNAT</i> : 8p11.21) (<i>GNS</i> : 12q14)	HS
MPS IV Morquio A Morquio B	Galactose-6-sulfatase β -galactosidase	Autosomal recessive (<i>GALNS</i> : 16q24.3) (<i>GLB1</i> : 3p22.3)	KS, CS KS
MPS VI (Maroteaux-Lamy)	Arylsulfatase B	Autosomal recessive (<i>ARSB</i> : 5q13–q14)	DS
MPS VII (Sly)	β -glucuronidase	Autosomal recessive (<i>GUSB</i> : 7q21.11)	DS, CS, HS
MPS IX (Natowicz)	Hyaluronidase 1	Autosomal recessive (<i>HYAL1</i> : 3p21.31)	Hyaluronan

This thesis specifically approaches the MPS II and MPS VI diseases, which are described with more detail henceforth.

1.1.1.1. Mucopolysaccharidosis type II

MPS II, or Hunter syndrome, is a rare LSD arising from reduced or absent activity of the lysosomal hydrolase iduronate-2-sulfatase (IDS) [14–16,18,21–24]. This recessive disorder differs from all other MPSs by the fact that presents an X-linked genetic heritage, occurring almost

exclusively in males; even so, rare female patients have also been reported, which can be due to a non-random X-chromosome inactivation in carrier females [14–16,18,21–24]. The estimated prevalence of MPS II is approximately 1.2 in Italy [9], 0.43 in the Czech Republic [10], 0.74 in Australia [11], and 0.67 per 100,000 live births in The Netherlands [12]. In the Portuguese population, this disease presents a prevalence of around 1.09 per 100,000 live births [13].

Molecular basis

MPS II occurs as a result of partially or completely defective activity of the enzyme IDS, a lysosomal sulfatase that is codified by the *IDS* gene positioned at the locus Xq28, which spans about 24kb and contains nine exons [14,15,21–23,25].

Within the lysosome, IDS is responsible for the correct degradation of both DS and HS by removing the sulfate group from the 2- position of *L*-iduronic acid residue situated at the non-reducing terminus of these GAGs [14,15,22,23]. The breakdown pathways of DS and HS, including the specific enzymatic reactions blocked in MPS II, are represented in Figure 1.1.

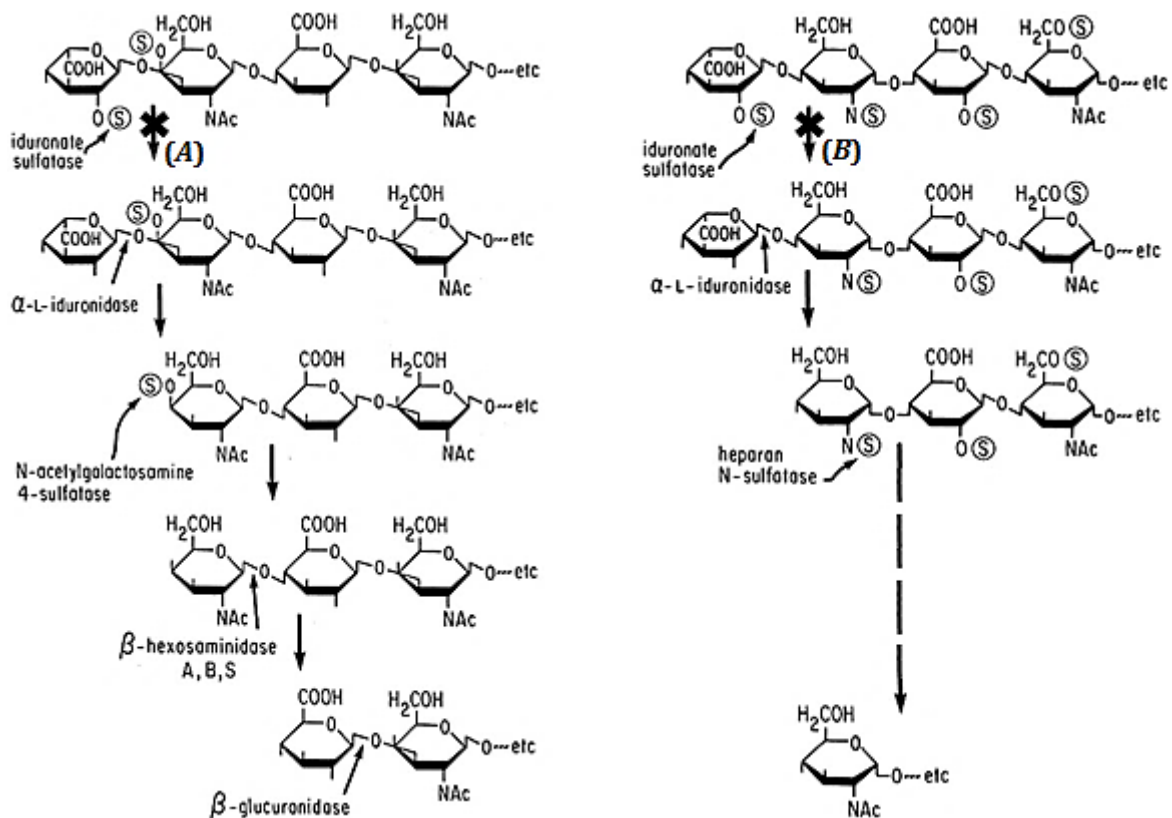


Figure 1.1. Deficiencies in GAG catabolism in MPS II disease. Adapted from [14]. Represented are the enzymatic reactions in the stepwise degradation pathways of DS (A) and HS (B) that are blocked in Hunter syndrome.

Numerous mutations can affect the *IDS* gene, namely small insertions (e.g. 1269insCC) and deletions (e.g. 383delAT), as well as missense (e.g. S71R), nonsense (e.g. Y234X), and altered splicing (e.g. 1122C→T) errors, many of which are private or non-recurrent mutations that together cause 75–80% of MPS II cases [14,21,22,25]. The remaining fifth of cases are due to gene rearrangements (e.g. recombination, followed by inversion, of the *IDS* gene with an IDS-like pseudogene) and large deletions (e.g. intragenic deletion of exons 4–7), which always result in a severe MPS II phenotype [14,21–23,25].

The diminution or lack of such enzymatic activity arising from mutations in the *IDS* gene leads to continuous storage of HS and DS, both inside cells and extracellularly, in nearly all cell types, in addition to causing the urinary excretion of excessive amounts of these two non-degraded GAGs [14,15,22,23]. In some cases, the secondary accumulation of GM2 and GM3 gangliosides occurs in the brains of affected individuals, owing to the inhibition of enzymes involved in ganglioside metabolism, elicited by primary intralysosomal storage of HS and DS [14].

Clinical presentation

In MPS II, neurological and somatic involvement are usually present, in which multiple manifestations affect the brain and musculoskeletal, cardiovascular, and respiratory systems [14–16,21,24]. Although many severity degrees exist, two major clinical entities are recognized as the extremes of a continuum of multisystemic symptoms: severe and mild MPS II [14,15,22–24].

About two-thirds of patients exhibit the severe form of MPS II, defined by progressive neurodegeneration and cognitive dysfunction, as well as serious somatic impairment, culminating in reduced life expectancy [14–16,21–24]. Around 2–4 years of age, a series of clinical symptoms arise: mental retardation, dysostosis multiplex, short stature, facial dysmorphia, umbilical and inguinal hernias, chronic diarrhea, hepatosplenomegaly, recurrent otitis and gradual hearing loss, retinal dystrophy, and small ivory-colored papules (pebbling) in the skin – a pathognomonic feature – are common findings [14,16,21–24]. In early childhood, patients also experience several cardiologic and pulmonary complications, such as myocardial disease and repetitive respiratory infections [14,16,21,22]. The communicating hydrocephalus and increased intracranial pressure aggravate the already extensive neurological deterioration, leading to a late-stage with seizures and lack of mobility [14,16,21,22]. Natural death generally occurs at the age of 10–15 years old, as a result of obstructive airway disease combined with cardiac failure [14–16,21–24].

Patients with the milder phenotype of MPS II possess normal intelligence, with little to no cognitive impairment, as well as attenuated somatic involvement compatible with survival into adulthood [14–16,21–24]. First symptoms have a late onset, usually between 4 and 8 years of age,

with joint stiffness, hepatosplenomegaly, spinal cord compression with cervical myelopathy, carpal tunnel syndrome, and hearing deficiency as classical manifestations [14,16,22]. Mildly affected patients display several somatic abnormalities that are also present in individuals with severe MPS II, but which develop with a slower progression [14,16,22]. Natural death may occur prematurely in late-teenage years or in early adulthood secondary to chronic cardiorespiratory problems, but some patients live until their fifth or sixth decades of life [14,16,22–24].

The overall clinical symptoms typically expressed in MPS II are summed up in Table 1.2 and the characteristic features of affected patients are shown in Figure 1.2.

Table 1.2. Clinical symptoms characteristic of MPS II disease [14,16,21,22,24]

Organ/system affected	Clinical manifestations	
Nervous system	<i>Restricted to the severe phenotype</i>	
	- Developmental delay	- Seizures
Nervous system	- Behavioral changes: aggressiveness and hyperactivity	
	<i>Commonly present in both mild and severe phenotypes</i>	
	- Carpal tunnel syndrome	- Spinal cord compression
Musculoskeletal system	- Communicating hydrocephalus	
	- Short stature	- Coarse facial features
	- Joint stiffness and contractures	- Overall restricted mobility
	- Spine deformities	- Hand and wrist deformities
Cardiovascular system	- Pelvic dysplasia	- Short neck and limbs
	- Cardiac valve lesions	- Coronary artery narrowing
	- Ventricular hypertrophy	- Pulmonary hypertension
Respiratory system	- Repetitive upper respiratory tract infections	
	- Obstructive sleep apnea	- Thick nasal/tracheal secretions
Gastrointestinal system	- Hepatomegaly	- Splenomegaly
	- Chronic diarrhea	- Umbilical and inguinal hernias
Visual system	- Retinal dystrophy	- Papilledema
	- Optic nerve atrophy	
Auditory system	- Recurrent otitis	- Gradual hearing loss
Skin	- Mongolian blue spots	- Pebbling



Figure 1.2. Typical features of MPS II patients [24]. Evidence of short stature, joint stiffness (inability to raise arms above head), short neck [*left*], and coarse facies (enlarged head, large jowls, thickened lips, broad nose, and prominent supraorbital ridges) [*right*].

Diagnosis

MPS II is usually suspected on the basis of clinical presentation, with patients exhibiting skeletal deformities, coarse facies, short stature, organomegaly, recurrent hearing infections, and thickened pebbled skin [24]. However, a suspicion based on clinical findings is not sufficient to diagnose MPS II, since it is phenotypically similar to other MPSs or even some other LSDs [24].

Quantitative and qualitative analyses of urinary GAGs are the first screening tests used to assess if a subject has a form of MPS, but elevated levels of total urinary GAGs, as well as the accumulation of DS and HS in urine, do not confirm a specific diagnosis of MPS II [23,24].

An enzyme assay performed on leukocytes, fibroblasts, plasma, or dried blood spots that reveals a deficiency of IDS activity is required for a definitive diagnosis [16,23,24]. The distinction between mild and severe MPS II has to be based on clinical symptoms, as IDS activity measured *in vitro* is equally deficient in both forms [14,15,23,24]. The evidence of the normal activity of other sulfatase is crucial, since low levels of IDS may also indicate multiple sulfatase deficiency [23,24].

Molecular genetic testing can be used to identify the pathologic mutation(s) that affect the *IDS* gene and also allows for genetic counselling and carrier testing to be offered to at-risk family members, as well as for identifying affected embryos in prenatal diagnosis [16,21,23,24].

Treatment

Given the wide range of clinical manifestations present in MPS II, medical support (e.g. from orthopedic surgeons, pneumologists, neurologists, cardiologists) has been essential to manage individual symptom complications and improve patients' quality of life [19,21,23,24].

Until the recent past, HSCT was the only disease-specific therapeutic tool available for MPS II that allowed correcting the deficient IDS activity [21]. Although some somatic benefits were obtained in few cases, the results at neurological level were not equally promising; thus, such improvements did not exceed the high rate of morbidity and mortality associated to this procedure [16,18,19,21,23,24]. Because the same benefits are achieved through specific ERT and with fewer risks, HSCT has not shown promise as a therapy for MPS II [16,21,24].

ERT with idursulfase (Elaprase®, Shire Human Genetic Therapies Inc.) – a recombinant enzyme analogous to native human IDS – is the treatment of choice for MPS II since its approval in the European Union, in 2007 [18,21–24]. ERT can be applied to all symptomatic patients with confirmed diagnosis, being performed on a weekly basis through intravenous infusion of a dose of 0.5mg/kg for 1–3 hours [21–24]. Providing the exogenous enzyme to IDS-deficient cells was shown to attenuate the progressive course of somatic involvement by reducing liver and spleen size, respiratory infections, facial coarseness, and urinary GAG excretion, as well as through the improvement in obstructive sleep apnea, joint mobility, and walking ability [18,19,21–24]. Still, as idursulfase does not cross the blood-brain barrier nor reaches the bone cells, ERT does not have neurocognitive benefit in severe MPS II patients neither corrects the bone disease [17–19,22–24].

New approaches for delivering the recombinant enzyme to the brain and bone structures are currently under study, such as ERT via intrathecal injections and gene therapy [17–19,23,24].

1.1.1.2. Mucopolysaccharidosis type VI

MPS VI, or Maroteaux-Lamy syndrome, is a rare LSD caused by deficit of the enzymatic activity of arylsulfatase B (ARSB, or *N*-acetylgalactosamine-4-sulfatase) [14–16,18,21,26]. As with most MPSs, this genetic disease is transmitted in an autosomal recessive pattern, occurring with equal frequency in males and females [14–16,21,26]. The prevalence of MPS VI is around 0.05 in the Czech Republic [10], 0.43 in Australia [11], and 0.15 per 100,000 live births in The Netherlands [12]. In Portugal, its prevalence is estimated in 0.42 per 100,000 live births [13].

Molecular basis

MPS VI is instigated by complete or partial loss of activity of the lysosomal sulfatase ARSB, which arises from mutations in the *ARSB* gene that is positioned at the locus 5q13–q14 and comprises 8 exons spread over 206kb [14,15,21,26,27].

Functionally, ARSB promotes the degradation of DS inside the lysosome by catalyzing the removal of the C4 sulfate ester group from *N*-acetylgalactosamine 4-sulfate sugar residue at the non-reducing end of this GAG [14,15,26,27]. The breakdown pathway of DS, including the enzymatic reaction blocked in MPS VI, is represented in Figure 1.3.

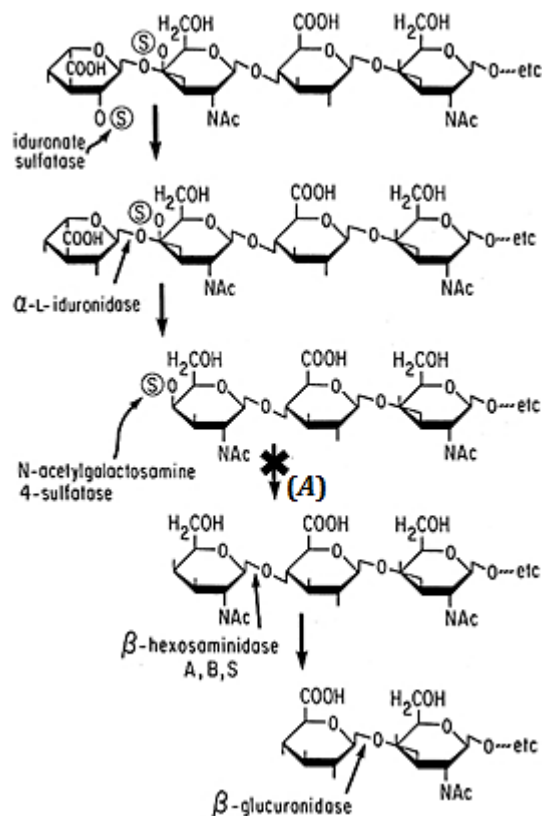


Figure 1.3. Deficiency in GAG catabolism in MPS VI disease. Adapted from [14]. Represented is the enzymatic reaction in the stepwise degradation pathway of DS (A) that is blocked in Maroteaux-Lamy syndrome.

A large number of private mutations in the *ARSB* gene were reported with relative low frequency in single families, which comprise insertion (e.g. 1161insC), deletion (e.g. 427delG), missense (e.g. Y210C), nonsense (e.g. R160X), and splice junction errors (e.g. 1143-8T>G) [14,21, 26,27]. This genetic heterogeneity may be a major contributing factor for the wide spectrum of clinical symptoms manifested by the affected individuals [27].

In consequence of the deficiency of such enzymatic activity determined by pathogenic mutations in the *ARSB* gene, MPS VI patients demonstrate an inability to efficiently degrade DS, resulting in the intralysosomal storage of this partially digested GAG material with subsequent cell and tissue injury, along with its excretion in urine [14,15,26,27].

Clinical presentation

MPS VI patients manifest a purely somatic disease with no primary cognitive impairment, characterized by a broad spectrum of clinical severity varying from slowly to rapidly progressing phenotypes, wherein the musculoskeletal, cardiopulmonary, gastrointestinal, and nervous systems, as well as the skin, cornea, and auditory tissue are frequently affected [14–16,21,26].

In the severe form of MPS VI, somatic symptoms may be present at birth, with newborns displaying enlarged head and deformed chest [14,26]. In the first 2–3 years of life, many features of dysostosis multiplex arise and physical growth stagnates around 6–8 years of age [14,16,21, 26]. Multisystemic manifestations of severely affected patients include: facial dysmorphism; joint stiffness and contractures; hepatosplenomegaly; umbilical and inguinal hernias; absent or delayed puberty; visual and auditory deficits, which impair cognitive and learning capabilities; and central nervous system findings, as carpal tunnel syndrome, but with preserved intellect [14,16,21,26]. After one decade of life, they exhibit shortened trunk with protuberant abdomen, thoracolumbar gibbus, and reduced mobility [14,21,26]. Patients older than 10 years have cardiac problems, namely heart valve stenosis, often aggravated by progressive airway narrowing, upon which natural death in the second or third decades occurs, due to right ventricular failure [14,16,21,26].

Patients with mild MPS VI develop attenuated or slowly progressing somatic involvement later in life, typically affecting few systems simultaneously [16,26]. In general, diagnosis is made in teenage years or early adulthood, when skeletal alterations and a decrease in overall functional status become evident [16,26]. Mildly affected patients experience severe complications at some point in their lives, as joint degeneration, reduced respiratory function, spinal cord compression with myelopathy, and valvular heart lesions [14,16,26]. Natural death from cardiopulmonary failure may occur between 20 and 30 years of age, although some patients survive longer [21,26].

The clinical symptoms generally manifested in MPS VI are summarized in Table 1.3 and the characteristic features of affected patients are shown in Figure 1.4.

Table 1.3. Clinical symptoms characteristic of MPS VI disease [14,16,21,26]

Organ/system affected	Clinical manifestations	
Musculoskeletal system	<ul style="list-style-type: none">- Macrocephaly- Coarse facies- Claw-hand deformities- Acetabulum hypoplasia- Shortened trunk	<ul style="list-style-type: none">- Thoracic deformity- Degenerative joint disease- Vertebral body anomalies- Dysplasia of the proximal femur- Thoracolumbar gibbus

Table 1.3. Clinical symptoms characteristic of MPS VI disease (cont.) [14,16,21,26]

Organ/system affected	Clinical manifestations
Cardiovascular system	<ul style="list-style-type: none"> - Aortic, mitral, and tricuspid valvular stenosis and/or insufficiency - Endocarditis fibroelastosis - Systemic hypertension - Cardiomyopathy
Respiratory system	<ul style="list-style-type: none"> - Chronic airway obstruction (secondary to short neck, hypoplastic mandible, elevated epiglottis, and tracheobronchomalacia) - Obstructive sleep apnea - Thick nasal discharge - Restrictive lung disease - Recurrent pneumonia
Gastrointestinal system	<ul style="list-style-type: none"> - Hepatomegaly - Umbilical and inguinal hernias - Splenomegaly
Visual system	<ul style="list-style-type: none"> - Corneal clouding - Optic nerve alterations - Glaucoma - Visual disability
Auditory system	<ul style="list-style-type: none"> - Otitis media - Hypoacusia
Skin	<ul style="list-style-type: none"> - Mild hirsutism
Nervous system	<ul style="list-style-type: none"> - Carpal tunnel syndrome - Meningeal thickening - Communicating hydrocephalus - Spinal cord compression

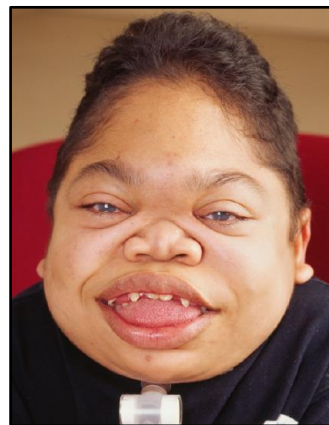


Figure 1.4. Typical features of MPS VI patients [26]. Evidence of short stature, spine curvature [*left*], and coarse facial features (enlarged tongue, gingival hypertrophy, delayed dental eruption, depressed nasal bridge, and frontal bossing) [*right*].

Diagnosis

The suspicion of MPS VI typically arises during clinical evaluation based on physical evidence: coarse facies, dysostosis multiplex, short stature, organomegaly, inguinal or umbilical

hernias, and corneal clouding are common findings [26,28]. Still, because this phenotype is similar to other MPSs, biochemical and genetic testing are required for an accurate diagnosis [26,28].

The elevation of total urinary GAGs can be used as a supportive test, in which levels above 200µg GAGs/mg creatinine are found in severely affected patients, whereas levels below the threshold of 100µg GAGs/mg creatinine are seen in the milder form of MPS VI [26–28]. Since this method is only suggestive of a MPS disorder, the demonstration of DS accumulation in urine, with concomitant absence of all other GAGs, is necessary to reinforce suspicion of MPS VI [26,28].

Even so, the “gold standard” for MPS VI diagnosis is the evidence of severe deficiency of the ARSB activity in fibroblasts, leukocytes, serum, or dried blood spots, usually below 10% of the lower limit of normal enzyme activity, with the greatest disease severity being correlated with no detectable ARSB activity *in vitro* [16,26,28]. The identification of the normal activity of other lysosomal sulfatases is essential to rule out multiple sulfatase deficiency [26,28].

Gene sequencing for identifying pathological mutations in the *ARSB* gene can confirm the diagnosis of MPS VI, being also critical in carrier testing and prenatal diagnosis [26,28].

Treatment

For many years, the clinical management of MPS VI was limited to supportive care and HSCT [26,28]. Because this disease affects multiple body systems, integrated care (e.g. physical and occupational therapy, nutrition counselling, symptom-based medications, and surgical interventions) has been important to optimize patients’ health and quality of life [18,21,26,28].

HSCT was, until recently, the only specific therapy available for MPS VI patients that provided long-term physiologic levels of ARSB delivered endogenously by donor cells [18,21,26, 28]. Although it was shown to attenuate some somatic symptoms, it was only used in few cases due to lack of suitable donors, as well as significant mortality and morbidity risks [16,18,21,26, 28]. After the availability of a specific ERT with proven efficacy and safety, HSCT has become an alternative therapeutic tool for this disease [16,18,21,28].

Since its approval in Europe, in 2006, ERT with genetically engineered human enzyme has been the first-line treatment for MPS VI [18,21,26,28]. This therapy with galsulfase (Naglazyme®, BioMarin Pharmaceutical Inc.) – a recombinant form of native human ARSB – is suitable for all symptomatic patients with confirmed diagnosis [18,21,26,28]. Regular treatment consisting of weekly intravenous administration of a dose of 1mg/kg, during a minimum infusion time of 4 hours, proved to improve walking ability and pulmonary function, showing also positive effects on growth and puberty, as well as in the reduction of urinary GAG excretion [18,21,26,28].

Even so, because ERT administered intravenously does not allow for galsulfase to reach the bone cells in order to correct the skeletal pathology, gene therapy is being investigated as a new approach to provide a stable source of exogenous enzyme to bone structures [17–19].

1.1.2. Immunological alterations in lysosomal storage diseases

The lysosome, whose function is impaired in LSDs, represents a vital component of many immune cell processes, such as: autophagy; protein and lipid antigen processing and presentation by antigen presenting cells (APCs); phagocytosis; release of pro-inflammatory mediators by mast cells; and perforin secretion by CD8+ T cells [29–31]. The intralysosomal accumulation of substrates was already demonstrated in different immune cells in the context of LSDs, including circulating B cells [32], CD4+ and CD8+ T cells, natural killer (NK) cells [33], and monocytes [34]. Thus, lysosomal dysfunction in LSDs has potentially a negative impact in the normal functioning of the immune system, for example by causing direct damage to immune cells affected by lysosomal storage, or by impairing the correct activation and development of immune cells as well as their subsequent capacity of mounting an efficient protective response [29,30,35].

Up to the present day, most studies that characterized the immune system in LSDs were performed in murine models. A reduction of CD4+ T cells and an increase of CD8+ T cells were identified in the liver and spleen of Fabry disease mice [36]. A deficiency of thymic, hepatic, and splenic invariant natural killer T (iNKT) cells was also reported in the mouse models of Tay-Sachs disease [35], Fabry disease [35,36], multiple sulfatase deficiency [37], Sandhoff disease [35,37], Niemann-Pick disease type C1 [35,38], GM1 gangliosidosis [35,39], and Niemann-Pick disease type C2 [39]. With respect to APCs, an increase of splenic macrophages and a decrease of dendritic cells (DCs) were described in Sandhoff disease and GM1 gangliosidosis mice [35]. However, the levels of T cells, as well as CD4+ and CD8+ T cell compartments, were normal in the thymus, liver, and spleen of Niemann-Pick disease type C1 [38], GM1 gangliosidosis, and Niemann-Pick disease type C2 [39] mice. In the murine models of metachromatic leukodystrophy and Krabbe disease, there were no anomalies concerning iNKT cells [37].

In humans, studies evaluating the frequency of circulating leukocyte populations in LSD patients remain scarce. In Fabry disease, no alterations were detected in peripheral blood T cells [36], CD4+ T cells, NK cells [40], iNKT cells [36,40,41], and iNKT CD8+ cells [41]. In contrast, decreased numbers of CD8+ T cells, DCs, monocytes [40], and iNKT CD4+ cells [41] were seen in Fabry disease patients, along with higher levels of B cells [40] and iNKT CD4–CD8– cells [41]. In

Gaucher disease, it was found a reduction of circulating DCs [42] and CD4+ T cells, as well as an increase of CD8+ T cells, but no anomalies in iNKT cells [43]. In Niemann-Pick disease type C1 patients, although the frequencies of iNKT cells [44], T cells, and B cells were normal, a deficiency of NK cells was observed [45].

In the particular case of MPSs, a limited number of studies have investigated, so far, the immune cell abnormalities present in this subclass of LSDs. In the mouse model of MPS VII, no alterations in CD4+ and CD8+ T cells were detected in the thymus, spleen, and lymph nodes, with the exception of a reduction in splenic CD4+ T cells [46]. The percentages of circulating DCs and CD4+, CD8+, and memory CD4+ T cell subsets were reduced in MPS I mice [30], but there were no changes in thymic, splenic, and hepatic iNKT cells [37]. In the MPS IIIB murine model, an increase of B cells, CD4+ and CD8+ T cells was identified in the spleen [47]. An analysis carried out in MPS II patients revealed normal levels of CD4+ and CD8+ T cells, but a decrease of circulating B cells and NK cells was reported [31].

In most studies regarding the immunological characterization of LSDs, iNKT cells were the lymphocyte population more frequently analyzed. Similarly, the iNKT cell frequency in MPS II and MPS VI diseases was also evaluated in our laboratory. The results showed no alterations in iNKT cells in MPS II patients [48] and MPS VI patients [49] as compared with control subjects, being consistent with previous works conducted in Fabry disease [36,40,41], Gaucher disease [43], and Niemann-Pick disease type C1 [44] patients. The B cell percentage was also assessed in our laboratory for MPS II and MPS VI diseases. Although no differences were observed in MPS II patients [48], a significant increase of B cells was found in MPS VI patients [49] comparing with control subjects, which was in accordance with a prior study in Fabry disease patients [40].

1.2. Invariant natural killer T cells

iNKT cells are a highly conserved T cell subpopulation defined by the expression of NK lineage markers (e.g. CD161) and a CD1d-restricted, lipid-specific T cell receptor (TCR) [50–55]. Unlike other natural killer T (NKT) cells that exhibit an oligoclonal $\alpha\beta$ TCR – type II NKT cells –, iNKT cells – type I NKT cells – express a semi-invariant TCR composed by an invariant α chain (V α 24] α 18 in humans and V α 14] α 18 in mice) combined with a limited, but not invariant, β chain repertoire (typically V β 11 in humans, although in mice can be V β 2, V β 7, or V β 8.2) [50–55].

The tissue distribution and frequency of iNKT cells vary considerably among humans, although remaining stable within individuals, with higher levels typically found in women [50, 53–55]. After developing in the thymus, some mature iNKT cells remain in this lymphoid organ whereas others migrate to the periphery, being mostly distributed between the adipose tissue, omentum, and liver, where they represent, respectively, 15–35%, 10%, and 1% of the lymphocyte population [50,53–55]. Lower similar iNKT cell levels are detected in the bone marrow, spleen, and peripheral blood, where they account for 0.01–1% of total lymphocytes [50,53,55].

Immune responses

iNKT cells are responsive to lipid antigens presented by CD1d, a monomorphic major histocompatibility complex (MHC) class I-like molecule; this feature distinguishes them from conventional T cells, which typically identify peptide ligands bound to highly polymorphic MHC class I and II molecules [50–54]. iNKT cells recognize not only foreign lipids, essentially derived from microorganisms (e.g. glycolipids from *Sphingomonas* spp., *Borrelia burgdorferi*, *Streptococcus pneumoniae*), but also self-antigen lipids (e.g. membrane phospholipids) [50–54]. One of the most potent lipids known to be able to stimulate iNKT cells is α -galactosylceramide (α -GalCer), an exogenous marine sponge-derived glycolipid commonly used to study these cells [50,51,53].

Upon specific binding of the TCR to a high-affinity lipid antigen loaded in CD1d molecules at the surface of an APC (e.g. DCs, macrophages, B cells), activation and proliferation of iNKT cells are quickly induced [50–54]. The TCR signaling culminates fundamentally in rapid and abundant secretion of several T helper (Th) type 1 (e.g. interferon (IFN)- γ , interleukin (IL)-2) and type 2 (e.g. IL-4, IL-10) cytokines [50–54]. This cytokine profile varies with CD4 and CD8 expression, according to which iNKT cells can be divided into three functional subsets: iNKT CD4+ cells release both Th1 and Th2 cytokines, while iNKT CD8+ cells and iNKT CD4–CD8– cells are mainly producers of Th1 cytokines [50,52–54]. Besides secreting copious amounts of Th1 and Th2 cytokines – based on which are classified into iNKT1 and iNKT2 cells, respectively –, iNKT cells can produce Th17 cytokines (e.g. IL-17, IL-22) – iNKT17 cells – or share functional features with follicular helper T cells and secrete IL-5 or IL-6 cytokines – iNKT_{FH}-like cells [51–53].

In addition to direct activation via TCR–CD1d/lipid interactions, iNKT cells may also be indirectly stimulated through cytokine production by APCs, readily recognized by constitutive cytokine receptors in resting iNKT cells [51–54]. Because many microbial pathogens do not express cognate lipid antigens, iNKT cell activity requires induction by pro-inflammatory cytokines (e.g. IL-12, IL-18), leading to responses that usually consist in the secretion of IFN- γ [51–54]. Besides providing an alternative pathway through which they can be activated in the absence of specific lipid antigens, this cytokine-driven stimulation of iNKT cells can also occur in

combination with TCR signals in the presence of low-affinity lipids, with both stimuli acting synergistically to promote a rapid and robust immune response [51–54].

The direct and indirect processes of iNKT cell activation are displayed in Figure 1.5.

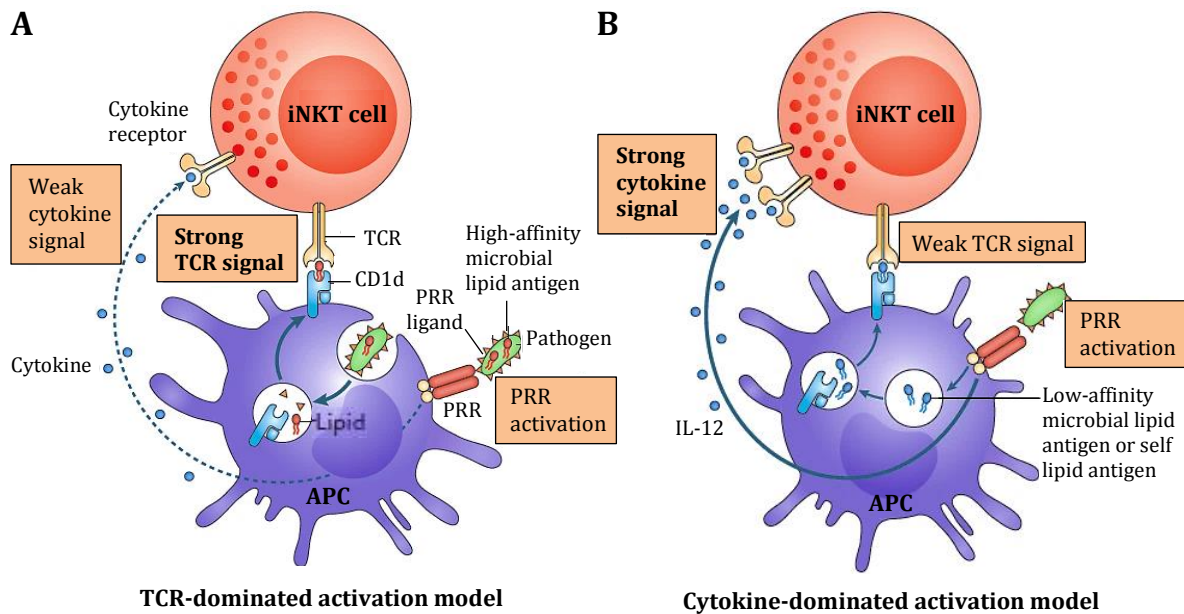


Figure 1.5. TCR- and cytokine-mediated activation of iNKT cells. Adapted from [53]. (A) iNKT cell activation by a strong foreign antigen is dominated by the TCR signal provided by a lipid–CD1d complex and has little dependence on APC-derived cytokines that are generated in response to the stimulation of pattern-recognition receptors (PRRs). (B) In cytokine-driven iNKT cell activation, PRR-mediated stimulation of APCs leads to the secretion of pro-inflammatory cytokines (e.g. IL-12) that bind to specific receptors in iNKT cells; TCR signal is still required in most cases, being provided by low-affinity microbial lipids or self-lipid antigens.

An additional iNKT cell action secondary to TCR-dependent signaling and inflammatory cytokines involves the acquisition of cytolytic activity, due to expression of cytotoxic granules (e.g. granzyme, perforin) like NK cells [50,52,54]. As a result, iNKT cells are able to kill different target cells, including APCs, regulatory T cells, as well as malignant and infected cells [50,53].

In this way, iNKT cells perform both innate-like and adaptive immune functions: the ability for rapidly mounting protective immune responses with minimal TCR involvement by releasing cytokines and producing cytolytic mediators, as well as the capacity to respond directly via specific TCR-mediated recognition of lipid antigens allow them to bridge the two arms of the immune system [50,52,54]. These actions can have either protective or harmful roles in several human pathologies, with the iNKT cells having already been implicated in cancer, allergic diseases, autoimmunity, and microbial infections [50,52–54].

1.3. B lymphocytes

As part of the humoral immunity of the adaptive immune system, B cells are widely recognized for their main role in the secretion of antibodies capable of recognizing an almost unlimited variety of antigenic epitopes (e.g. polysaccharides, proteins, lipids) of bacteria, viruses, and other disease-causing organisms [56–58]. Antibodies are immunoglobulin (Ig) molecules composed of four polypeptide chains – two heavy and two light chains –, both of which contain a variable region and a constant one [59,60]. The variability that enables each antibody to specifically bind a cognate antigen is conferred by the variable region, whereas the constant region allows Ig molecules to mediate effector functions [59,60]. Antibodies exist in two physical forms: (i) membrane-bound antibodies are a constitutive part of the B cell receptor (BCR), whose interaction with specific antigens elicits activation and proliferation of B cell clones, leading to abundant secretion of Ig molecules; (ii) soluble antibodies are released into the peripheral blood as effectors of the humoral immune system for neutralizing antigens or marking them for destruction [57,59,60]. According to the unique amino acid sequences present in the heavy chain's constant region, five antibody isotypes can be distinguished: IgM, IgD, IgG, IgA, and IgE [60]. The general structure of an Ig molecule, as well as of the antigen-binding receptor of B cells, is represented in Figure 1.6.

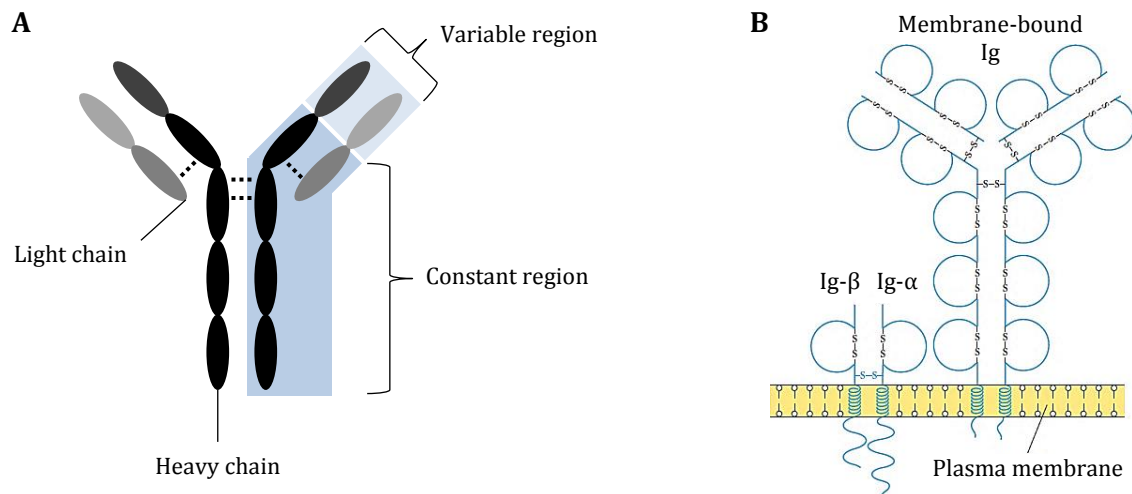


Figure 1.6. Basic structure of an antibody and of BCR. Adapted from [60]. (A) Two identical combinations of light and heavy chains are bound to each other to form a Y-shaped, four-chain Ig molecule. A variable region exists in each light and heavy chain, with the remainder of each chain forming a constant region. (B) The BCR is a multiprotein complex consisting of an antigen-binding surface Ig molecule associated with the signal-transducing Ig- α /Ig- β heterodimer, responsible for cellular activation upon specific ligand recognition.

Additional functions of B cells include antigen presentation via MHC molecules to activate T cell-dependent immune responses, regulation of DC and T cell actions through production of immunomodulatory cytokines, lymphoid tissue organization, and tumor immunity [57,58].

1.3.1. Development of B cell subpopulations

In humans, several B cell compartments are encountered in the peripheral blood, together accounting for 5–15% of circulating lymphocytes, wherein the total B cell population generally changes with age: the global number of B cells in circulation usually rises during the first 2 years of life, followed by a decrease until early adulthood and stabilization in adult people, after which it starts to diminish again when individuals reach the sixth decade of life [57,61].

The various human peripheral blood B cell subsets are generated through a continuum of differentiation stages that take place in many tissues [56–58,61]. The development of B cells is initiated in primary lymphoid tissues (e.g. bone marrow and fetal liver), wherein committed precursors give rise to immature B cells of two different lineages – B-1 cells and B-2 cells –, which recirculate in the peripheral blood to complete their maturation in secondary lymphoid tissues (e.g. spleen, lymph nodes, mucosa-associated lymphoid tissues) and in bone marrow [56–58,61]. The developmental progression from pluripotent progenitors to functional B cells is defined by a changing in the expression pattern of several surface markers [58,62,63].

❖ Initial development of B cells in the fetal liver and bone marrow

During embryonic life, hematopoietic stem cells (HSCs) in the fetal liver give rise to committed precursors that differentiate into the B-1 cell lineage [57,62,63]. After birth, bone marrow-derived HSCs generate committed progenitor cells that continually develop into the B-2 cell lineage, which includes most B cell subpopulations, together known as B-2 cells [57,62,63].

The limitation of lifespan and differentiation-inducing factors (e.g. bone marrow stromal cells' surface receptors, lineage-specific cytokines, BCR ligands) drives B cell ancestors to compete among each other for growth resources, which subsequently stimulates them to go through a stepwise differentiation into functionally mature B cells [61,63]. Irrespective of whether they are generated in the bone marrow or fetal liver, early B cell progenitors (i.e. pro- and pre-B cells) are

Ig negative [56,58,61–63]. Once the rearrangement of Ig heavy and light chain gene segments is complete, these precursors evolve into immature B cells by expressing surface IgM antibodies, an event that triggers egress into the peripheral blood [56,58,61–64]. At this point, immature B cells have an intact BCR, required for B cell development and survival in the periphery [56,58,62–64].

❖ *Further development of B cells in peripheral lymphoid tissues: differentiation into functionally and phenotypically distinct subpopulations*

After the negative selection process, the functionally immature IgM⁺ B cells whose BCRs do not exhibit self-reactivity leave the hematopoietic lymphoid tissues and migrate to secondary lymphoid organs for further maturation [56,61–64]. On the one hand, IgM-expressing immature B cells produced in the fetal liver enter the peripheral circulation to differentiate into B-1 cells [57, 62]. On the other hand, IgM⁺ immature B cells originated in the bone marrow recirculate in the peripheral blood to finalize early B-2 cell development mainly in the spleen, as well as terminal differentiation of mature B-2 cells before migrating to other peripheral lymphoid organs, namely lymph nodes and mucosa-associated lymphoid tissues [56,57,61,62]. According to the maturation status, circulating B-2 cells are typically classified as transitional B cells, naïve follicular B cells, plasma B cells, and memory B cells [56,61]. Essentially all peripheral blood B-lineage cells are identified by CD19 expression, a component of the B cell co-receptor that provides stimulatory signals to BCR, contributing to the activation of mature B cells in the periphery [58,62,63].

1.3.1.1. B-1 cells

B-1 cells represent a small IgM⁺ B cell subset that develops earlier in life than B-2 cells, being encountered primarily in the peripheral blood, peritoneum, and mucosae of human adults as a self-replenishing population, which comprises 1–9% of all circulating B cells [57,62,63,65].

Immune responses

As part of the innate immune system, B-1 cells secrete spontaneously and constitutively the majority of natural, low-affinity IgM antibodies that recognize a variety of carbohydrate and lipid antigens present in most common microbial pathogens [57,58,62,63,65]. In this way, they

immediately provide an initial immune response against infection within the naïve host, especially in the peritoneal cavity, through T cell-independent mechanisms [57,62,63,65]. In addition, B-1 cells have immunosuppressive properties owing to secretion of IL-10 and can also act as APCs by presenting antigens and strongly stimulating T cells via CD80/86 [65].

Phenotypic characterization

Despite the evidence for the existence of human circulating B-1 cells, their phenotype is not clearly defined as it is in mice, since they share surface antigens with memory B cells, monocytes/macrophages, and T cells; therefore, the profile of cell-surface marker expression in human B-1 cells has not yet been universally established and accepted [65–67].

1.3.1.2. Transitional B cells

Immature IgM⁺ B-2 cells begin to mature rapidly in the peripheral blood and spleen via three transitional stages, wherein they successively give rise to T1, T2, and T3 B cells that express both IgM and IgD molecules, together accounting for 2–4% of all circulating B cells in adult people [56,61,62,64,68,69]. Transitional B cells then complete the first stage of B-2 cell differentiation in the spleen, where they mature into follicular or marginal zone B cells [56,61,62,64,68,69].

Immune responses

Transitional B cells appear to respond to antigens that trigger T cell-independent immune responses (e.g. lipopolysaccharides) via rapid antibody production [58,69], but they also seem to exhibit a lower ability to proliferate and develop into antibody-secreting B cells in comparison with mature naïve follicular B cells [61]; therefore, their functions are not fully understood.

Phenotypic characterization

Transitional B cells exhibit features of an immature phenotype, as lack of responsiveness to BCR-mediated signaling due to overexpression of negative regulators (e.g. CD5) that counteract the reduced activation of BCR co-receptors (e.g. CD21) [61,68]. However, they also co-express surface IgM and IgD molecules like mature naïve follicular B cells, although transitional B cells present higher IgM and lower IgD expression as compared with naïve follicular B cells [58,61,68].

1.3.1.3. Follicular B cells

Most mature B-2 cells constitute the follicular B cell subset, defined by the production of both membrane-bound IgD and IgM antibodies with a single antigenic specificity [61–63]. Their co-expression is associated with the capacity to migrate between secondary lymphoid organs and the acquisition of functional competence, in which the naïve follicular B cells become responsive to antigen-specific BCR activation [61,62]. In human adults, they represent 60–70% of B cells in the peripheral blood, which they habitually recirculate while migrating between the spleen, lymph nodes, and mucosa-associated lymphoid tissues, where they reside in specialized niches – the B cell follicles [57,58,61,62,70].

Immune responses

Mature naïve follicular B cells not yet exposed to an antigen circulate between the peripheral blood and secondary lymphoid tissues, searching for specific antigens while competing for entry into B cell follicles; unless these cells encounter their cognate antigen, they die within a few weeks by apoptosis [57,61–63].

Upon first exposure of naïve follicular B cells to a foreign antigen presented by APCs (e.g. follicular DCs, marginal zone B cells) and recognized by surface IgM or IgD molecules of the BCR complex, they are committed to one of three effector fates of humoral immunity, depending on the inherent BCR affinity and antigenic nature [58,61,63,64,70,71]. Those B cell clones bearing high-affinity BCRs during T cell-dependent responses, or that bind to polysaccharide or lipid antigens and undergo activation without T cell help, are firstly selected for the generation of (i) short-lived plasma B cells outside lymphoid follicles, leading to immediate local antibody secretion early during an immune challenge [58,63,70,71]. In turn, low-affinity counterparts binding to protein antigens require direct contact with activated CD4+ T cells to complete the final stage of B-2 cell development in germinal centers (GCs) – central proliferative areas in lymphoid follicular loci –, being directed towards (ii) long-lived plasma B cell and (iii) memory B cell differentiation pathways to improve antibody affinity [56,58,61,63,64,70,71].

During the GC reaction in spleen, lymph node, and mucosa-associated lymphoid tissue follicles, antigen-activated B cells migrate repetitively between two distinct GC areas [56,58,61,63, 71]. In the dark zone, they undergo vigorous proliferation, somatic hypermutation – increase in antigen binding capacity of antibodies due to point mutations in heavy and light chain genes –, and, eventually, Ig class switch recombination – change of Ig isotype from IgM/IgD to IgG, IgA, or IgE [56,58,61,63,64,70–72]. In the light zone, the improvement in Ig affinity is verified via re-

-contact of B cells with cognate antigens presented by follicular DCs [56,58,61,63,64,70,71]. After passing through many cycles of proliferation, affinity maturation, and antigen-driven selection, B cell clones with high-affinity surface antibodies are positively selected by CD4+ T cells to survive and proliferate, whereas low-affinity counterparts die by apoptosis [61,63,64,70–72]. The major outcome of GC reactions is the differentiation of higher affinity long-lived plasma B cells and memory B cells, which dominate the immune response, from low-affinity naïve B cells [61,63,70].

The antigen-dependent developmental stage of mature naïve follicular B cells occurring in the periphery that relies on T cell-mediated activation is represented in Figure 1.7.

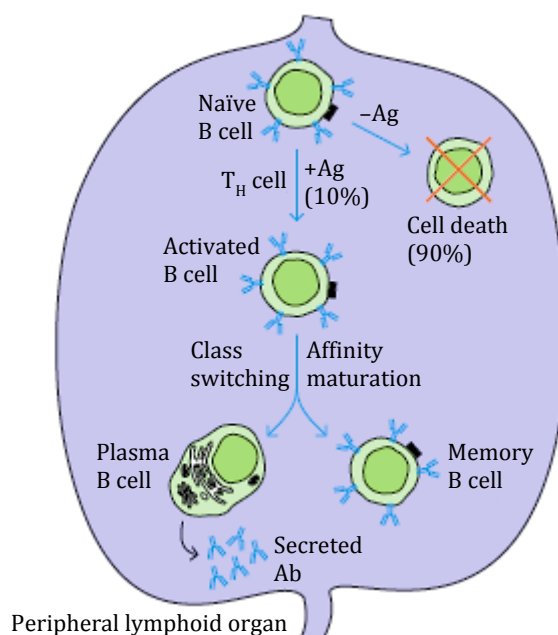


Figure 1.7. Differentiation of follicular B cells in secondary lymphoid tissues. Adapted from [63]. During antigen-dependent maturation, circulating naïve follicular B cells die within a few weeks unless they bind an antigen (Ag) specific to its surface Ig molecule. In T cell-mediated GC reactions, the antigen–BCR complex is internalized and the processed epitopes are presented to helper T cells (T_H cells), which induce B cell proliferation, affinity maturation, and Ig class switching in peripheral lymphoid tissues. B cell clones bearing high-affinity surface Ig molecules are selected to develop into memory B cells and long-lived plasma B cells, culminating in high-affinity antibody (Ab) secretion.

Phenotypic characterization

The combination of IgM (or IgD) and CD27 surface markers – the last one being typically associated with the occurrence of somatic hypermutation in GCs – is a strategy frequently used to discriminate B cells with a more naïve phenotype (IgM+) from those that are more differentiated (CD27+) [64,69,73]. In this way, mature naïve follicular B cells are identified as CD19+IgM+CD27– cells (this phenotypic profile is also applicable to circulating transitional B cells) [64,69,73].

1.3.1.4. *Plasmablasts and plasma B cells*

Most of the progeny of naïve follicular B cells that proliferated in response to antigen stimulation and T cell help gives rise initially to plasmablasts, pre-effector B cells showing on-going cell division and antibody production [57,61,64,71]. Plasmablasts look for survival niches in the bone marrow or mucosa-associated lymphoid tissues to differentiate into plasma B cells, defined by enlarged size, lacking of proliferative activity, and presence of few or none surface Ig molecules [56,57,61,63,64,71]. In humans, both subsets are found at very low frequencies in the peripheral blood of healthy individuals, corresponding to 1–3% of adult circulating B cells [61,64]. However, under circumstances of immune activation (e.g. acute infections), high levels of newly-generated plasmablasts and mature plasma B cells are detected in circulation [61,64].

Immune responses

Plasma B cells constitute terminally differentiated B cells that are committed to abundant antibody secretion to assist the destruction of pathogens [57,61,64,71]. While differentiation of naïve follicular to plasma B cells conduces mostly to the secretion of IgM in primary immune responses, activation of memory B cells during subsequent exposures to the same antigen leads to the production of enormous amounts of high-affinity, somatically mutated IgG or IgA [57,61,71].

For humoral immunity to be sustained throughout a person's life, continuous generation of antibodies is mandatory due to its very short half-life, which can fluctuate from only a few days (e.g. IgM, IgA) to some weeks (e.g. IgG) [61]. On this basis, two types of antibody-secreting cells are distinguished [56,70,71]. Short-lived plasma B cells are originated during T cell-independent reactions in extrafollicular foci and early in T cell-mediated responses in B cell follicles, being found in secondary lymphoid organs and non-lymphoid tissues [70,71]. By producing low-affinity antibodies that form immune complexes with antigens in B cell follicles, they provide an initial, temporary rapid defense while GCs are being prepared to yield a more sustained protection [58, 70,71]. In turn, long-lived plasma B cells are generated during T cell-dependent GC reactions and acquire the ability to home to the bone marrow, where they are maintained for extended periods by cytokines of the BAFF family [56,58,61,64,70,71]. Through the persistent secretion of low levels of high-affinity antibodies for months or even years after an infection be eradicated, they confer immediate protection if the same invading organism is encountered later [58,61,64,70,71].

Phenotypic characterization

The peripheral blood fraction of newly-generated plasmablasts and mature plasma B cells

migrating from the bone marrow exhibits low levels of membrane-bound Ig molecules and heterogeneous CD138 expression [61,64]. Since the adhesion molecule CD138 is acquired during plasmacytic differentiation and, hence, is restricted to circulating plasmablasts and plasma B cells as compared with other peripheral blood B cells, the subset of plasmablasts and plasma B cells in the peripheral circulation is typically defined as CD19⁺CD138^{+/-} cells [61,64,65].

1.3.1.5. Memory B cells

A minority of antigen-activated follicular B cells emerges from GCs during T cell-mediated reactions and acquires the ability to survive in the periphery for long periods without continuous antigenic stimulation [56,57,71]. These memory B cells are antigen-experienced cells capable of mounting rapid adaptive responses for neutralizing and eliminating antigens already encountered in the past, and express high levels of the anti-apoptotic protein Bcl-2 that contribute to their long lifespan [58,64,70,71]. In human adults, some memory B cells reside in the lymphoid organ where they were generated, whereas others circulate between the peripheral blood and antigen-draining lymphoid tissues, representing 30–40% of all circulating B cells [61,71].

Immune responses

In a secondary immune reaction, memory B cells recognizing specific antigens rapidly go through several additional cycles of proliferation in GCs, after which many of them provide the host with a burst of short-lived plasma B cells or differentiate into high-affinity long-lived plasma B cells, while a small fraction still persists as memory B cells [57,58,61,70–72]. Due to such ability to promptly generate intensified immunizing responses against invading pathogens that formerly infected the host – immune memory –, they can eradicate a second infection more quickly than naïve follicular B cells in a primary challenge (3–5 *versus* 7–10 days, respectively) [63,70–73].

The repeated activation of memory B cells via antigen binding and T cell help conduces to extensive Ig isotype switching in GCs and increased expression of surface Ig molecules other than IgM and IgD [57,61,63,71]. About half of peripheral blood memory B cells exhibit mutated antigen receptors with high-affinity IgG or IgA antibodies – switched memory B cells [57,61,64,71]. Most of the remaining memory B cells still exhibit both membrane-bound IgM and IgD – non-switched memory B cells – or IgM molecules solely – IgM-only memory B cells –, being collectively known as IgM memory B cells, whose development seems to be independent of GC formation [61,72,73]. Beyond that, some IgG⁺ and IgA⁺ memory B cells are not classical switched memory B cells due to

lack of CD27 expression – double-negative memory B cells –, which account for 5% of circulating B cells and appear to be transient effectors that did not yet conclude the GC reaction and acquire CD27, being at an earlier stage of development regarding affinity maturation [61,64,73].

Phenotypic characterization

Memory B cells are recognized for expressing CD27, an activation marker correlated with great proliferative capacity, aptitude for antigen presentation, and differentiation into antibody-secreting cells [64,69,73]. Since plasmablasts and plasma B cells are rare in the peripheral blood of healthy individuals, most circulating CD27+ B cells are identified as memory B cells [64,73]. To distinguish the various memory B cell subsets, the expression of IgM (or IgD) and CD27 surface markers is evaluated: switched memory B cells are CD19+IgM–CD27+, IgM memory B cells are CD19+IgM+CD27+, and double-negative memory B cells are CD19+IgM–CD27– [64,69,73].

1.3.1.6. Marginal zone B cells

Mature marginal zone B cells constitute a B-2 cell subpopulation with limited diversity that expresses high levels of membrane-bound IgM molecules [62]. In humans, they do not generally circulate in the peripheral blood; instead, they can be found primarily residing near the marginal sinus of the spleen and in the outer extrafollicular rim in lymph nodes [57,62,72,74].

Immune responses

Marginal zone B cells are innate-like cells that, similarly to B-1 cells, secrete natural IgM antibodies against polysaccharide and lipid ligands in the absence of antigenic stimulation [57,58, 62,74]. Upon direct contact with antigens and supported by splenic B cell helper neutrophils, they are capable of rapidly developing into extrafollicular short-lived plasma B cells that release IgM antibodies, being the first line of defense against blood-borne pathogens [56,62,74]. Besides their actions in T cell-independent humoral immunity, marginal zone B cells mediate antigen capture, transport into spleen and lymph node follicles, and presentation to follicular B cells [57,62,74].

Phenotypic characterization

Marginal zone B cells are best defined in rodents and, although they seem to share the phenotype of IgM memory B cells, there is still uncertainty on their identity in humans [58,62,74].

1.3.1.7. Regulatory B cells

A novel, yet less well understood, human B-2 cell subset includes regulatory B cells, which are thought to be representative of 1–3% of splenic B cells [57]. These cells appear to suppress excessive tissue-specific inflammation and immune reactions that can lead to autoimmunity, via secretion of the anti-inflammatory cytokine IL-10 and the growth factor TGF- β [57,58,64]. The surface marker expression in human regulatory B cells remains a matter of debate [57,64].

The overall developmental process of the B-2 cell lineage is schematized in Figure 1.8.

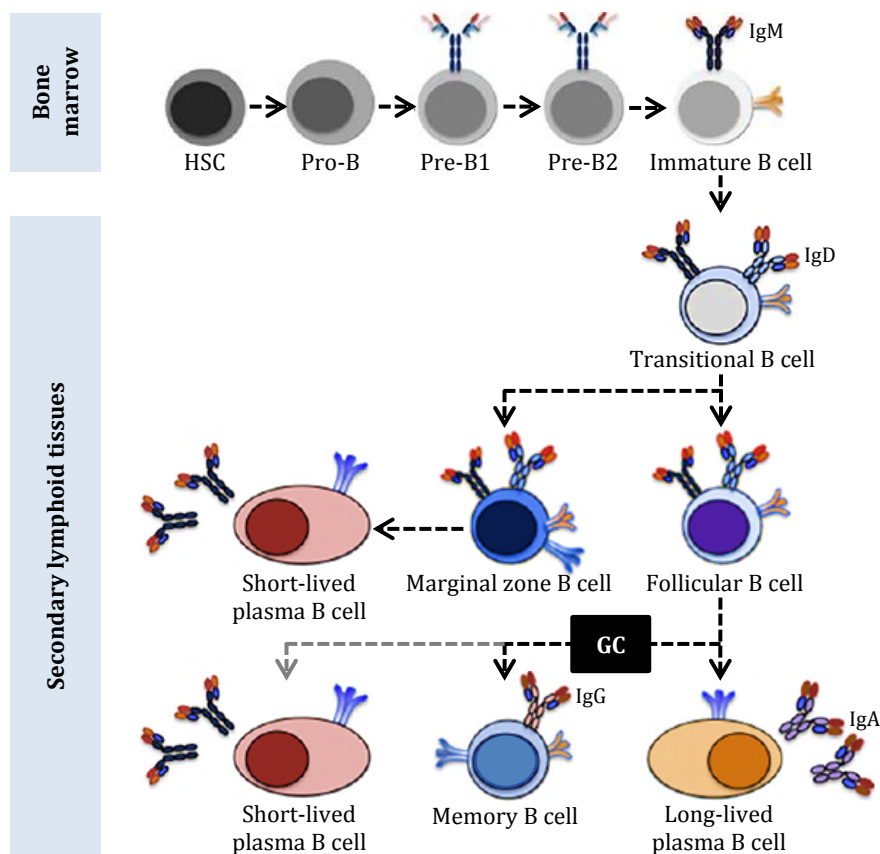


Figure 1.8. Developmental stages of the B-2 cell lineage. Adapted from [56]. Early B-2 cell development produces immature IgM-expressing B cells from bone marrow-derived HSCs that, after few transitional stages in the peripheral blood, mature into IgM+IgD+ follicular and marginal zone B cells. The latest generate IgM-secreting short-lived plasma B cells outside B cell follicles. Follicular B cells complete differentiation into short-lived plasma B cells without T cell help, or into long-lived plasma B cells and memory B cells, which express high-affinity IgG or IgA antibodies, under T cell-dependent activation in GCs.

1.3.2. Transformation of peripheral B cells by Epstein–Barr virus

Epstein–Barr virus (EBV) is a human lymphocryptovirus that belongs to the subfamily *Gammaherpesvirinae* of herpesviruses [75]. As a member of the family *Herpesviridae*, EBV is a double-stranded DNA virus composed mainly of: a core, containing the viral genome; a protein capsid, where the linear DNA molecule is densely packaged; a tegument, which consists of a proteinaceous layer surrounding the nucleocapsid; and an envelope, an external lipid bilayer carrying viral glycoproteins [75,76].

By adulthood, most humans have been infected by EBV, which is associated with several pathologies as Burkitt's lymphoma and infectious mononucleosis [75,77,78]. EBV is particularly known for having tropism for resting primary B cells, wherein naïve follicular and memory B cell subsets are the main cellular targets both *in vivo* and *in vitro*, though this orally transmitted herpesvirus can also infect epithelial cells [76,77,79–81]. The generation of EBV-transformed B cell lines *in vitro* is possible owing to the capacity of the virus to establish a latent infection that continuously induces the stable expansion of B cells, via expression of few viral genes that prevent apoptosis, regulate cellular activation and proliferation, and maintain viral latency [76–81].

The entry of EBV virions into B cells relies on the high-affinity interaction between the major viral envelope glycoprotein gp350/220 and the complement receptor type 2 (CR2, or CD21), which acts as an EBV receptor on the surface of target cells [76,78,79]. A second viral envelope glycoprotein gp42 attaches to human leukocyte antigen (HLA) class II molecules that serve as a cellular co-receptor [76,78,79]. Both interactions are essential for the effective entry of EBV into B cells, although they are not required for the much less efficient infection of epithelial cells [76,79].

After such interactions have been established, adsorption and endocytosis of EBV virions are quickly triggered, followed by fusion of the viral envelope with a cellular endocytic vesicle [76, 78]. As a consequence of EBV uncoating, the genomic material encapsidated in the protein shell is released into the cytoplasm, after which viral DNA is delivered into the nucleus [76,78].

During subclinical primary infections *in vivo* and B cell transformation *in vitro*, the double-stranded DNA molecule of EBV does not enter the cell nucleus in order to be massively replicated and produce progeny virions; instead, the viral genome is maintained as a covalently closed, circular extrachromosomal episome with only 5–100 copies per infected cell, which replicates synchronically with cellular DNA [77,78,80,82,83]. In this non-producing latent infection, a limited number of viral genes are expressed under careful regulation to generate nine virally

encoded proteins that drive the target B cell into cell cycle while maintaining viral latency, thus inducing the survival and continuous outgrowth of EBV-infected B cells [77-80,82,83]. Their phenotype is typically characterized by the expression of six Epstein-Barr nuclear antigens (EBNAs-1, -2, -3A, -3B, -LP, and -3C; alternatively, EBNAs-1-6) and three latent membrane proteins (LMPs-1, -2A, and -2B) [77-81,83]. Of these, EBNAs-1, -2, -3A, -LP, and -3C, as well as LMP-1, are required for the immortalizing effect of EBV, with EBNA-2 and LMP-1 as the most relevant viral proteins [77,78,80,81,83].

The phenotypic change resulting from expression of virally encoded proteins renders the infected B cells immunogenic and, therefore, stimulates T cell surveillance, wherein CD8+ T cells are dedicated to readily detect and eradicate transformed B cells [77,79,80]. However, before this EBV-mediated cell expansion is contained by the immune system, some infected B cells manage to switch off viral gene expression and counteract antigen presentation by down-regulating surface HLA expression, in order to escape from T cell recognition; as so, these cells are able to reach the memory B cell pool and achieve long-term persistency as resting cells that carry silent viral genomes and are not immunogenic [77,79,80,83].

2. AIMS

Considering a previous work conducted in our laboratory that identified a significant increase in the frequency of B cells in MPS VI patients [49], the main purpose of this thesis was to study the B cells in MPS II and MPS VI diseases. The more specific aims were:

- ❖ To analyze the frequency of the major peripheral blood leukocyte populations in MPS II and MPS VI patients;
- ❖ To characterize the frequency of the B cell and T cell subsets in MPS II and MPS VI patients;
- ❖ To produce EBV-transformed B cell lines from MPS II and MPS VI patients;
- ❖ To evaluate the efficacy in the production of EBV-transformed B cell lines from MPS II and MPS VI patients;
- ❖ To assess the phenotype of EBV-transformed B cell lines from MPS II and MPS VI patients.

3. MATERIALS AND METHODS

During the period of my thesis, the experimental activities comprising (i) the analysis of the B cell and T cell populations by flow cytometry and (ii) the production of EBV-transformed B cell lines *in vitro* were performed using peripheral blood samples from MPS II and MPS VI patients as well as control subjects. Upon their isolation, peripheral blood mononuclear cells (PBMCs) were incubated with EBV infectious virions (previously obtained from B95-8 cell cultures) to induce B cell transformation. The remaining PBMCs were used for flow cytometry in order to determine the frequency of circulating B cell and T cell subsets. After the culture of infected B cells over a period of 35 days, the phenotypic characterization through flow cytometry and the freezing of EBV-transformed B cell lines were executed. The experimental design of the study conducted during the time I worked in the laboratory is shown in Figure 3.1.

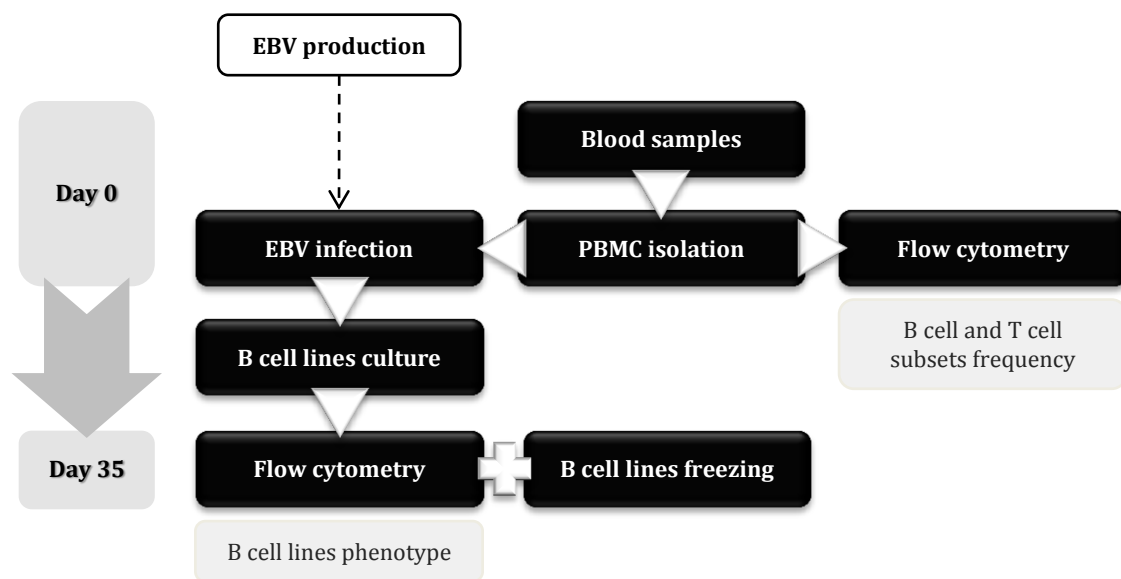


Figure 3.1. Experimental design of the study.

Prior to the start of this thesis, a first analysis of the frequency of several leukocyte populations – T cells, NK cells, B cells, and monocytes – was carried out by Luz Maia, Nuno Lopes, and Cátia Pereira for six of the ten MPS II patients and for all the sixteen MPS VI patients included in the study of the immune system alterations in MPS II and MPS VI diseases. During my work in the laboratory, I performed a second determination of the percentage of B cells and T cells for two of the ten MPS II patients and for ten of the sixteen MPS VI patients, as well as the analysis of four MPS II patients for the first time.

3.1. Subject selection and blood sample collection

In the study that focused on the characterization of the immune system in MPS II and MPS VI diseases and which was mostly performed before I have worked in the laboratory, a total of ten MPS II patients, sixteen MPS VI patients, and twenty-seven control subjects were evaluated. More specifically, during the period of my thesis, a total of six MPS II patients and ten MPS VI patients, as well as nine control subjects were analyzed for the frequency of circulating B cell and T cell populations. Of these, five MPS II patients, five MPS VI patients, and all control subjects were included in the study concerning the production and phenotyping of EBV-transformed B cell lines.

The group of MPS II patients was composed entirely by males as this is an X-linked disease, while the MPS VI patient group comprised eight females and eight males. These patients were recruited by their physicians, after their and/or their parents' informed consent, and the blood samples collected at *Centro Hospitalar de São João* (Porto, Portugal), *Hospital Geral de Santo António* (Porto, Portugal), *Hospital de Santa Maria* (Lisbon, Portugal), *Hospital Pediátrico de Coimbra* (Coimbra, Portugal), *Hospital Clínicas de Porto Alegre* (Porto Alegre, Brazil), and *Hospital São João de Deus* (Barcelona, Spain), under an agreement between *Instituto de Biologia Molecular e Celular* (IBMC; Porto, Portugal) and these institutions, relying on the approval of their ethical committees. With the exception of two MPS II patients, all individuals in both groups were under ERT at the time of the first analysis. The treatment consisted in the intravenous infusion of a recombinant form of the enzyme iduronate-2-sulfatase (idursulfase, Elaprase®) for MPS II patients or arylsulfatase B (galsulfase, Naglazyme®) for MPS VI patients. The main characteristics of the MPS patients (age at the first analysis, sex, genetic mutation(s), and ERT information) that participated in the studies on the immune system in MPS II and MPS VI diseases as well as on the generation of EBV-transformed B cell lines are described in Table 3.1.

The control group analyzed with the aim of characterizing the immunological alterations in MPS II and MPS VI patients consisted of nine females and eighteen males, including sixteen children and eleven adults. Upon receiving the informed consent from these subjects, which were blood donors at *Centro Hospitalar de São João* and *Hospital de Valongo* (Valongo, Portugal), the blood samples were obtained under a protocol between IBMC and these institutions, with the approval of their ethics commission. In the control group of the work performed for producing EBV-transformed B cell lines, six females and three males were recruited by Fátima Macedo at IBMC, after the approval of the internal ethics board and obtainment of the informed consent from these adult voluntary donors. The blood samples were collected at *Centro de Genética Preditiva e Preventiva* (Porto, Portugal) by the nurse that collaborated in this project.

Table 3.1. Characterization of the MPS II and MPS VI patients included in the analysis of the immune system in MPS II and MPS VI diseases, as well as in the production of EBV-transformed B cell lines

Patient	Age	Sex	Mutation(s)	ERT	Study	
MPS II	#1	28	M	C2846G>C; tR95T, exon 3	Yes	1
	#2	9	M	NA	Yes	1
	#3	23	M	NA	Yes	1
	#4	9	M	p.G340R; c.1018G>C	Yes	1, 2
	#5	7	M	c.241C>T; p.Q81X	Yes	1, 2
	#6	15	M	c.1130G>C; p.G336R	Yes	1
	#7	16	M	NA	Yes	1, 2
	#8	12	M	NA	No	1, 2
	#9	17	M	NA	No	1, 2
	#10	18	M	NA	Yes	1
MPS VI	#1	18	F	c.944G>A; p.R315Q	Yes	1
	#2	20	M	R315Q	Yes	1
	#3	23	F	c.215T>G; p.L72R	Yes	1
	#4	18	M	p.D54N	Yes	1
	#5	4	F	NA	Yes	1
	#6	14	F	NA	Yes	1, 2
	#7	27	F	NA	Yes	1
	#8	23	M	NA	Yes	1
	#9	13	M	NA	Yes	1
	#10	11	F	IVS5+2; c.238delG	Yes	1
	#11	11	F	IVS5+2; c.238delG	Yes	1
	#12	13	F	NA	Yes	1
	#13	19	M	R315Q+S384N; L72R	Yes	1, 2
	#14	13	M	Heterozygous IVS5-8T>G; c.1143-8T>G; c.149T>A (p. L50X)	Yes	1, 2
	#15	7	M	Heterozygous c.1533_1555Del; c.1336G>A (p.G446S)	Yes	1, 2
	#16	13	M	Homozygous IVS5-8T>G; c.1143-8T>G	Yes	1, 2

M: male; F: female; NA: not available; ERT: enzyme replacement therapy; Study 1: study on the characterization of the immune system in MPS II and MPS VI diseases; Study 2: study on the generation and phenotypic characterization of EBV-transformed B cell lines.

The samples of peripheral blood from MPS II and MPS VI patients were collected into ethylenediamine tetraacetic acid (EDTA)-containing tubes. For MPS patients that were under ERT, blood collection was executed before intravenous administration of the recombinant enzyme.

3.2. Isolation of peripheral blood mononuclear cells

Within 24 hours upon receipt of the blood samples, PBMCs were isolated through a process of density gradient centrifugation using the Histopaque[®]-1077 medium (Sigma), under sterile conditions. The blood was laid over an equal amount of Histopaque[®]-1077 and centrifuged at 400g for 30 minutes, without break. After centrifugation, the various blood constituents could be distinctly visualized as separate layers: PBMCs were positioned between the plasma and the Histopaque[®]-1077 medium as a narrow cell ring, as represented in Figure 3.2. Most plasma was collected, centrifuged at 2,500rpm, 4°C, for 30 minutes, and stored at -20°C. Following PBMC collection, cells were washed with 10mL of phosphate buffered saline 1x (PBS 1x; see appendix) and centrifuged at 250g for 10 minutes. Then, PBMCs were incubated for 10 minutes with 10mL of ammonium-chloride-potassium (ACK) lysing buffer (see appendix), after which 10mL of PBS 1x were added and cells centrifuged at 250g for 10 minutes. Upon resuspension of PBMCs in 10mL of PBS 1x, viable cells were counted under the microscope through the method of trypan blue and utilizing a Neubauer chamber. Following cell count, PBMCs were used for the generation of EBV-transformed B cell lines and for flow cytometry analysis.

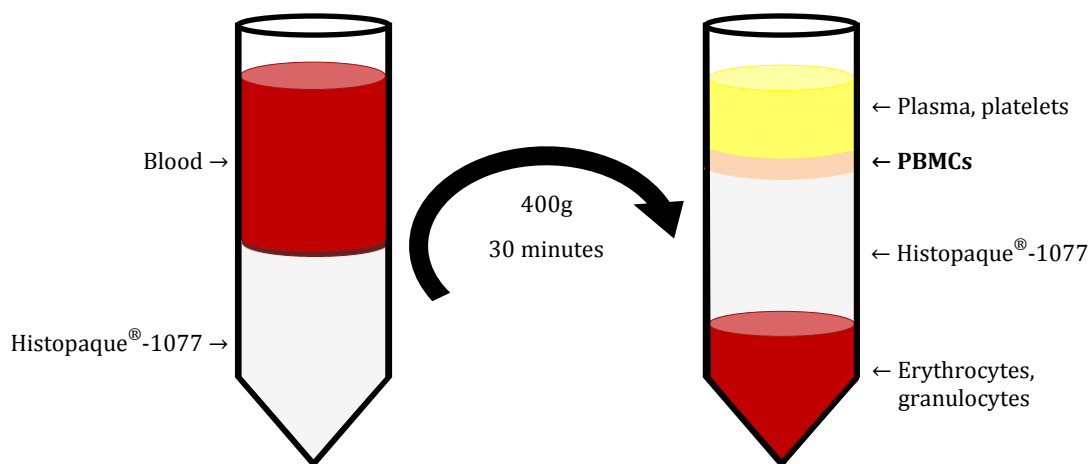


Figure 3.2. PBMC isolation by density gradient centrifugation with Histopaque[®]-1077 medium.

3.3. Production of EBV infectious virions

For the production of high titers of EBV infectious virions, the marmoset B95-8 cell line available in our laboratory was used. Under sterile conditions, cells were cultured in 10mL of RPMI 10% inactivated fetal bovine serum (iFBS) (see appendix), and incubated at 37°C, 5% CO₂. On the following day, the B95-8 cell culture was splitted 1:3 in RPMI 10% iFBS and incubated at 37°C, 5% CO₂, until the medium had a strong yellow coloration. A week later, cells were centrifuged at 1,200rpm for 10 minutes, after which the supernatant with EBV infectious virions was collected and passed through a 0.45µm filter. Aliquots of 1mL and 4,5mL of the filtered EBV-containing supernatant were stored at -80°C until their use for the generation of EBV-transformed B cell lines. Given that the lifetime of EBV is reduced when maintained at 37°C, the aliquots of infectious virions were only thawed for use once; they were not frozen again for reutilization due to the risk of EBV's infectivity being affected by successive thawing processes.

3.4. Transformation of B cells by EBV

For the viral infection and transformation of peripheral blood B cells, EBV infectious virions from the B95-8 culture supernatant were used, along with the previously isolated PBMCs. After quick thawing on a 37°C water bath, 1mL per well of EBV-containing supernatant was plated in a 24-well plate, under sterile conditions. Upon resuspension of PBMCs at 2x10⁶ cells/mL in RPMI 20% iFBS (see appendix), 1mL per well of PBMCs was transferred to the previous wells. Finally, cyclosporine A (Calbiochem) at 1µg/mL was added to each well to suppress T cell and NK cell function, after which the cultures were incubated at 37°C, 5% CO₂. Of note, the aliquots of EBV-containing supernatant used in the production of all EBV-transformed B cell lines came from the same stock of EBV infectious virions.

3.5. Culture of EBV-transformed B cells

On day 7 post-infection, approximately half the transformation medium in each well was discarded and replaced by an equal volume of RPMI 20% iFBS (see appendix), followed by cell

incubation at 37°C, 5% CO₂. On days 14 and 21 post-infection, after removing about half the culture medium in each well, the rupture of EBV-transformed cell clusters was promoted through vigorous resuspension of the cultures in order to stimulate cell proliferation. The final volume of each well was again adjusted to 2mL by adding RPMI 20% iFBS and cells were incubated at 37°C, 5% CO₂. From that moment, this procedure was performed twice a week until day 35 post-infection and, occasionally, the cultures were splitted in RPMI 20% iFBS.

The growth of virally infected cell cultures was evaluated by weekly observation under the microscope, along with its documentation through photographs. The wells still showing actively proliferating cell aggregates after 35 days of culture were considered to contain EBV-transformed B cell lines.

3.6. Flow cytometry

For studying the frequency of the major peripheral blood leukocyte populations – T cells, NK cells, B cells, and monocytes –, up to 1x10⁶ PBMCs per well were stained extracellularly in a round-bottomed 96-well plate. Upon cell addition to the wells, PBMCs were collected through a short spin at 1,200rpm for 2 minutes. After discarding the supernatant and vortexing the plate, PBMCs were resuspended in 25µL of fluorochrome-conjugated antibody/tetramer mixes diluted in PBS 0.2% BSA 0.1% NaN₃ (flow cytometry solution; see appendix) and incubated during 20 minutes, at 4°C, in the dark. The antibodies and tetramer listed in Table 3.2 were used in PBMCs flow cytometry.

Once the incubation period ended, stained PBMCs were washed three times by adding 100–200µL of flow cytometry solution, followed by centrifugation at 1,200rpm for 2 minutes, rejection of the supernatant, and resuspension of cells in the vortex. Then, PBMCs were resuspended in 400µL of PBS 1% formaldehyde (cell fixing solution; see appendix) and transferred to FACS tubes provided with a filter. The filtered PBMCs were acquired on the same day, or kept at 4°C in the dark to be acquired on the next day.

Furthermore, for the phenotypic characterization of EBV-transformed B cell lines, the extracellular staining of transformed B cells was executed on day 35 post-infection by following the experimental protocol described above and using the fluorochrome-labelled antibody mix listed in Table 3.3.

Table 3.2. Antibodies and tetramer used in flow cytometry to identify and characterize phenotypically the T cell, iNKT cell, NK cell, and B cell populations

Antibody	Clone	Fluorochrome	Brand
Anti-human CD3	SK7	PerCP-Cy5.5	eBioscience
Anti-human CD4	RPA-T4	PE-Cy7	eBioscience
Anti-human CD8	RPA-T8	APC-eFluor 780	eBioscience
Anti-human CD19	HIB19	FITC	eBioscience
Anti-human CD27	O323	PE	eBioscience
Anti-human CD45RA	MEM-56	APC	ImmunoTools
Anti-human CD56	MEM-188	FITC	eBioscience
Anti-human CD138	MI15	APC	BioLegend
Anti-human CD161	HP-3G10	eFluor 450	ImmunoTools
Anti-human CCR7	150503	FITC	R&D Systems
Anti-human IgM	MHM-88	APC	BioLegend
PBS57-loaded hCD1d tetramer	-	PE	National Institute of Health tetramer core facility

APC: allophycocyanin; APC-eFluor 780: allophycocyanin conjugated with eFluor 780; FITC: fluorescein isothiocyanate; PE: phycoerythrin; PE-Cy7: phycoerythrin conjugated with cyanin-7; PerCP-Cy5.5: peridinin-chlorophyll protein complex conjugated with cyanin-5.5.

Table 3.3. Antibodies used in flow cytometry to characterize phenotypically the EBV-transformed B cell lines

Antibody	Clone	Fluorochrome	Brand
Anti-human CD19	HIB19	PE-Cy7	eBioscience
Anti-human CD27	O323	PE	eBioscience
Anti-human IgM	MHM-88	APC	BioLegend

APC: allophycocyanin; PE: phycoerythrin; PE-Cy7: phycoerythrin conjugated with cyanin-7.

PBMCs and EBV-transformed B cells were acquired in a 3-laser BD FACSCanto™ II (BD Biosciences) flow cytometer, using the BD FACSDiva™ software (BD Biosciences). Before data acquisition, both unstained and single stained controls were analyzed to adjust the voltage of sample acquisition and compensate samples. In PBMCs flow cytometry, data acquisition was performed as follows: up to 20,000 events for B cells, up to 2,000 events for iNKT cells, and up to

10,000 events for monocytes were acquired. In the case of EBV-transformed B cell lines, up to 40,000 events were acquired inside the gate of B cells. All flow cytometry analyses were performed using the FlowJo software (Tree Star).

3.7. Cryopreservation of EBV-transformed B cell lines

EBV-transformed B cell lines were centrifuged at 1,600rpm for 5 minutes, after which up to $5\text{--}20 \times 10^6$ cells were gently resuspended in 1mL of iFBS 10% DMSO (freezing medium; see appendix) and quickly transferred to cryovials placed on ice by slowly pipetting 1mL per vial. Cells were gradually cooled by placement of the cryovials into a freezing container (Mr. Frosty®), which was stored overnight at -80°C . In the following day, the vials were moved to the liquid nitrogen tank for prolonged storage at -160°C .

3.8. Thawing of EBV-transformed B cell lines

Two cryovials containing EBV-transformed B cells (14×10^6 cells) were removed from the liquid nitrogen tank and immediately placed on a 37°C water bath. When cell suspension was completely thawed, cells were resuspended in 10mL of cold PBS 1x (see appendix) and centrifuged at 1,600rpm for 5 minutes. Upon resuspension in 5mL of RPMI 20% iFBS (see appendix), cells were transferred to a T25 culture flask and incubated at 37°C , 5% CO_2 . Cells were cultured over a week and growth documented through photographs, after which they were stored again in liquid nitrogen following the protocol described above.

3.9. Statistical analysis

All statistical analyses were performed using the GraphPad Prism 6 software. The normal distribution of each variable was determined using the Shapiro–Wilk test. For the comparison of each variable between several groups, the parametric one-way ANOVA test was applied when

variables were normally distributed, whereas the non-parametric Kruskal-Wallis test was used when variables did not follow a normal distribution. For the comparison of two analysis of a certain variable within each group, the parametric Student's *t*-test was employed when variables followed a normal distribution, while the non-parametric Mann-Whitney *U* test was utilized when variables were not normally distributed. The correlations were assessed through the parametric Pearson correlation coefficient when variables presented a normal distribution or through the non-parametric Spearman correlation coefficient when variables did not follow a normal distribution. Values of $p < 0.05$ were considered statistically significant.

CHAPTER I

*CHARACTERIZATION OF THE IMMUNE SYSTEM IN MPS II
AND MPS VI PATIENTS – MANUSCRIPT IN PREPARATION*

4. CHAPTER I – RESULTS

Most of the results concerning the characterization of the immune system in MPS II and MPS VI diseases were already available in our laboratory when I started to develop this thesis. During the time I worked in the laboratory, I completed the study of the frequency of B cell and T cell populations in some MPS II and MPS VI patients, either for the first time in the case of four of the ten MPS II patients, or as a second determination for two out of ten MPS II patients and for ten out of sixteen MPS VI patients. In addition, I contributed to the statistical analysis of the results presented hereinafter in this chapter, as well as to the writing of the respective research paper.

4.1. MPS patients and control subject characteristics

In the study on the frequency of peripheral blood leukocyte populations in MPS II and MPS VI diseases, ten male MPS II patients with a mean age of 15.4 ± 6.6 years (range: 7–28 years), as well as sixteen MPS VI patients, including eight females and eight males, with a mean age of 15.4 ± 6.1 years (range: 4–27 years) were analyzed.

In turn, the control group consisted of twenty-seven apparently healthy individuals with a mean age of 16.8 ± 7 years (range: 6–30 years), of which nine were females and eighteen were males. There is no statistically significant difference with respect to age between these control subjects and both groups of MPS patients since they were age-matched.

4.2. T cell and T cell subset frequency in MPS II and MPS VI patients

T cells are involved in the recognition of peptide and lipid antigens, constituting the mediators of cellular immune responses of the adaptive immunity. In this study, the percentage of T cells (CD3+ cells) and their two major subsets – helper T cells (CD3+CD4+ cells) and cytotoxic T cells (CD3+CD8+ cells) – was evaluated in all MPS II and MPS VI patients as well as control subjects. The gating strategy used to identify T cells and their subpopulations by flow cytometry is shown in Figure 4.1.

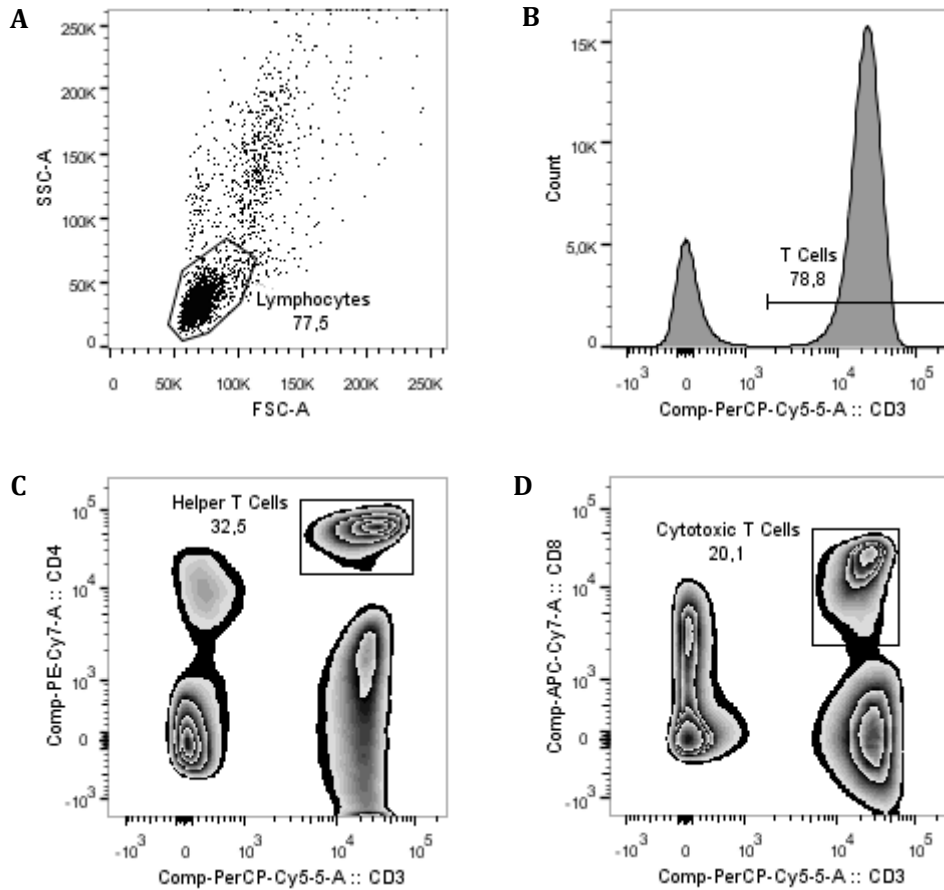


Figure 4.1. Flow cytometry analysis of T cells and T cell subsets. After creating a lymphocyte gate in a forward scatter and side scatter cytogram (A), T cells are identified as CD3-expressing lymphocytes (B). Helper T cells and cytotoxic T cells are recognized, respectively, by the expression of CD3 and CD4 (C) or CD3 and CD8 (D) surface markers inside the lymphocyte gate.

The results relative to the frequency of T cells and their two major compartments are displayed in Figure 4.2. In the MPS II and MPS VI patient groups, the percentages of total T cells (Figure 4.2-A), CD4+ helper T cells (Figure 4.2-B), and CD8+ cytotoxic T cells (Figure 4.2-C) are normal when comparing with the group of control subjects. Surprisingly, an increase of the CD4+ T cell subset (Figure 4.2-B) is observed in the case of MPS VI patients ($p=0.0333$) in comparison with MPS II patients.

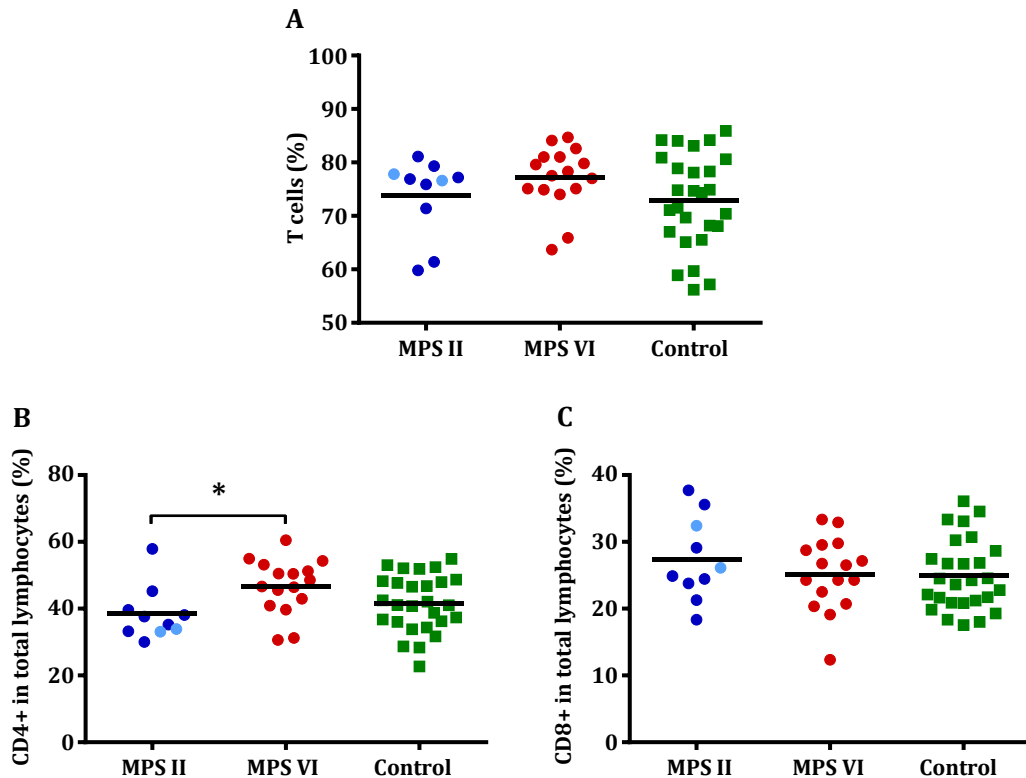


Figure 4.2. T cell and T cell subset frequency in MPS II and MPS VI patients. Frequency of (A) total T cells, (B) CD4+ T cells in total lymphocytes, and (C) CD8+ T cells in total lymphocytes. Dark blue circles represent cell frequency in MPS II patients under ERT; light blue circles represent cell frequency in untreated MPS II patients; red circles represent cell frequency in MPS VI patients under ERT; green squares represent cell frequency in control subjects; horizontal bars represent mean values. * $p < 0.05$.

Further characterization of the T cell population was performed through analysis of the naïve (CD45RA+CCR7+), effector memory (CCR7-), and central memory (CD45RA-CCR7+) phenotypes in both CD4+ and CD8+ T cell compartments. A total of five MPS II patients, all MPS VI patients, and all control subjects were studied by flow cytometry for these parameters.

The results regarding the frequency of naïve, effector memory (EM), and central memory (CM) CD4+ helper T cells and CD8+ cytotoxic T cells are represented in Figure 4.3. MPS II patients show no differences in the percentage of naïve (Figure 4.3-A,D), effector memory (Figure 4.3-B,E), and central memory (Figure 4.3-C,F) subsets in both CD4+ and CD8+ T cell populations as compared with control subjects. In the case of MPS VI patients, significant increases of naïve CD4+ T cells ($p=0.0029$) (Figure 4.3-A) and naïve CD8+ T cells ($p=0.0037$) (Figure 4.3-D), with concomitant alterations of the memory phenotypes in both CD4+ and CD8+ T cells, are seen when comparing with the control group. In particular, significant decreases of central memory CD4+ T cells ($p=0.0004$) (Figure 4.3-C) and effector memory CD8+ T cells ($p=0.03$) (Figure 4.3-E) are

identified in these patients, with normal levels of effector memory CD4+ T cells (Figure 4.3-B) and central memory CD8+ T cells (Figure 4.3-F) being found.

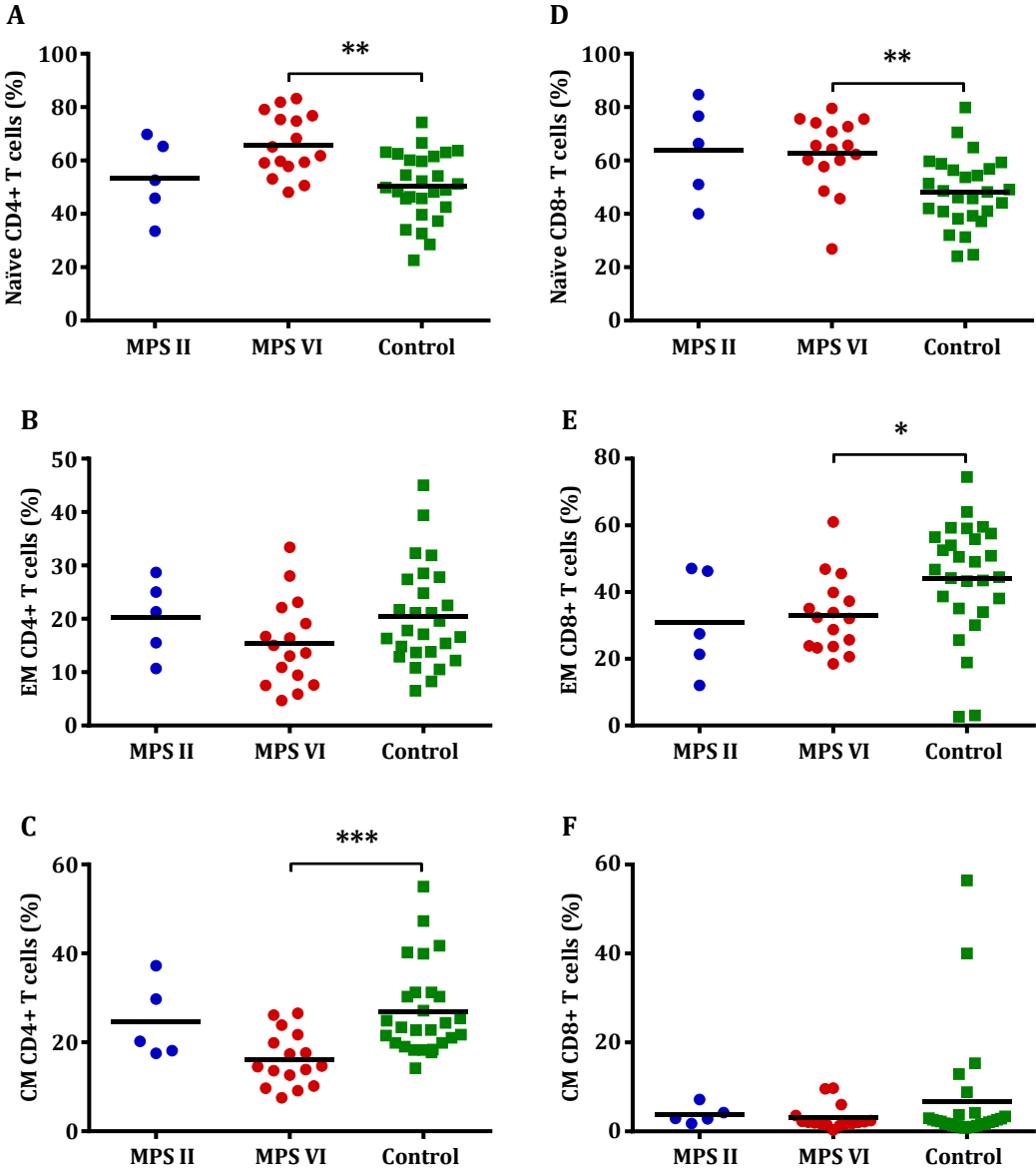


Figure 4.3. Naïve, effector memory, and central memory T cell subset frequency in MPS II and MPS VI patients. Frequency of (A) naïve cells in CD4+ T cells, (B) effector memory cells in CD4+ T cells, (C) central memory cells in CD4+ T cells, (D) naïve cells in CD8+ T cells, (E) effector memory cells in CD8+ T cells, and (F) central memory cells in CD8+ T cells. Dark blue circles represent cell frequency in MPS II patients under ERT; red circles represent cell frequency in MPS VI patients under ERT; green squares represent cell frequency in control subjects; horizontal bars represent mean values. * $p < 0.05$; ** $p < 0.01$; *** $p < 0.001$.

4.3. NK cell frequency in MPS II and MPS VI patients

NK cells are part of the innate immune system. In this work, NK cells (CD3-CD56+ cells) were also analyzed in six MPS II patients, all MPS VI patients, and all control subjects. The gating strategy used to recognize NK cells by flow cytometry is shown in Figure 4.4.

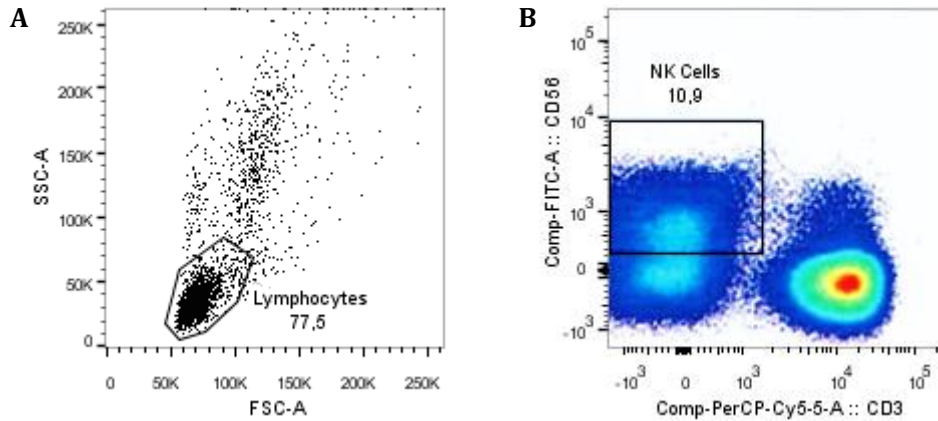


Figure 4.4. Flow cytometry analysis of NK cells. A lymphocyte gate is firstly established in a forward scatter and side scatter cytogram (A) and NK cells are then selected as CD3-CD56+ cells (B).

The results regarding the NK cell frequency are displayed in Figure 4.5. A significant decrease of the levels of NK cells is observed in MPS VI patients ($p=0.0107$) in comparison with control subjects, but no alterations are detected in MPS II patients or between the two patient groups.

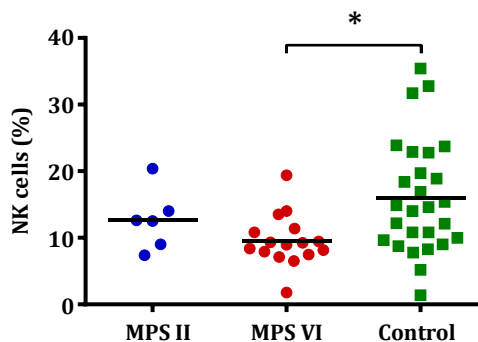


Figure 4.5. NK cell frequency in MPS II and MPS VI patients. Dark blue circles represent cell frequency in MPS II patients under ERT; red circles represent cell frequency in MPS VI patients under ERT; green squares represent cell frequency in control subjects; horizontal bars represent mean values. $*p<0.05$.

4.4. iNKT cell and iNKT cell subset frequency in MPS II and MPS VI patients

iNKT cells are involved in the recognition of lipid antigens and play a role in both innate and adaptive immunity, sharing diverse characteristics with T cells and NK cells. In this study, the percentage of iNKT cells (CD3+ PBS57-loaded hCD1d tetramer+ cells) was assessed in nine MPS II patients, all MPS VI patients, and all control subjects. Their three major subpopulations – iNKT CD4+ cells (CD4+CD8- iNKT cells), iNKT CD8+ cells (CD4-CD8+ iNKT cells), and iNKT double-negative cells (CD4-CD8- iNKT cells) – were also studied in eight MPS II patients as well as all MPS VI patients and control subjects. The gating strategy used to identify iNKT cells and their subsets by flow cytometry is described in Figure 4.6.

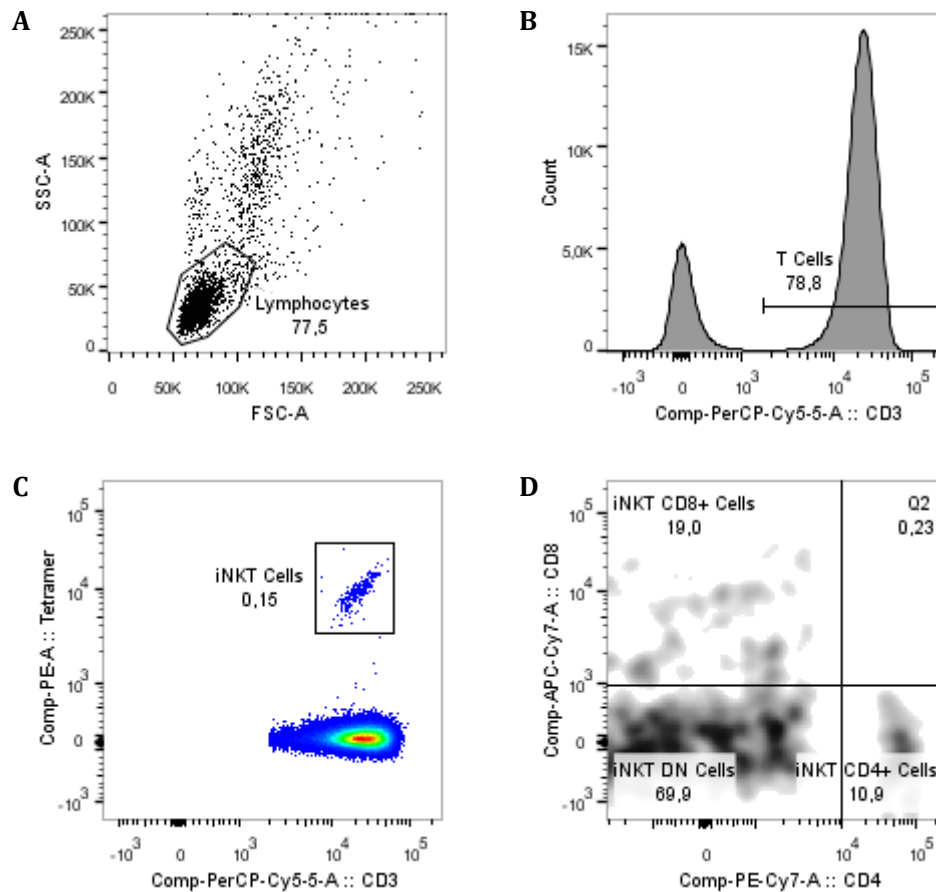


Figure 4.6. Flow cytometry analysis of iNKT cells and iNKT cell subsets. Upon definition of a lymphocyte gate in a forward scatter and side scatter cytogram (A), a second gate comprising CD3+ cells is selected (B), after which iNKT cells are identified by the expression of both CD3 marker and PBS57-loaded hCD1d tetramer (C). The subpopulations of iNKT CD4+ cells, iNKT CD8+ cells, and iNKT double-negative cells are then distinguished according to CD4 and CD8 differential expression (D).

The results relative to the frequency of iNKT cells and their compartments are presented in Figure 4.7. No differences in the iNKT cell percentage among total T cells are found between MPS II or MPS VI patients and control subjects or when comparing the two patient groups (Figure 4.7-A). In a similar way, both MPS II and MPS VI patients show normal levels of iNKT CD4+ cells (Figure 4.7-B), iNKT CD8+ cells (Figure 4.7-C), and also iNKT double-negative (DN) cells (Figure 4.7-D) as compared with the control group.

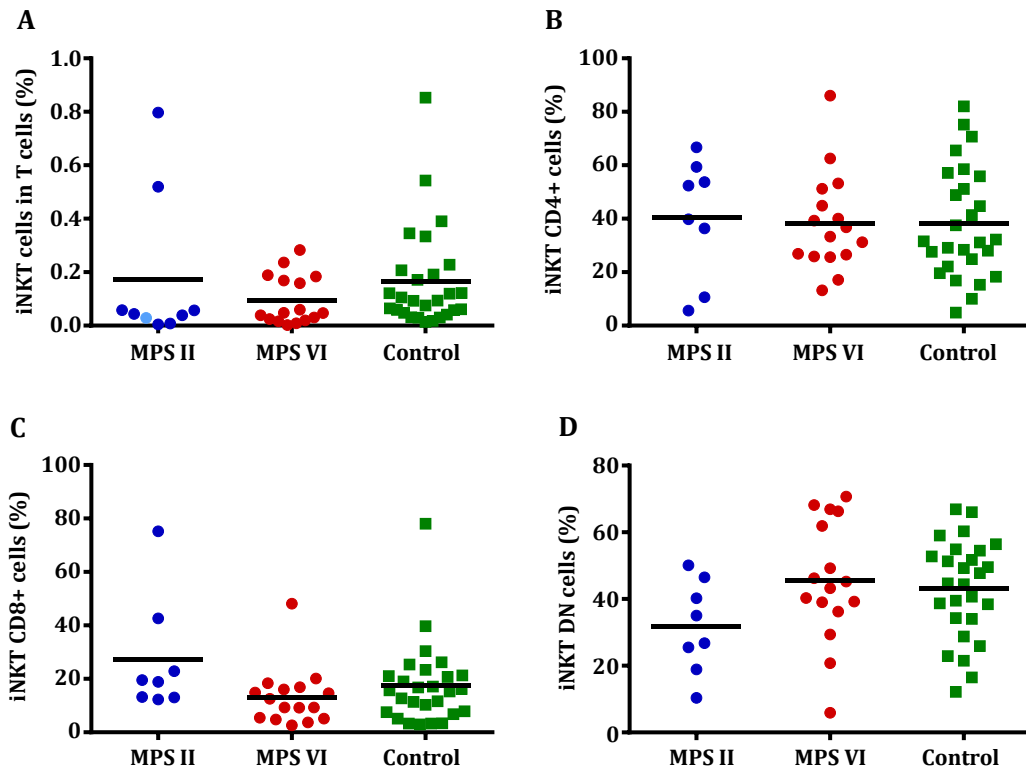


Figure 4.7. iNKT cell and iNKT cell subset frequency in MPS II and MPS VI patients. Frequency of (A) iNKT cells in total T cells, (B) CD4+CD8- cells in iNKT cells, (C) CD4-CD8+ cells in iNKT cells, and (D) CD4-CD8- cells in iNKT cells. Dark blue circles represent cell frequency in MPS II patients under ERT; the light blue circle represents cell frequency in the untreated MPS II patient; red circles represent cell frequency in MPS VI patients under ERT; green squares represent cell frequency in control subjects; horizontal bars represent mean values.

To further characterize the iNKT cells, the expression of the NK cell marker CD161 was analyzed by flow cytometry in six MPS II patients, all MPS VI patients, and twenty-six control subjects.

As shown in Figure 4.8, a significant decrease in the frequency of CD161-expressing iNKT cells is identified in MPS II patients ($p=0.0364$) and MPS VI patients ($p=0.0087$) in comparison with control subjects.

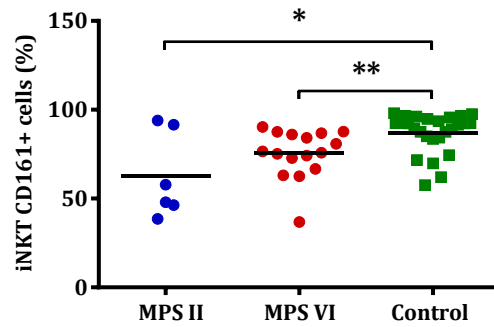


Figure 4.8. CD161-expressing iNKT cell frequency in MPS II and MPS VI patients. Dark blue circles represent cell frequency in MPS II patients under ERT; red circles represent cell frequency in MPS VI patients under ERT; green squares represent cell frequency in control subjects; horizontal bars represent mean values. * $p < 0.05$; ** $p < 0.01$.

4.5. B cell frequency in MPS II and MPS VI patients

B cells mediate humoral responses of the adaptive immune system through antibody secretion, in addition to playing a role in antigen presentation to T cells. In this work, the B cell population (CD19+ cells) was studied in all MPS II and MPS VI patients as well as control subjects. The gating strategy used to recognize B cells by flow cytometry is represented in Figure 4.9.

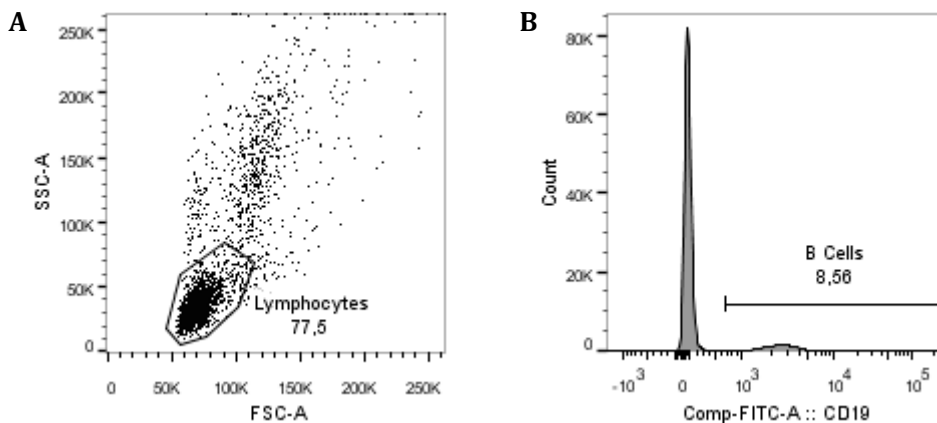


Figure 4.9. Flow cytometry analysis of B cells. A lymphocyte gate is firstly selected in a forward scatter and side scatter cytogram (A), followed by recognition of B cells as CD19-expressing lymphocytes (B).

As demonstrated in Figure 4.10, MPS II and MPS VI patients display no alterations in the B cell levels between each other or when comparing with the group of control subjects.

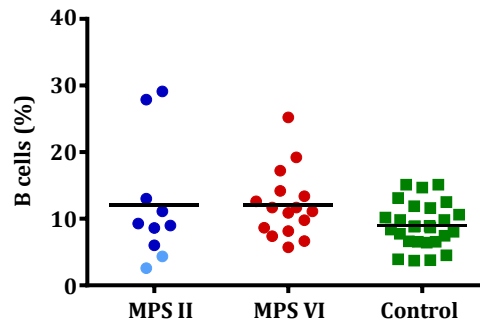


Figure 4.10. B cell frequency in MPS II and MPS VI patients. Dark blue circles represent cell frequency in MPS II patients under ERT; light blue circles represent cell frequency in untreated MPS II patients; red circles represent cell frequency in MPS VI patients under ERT; green squares represent cell frequency in control subjects; horizontal bars represent mean values.

4.6. Monocyte frequency in MPS II and MPS VI patients

Monocytes are innate immune cells important for the normal T cell function through the presentation of antigens. In this study, the percentage of monocytes was assessed in six MPS II patients, fourteen MPS VI patients, and twenty-six control subjects. The gating strategy used to identify monocytes by flow cytometry is shown in Figure 4.11.

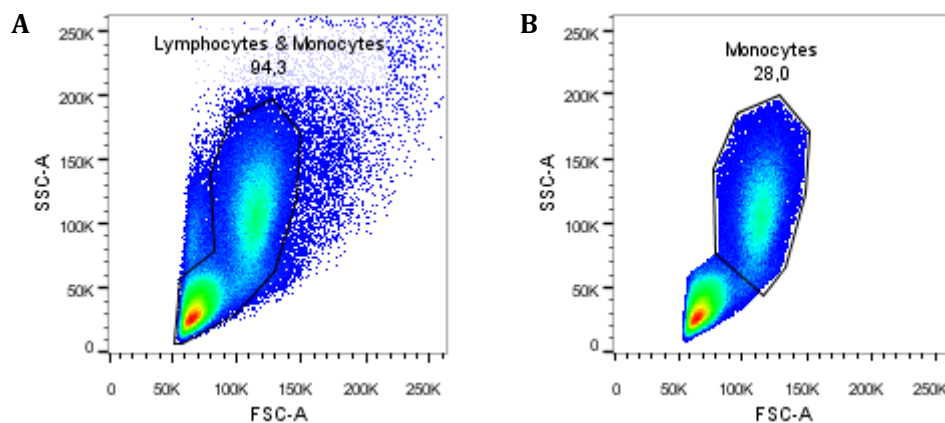


Figure 4.11. Flow cytometry analysis of monocytes. A gate comprising both lymphocytes and monocytes is firstly created in a forward scatter and side scatter cytogram (A), from which monocytes are then selected (B).

The results relative to the monocyte frequency are presented in Figure 4.12. Although normal levels are found between MPS II patients and control subjects or when comparing the two

patient groups, a significant decrease in the percentage of monocytes is observed in MPS VI patients ($p=0.0305$) as compared with control subjects.

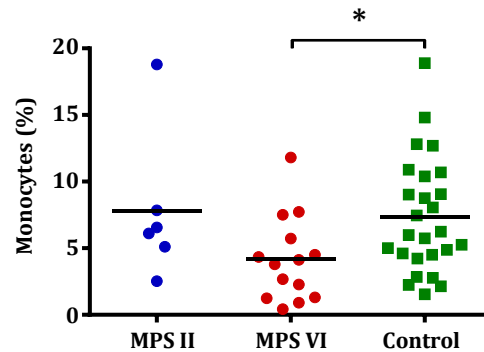


Figure 4.12. Monocyte frequency in MPS II and MPS VI patients. Dark blue circles represent cell frequency in MPS II patients under ERT; red circles represent cell frequency in MPS VI patients under ERT; green squares represent cell frequency in control subjects; horizontal bars represent mean values. $*p<0.05$.

4.7. Longitudinal study in MPS VI patients

The frequency of various peripheral blood leukocyte populations, namely B cells, T cells and their two major compartments, as well as iNKT cells, was evaluated twice, in 2012/2013 and 2015, in a total of ten MPS VI patients.

The results of this longitudinal study are displayed in Figure 4.13. There is a tendency toward a decrease in the percentage of B cells and also a trend to an increase in the levels of T cells in MPS VI patients between the two analyses. Apart from that, no significant alterations during the period between 2012/2013 and 2015 are demonstrated in regards to the CD4+ and CD8+ T cell subsets, wherein the evolution of their frequency is highly variable among the MPS VI patients, as well as in the case of iNKT cell percentage, whose values show certain stability in this group.

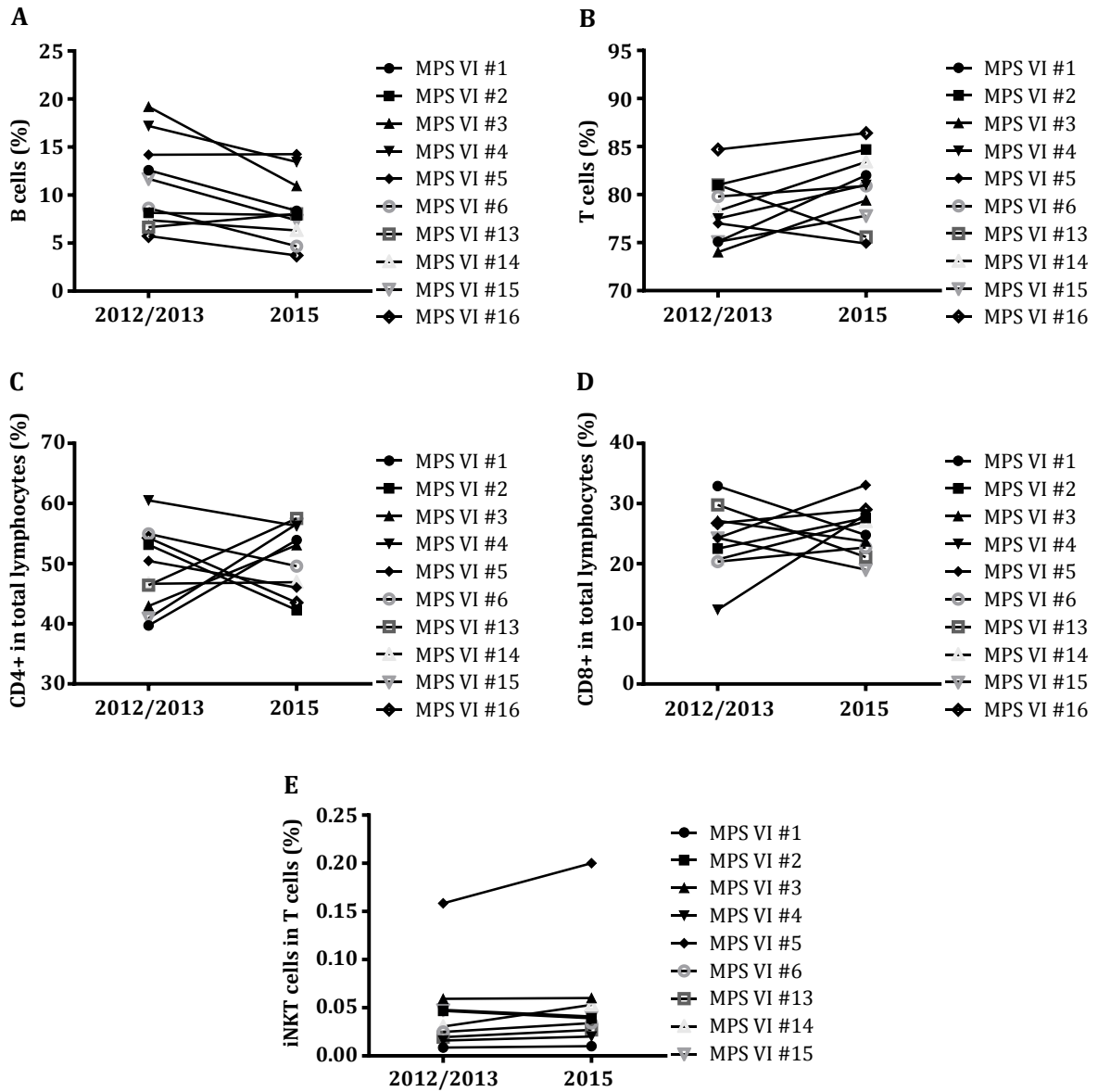


Figure 4.13. Longitudinal study of the frequency of B cells, T cells, T cell subsets, and iNKT cells in MPS VI patients. Evolution of the frequency of (A) B cells, (B) T cells, (C) CD4+ T cells in total lymphocytes, (D) CD8+ T cells in total lymphocytes, and (E) iNKT cells in total T cells in 2012/2013 and 2015 in MPS VI patients.

5. CHAPTER I – DISCUSSION

The lysosome plays a crucial role in many immune processes (e.g. antigen presentation), thus being important for the normal function of immune cells. The intralysosomal accumulation of non-degraded or partially digested macromolecular substrates that occurs in LSDs led, therefore, to the hypothesis that the immune system may potentially be altered in these diseases, either as a result of impairment of the protective immune cell processes against invading organisms or, alternatively, owing to disruption of the biology of immune cells affected by lysosomal storage. In line with this, alterations in different leukocyte populations were already reported in several LSDs; however, little is known about the immunological abnormalities in the MPS disorders, with studies in murine models and especially in humans remaining scarce up until this moment.

Herein, we analyzed the frequency of T cells and their subsets, B cells, NK cells, and monocytes in the peripheral blood of MPS II and MPS VI patients, with the main purpose of characterizing the immune system in these two diseases. The results of this study, with emphasis on the imbalances identified between MPS II or MPS VI patients and control subjects, are summed up in Table 5.1.


Table 5.1. Results of the analysis of the immune system in MPS II and MPS VI diseases


Leukocyte population	MPS II	MPS VI	Control
T cells	73.7 ± 7.4%	77.1 ± 5.8%	72.8 ± 8.8%
CD4+ T cells	38.4 ± 8.1%	46.7 ± 8.2%	41.6 ± 8.5%
Naïve CD4+ T cells	53.4 ± 14.7%	65.9 ± 11.4%	50.3 ± 12.5%
EM CD4+ T cells	20.2 ± 7.2%	15.4 ± 8.1%	20.4 ± 9.4%
CM CD4+ T cells	24.5 ± 8.6%	16.2 ± 6%	27 ± 10%
CD8+ T cells	27.4 ± 6.2%	25.2 ± 5.4%	25 ± 5.3%
Naïve CD8+ T cells	63.7 ± 18.3%	62.8 ± 13.5%	48.1 ± 13.2%
EM CD8+ T cells	30.9 ± 15.5%	33 ± 11.3%	44.2 ± 17.1%
CM CD8+ T cells	3.8 ± 2.1%	3.1 ± 2.8%	6.6 ± 12.7%
iNKT cells	0.17 ± 0.28%	0.09 ± 0.09%	0.16 ± 0.19%
iNKT CD4+ cells	40.6 ± 22.3%	38.4 ± 18.3%	38.1 ± 20.7%
iNKT CD8+ cells	27.2 ± 21.7%	13.2 ± 10.8%	17.5 ± 15.1%
iNKT DN cells	31.7 ± 13.7%	45.5 ± 18.2%	43.1 ± 14.8%
iNKT CD161+ cells	62.7 ± 24.1%	75.4 ± 13.6%	87.1 ± 11.1%

**Table 5.1. Results of the analysis of the immune system in MPS II and MPS VI diseases
(cont.)**

Leukocyte population	MPS II	MPS VI	Control
B cells	12.1 ± 9.2%	12.1 ± 5%	9 ± 3.3%
NK cells	12.7 ± 4.5%	9.6 ± 3.9%	16 ± 8.5%
Monocytes	7.8 ± 5.7%	4.2 ± 3.2%	7.4 ± 4.3%

EM: effector memory; CM: central memory; DN: double-negative.

 : increase of cell frequency as compared with control subjects.

 : decrease of cell frequency in comparison with control subjects.

5.1. T cell, B cell, NK cell, and monocyte frequency in MPS II and MPS VI patients

In the analysis of the percentage of the major peripheral blood leukocyte populations, MPS II and MPS VI patients showed normal T cell and B cell levels in comparison with control subjects, and also no differences were found between the two patient groups. The frequency of T cells was already evaluated and described as normal in other human LSDs, namely Fabry disease [36] and Niemann-Pick disease type C1 [45]. Similar results regarding the B cell percentage were previously reported in Gaucher disease [84] and Niemann-Pick disease type C1 [45] patients. In Fabry disease, however, an increase of B cells was demonstrated [40]. A prior work conducted in our laboratory did also identify higher B cell levels in MPS VI patients comparing with the control group [49], but the same result was not observed herein. Likely explanations for this discrepancy are that a larger number of MPS VI patients as well as age-matched control subjects were included in the present study, which was not possible to accomplish during the primary work carried out in the laboratory.

The two untreated MPS II patients that participated in this study were analyzed for the frequency of circulating T cell and B cell populations. Despite the fact that both individuals presented a T cell percentage near the mean value of the MPS II patient group, they also registered the two lowest B cell levels. This finding, along with the previous demonstration of the existence of disease-specific intralysosomal storage substances in B cells from MPS II patients [32], raises the question of whether ERT may have an effect on immune cell numbers, particularly on B cells.

On the other hand, in this work, a significant decrease in the frequency of NK cells and monocytes was uncovered in MPS VI patients as compared with control subjects. This defect appeared to be disease-specific since MPS II patients showed normal levels of both leukocyte populations, which led to the hypothesis that the causative mutation(s) of the LSD disorder or the lysosomal storage compound(s) might have an influence on these results. In line with this, several authors already documented alterations in these groups of immune cells in the context of other human LSDs. A decreased NK cell percentage was identified in Niemann-Pick disease type C1 [45] and Gaucher disease [84], but not in Fabry disease [40] patients. Monocytes were also shown to be reduced in Gaucher disease [85] and Fabry disease [40]. In accordance with the findings of our study, a prior report described a normal frequency of NK cells in MPS II patients [31]. The presence of disease-specific intralysosomal storage material was previously reported in monocytes from MPS VI patients [34]; thus, it is possible that a toxic effect of the accumulated GAG substrate – dermatan sulfate – conduces to significant cell morphology and function impairment, culminating in a higher apoptotic rate of these immune cells. Overall, the fact that the alterations in the peripheral blood levels of NK cells and monocytes are restricted to some LSDs suggests that lysosomal accumulation *per se* does not cause such deficiencies, but there is rather a particular negative effect of the compounds that are stored inside the lysosome or, alternatively, of the specific genetic mutation(s) leading to these disorders.

5.2. T cell subset frequency in MPS II and MPS VI patients

In terms of the frequency of the two major T cell compartments, no differences were found in helper CD4⁺ T cells and cytotoxic CD8⁺ T cells between each patient group and control subjects. Surprisingly, in the present work, an increase of CD4⁺ T cells was observed in MPS VI patients as compared with the MPS II patient group. A previous study carried out in MPS II patients revealed no abnormalities in both T cell subpopulations [31], thus being in agreement with the results presented herein. Nevertheless, the findings documented in several reports relative to other human LSDs are more variable. For instance, normal levels of CD4⁺ T cells, but a decreased percentage of CD8⁺ T cells, were detected in Fabry disease patients [40]. In the case of Gaucher disease, an increase of CD8⁺ T cells with a concomitant reduction of CD4⁺ T cells were demonstrated [43]. Another study, however, identified no alterations in the two T cell subsets in Gaucher disease, but only seven patients were analyzed [84]. The frequency of helper and cytotoxic T cells was also evaluated in various MPS murine models, wherein the results showed also certain variability among the different disorders. MPS IIIB mice were described to display an

increase of both splenic T cell compartments [47], whereas reduced levels of circulating CD4+ and CD8+ T cells were observed in MPS I mice [30], but no anomalies concerning these groups of immune cells were found in the thymus, spleen, and lymph nodes of MPS VII mice [46].

Interestingly, despite the normal frequency of the two major T cell subpopulations, the analysis of their memory status revealed significant alterations in MPS VI patients, including increases of naïve with concomitant decreases of memory CD4+ and CD8+ T cells in comparison with control subjects. Importantly, these abnormalities cannot be attributed to age differences between the two groups of individuals, given that they were age-matched. Similarly, a study performed in the MPS I mouse model did also identify a reduction in the percentage of peripheral blood memory CD4+ T cells [30]. In Gaucher disease patients, a reduction of naïve CD4+ T cells and an increase of memory CD4+ T cells were already documented, along with normal levels of both phenotypes within the CD8+ T cell subset [84].

Also in the present work, MPS II patients did not show anomalies in the memory state of both helper and cytotoxic T cells when comparing with control subjects. Although these results can be explained by the accumulation of different types of substrate inside the lysosome, it is also possible that the absence of significant alterations in the MPS II patient group is related to the small number of individuals that were analyzed for these parameters in our study (five MPS II patients *versus* sixteen MPS VI patients).

5.3. iNKT cell and iNKT cell subset frequency in MPS II and MPS VI patients

The analysis of the iNKT cell percentage within the T cell population demonstrated no differences between MPS II and MPS VI patients or when comparing each patient group with control subjects. In a similar way, normal iNKT cell levels were described in previous studies carried out in Fabry disease [36,40,41], Gaucher disease [43], and Niemann-Pick disease type C1 [44] patients. Given that the frequency of iNKT cells in the peripheral blood is highly variable among the general human population, the detection of smaller alterations between patients and healthy subjects may be difficult to accomplish.

Although both untreated MPS II patients included in this work were also analyzed for this parameter by flow cytometry, it was only possible to assess the percentage of iNKT cells in one of them, due to the corresponding reduced number of events that were acquired from the sample of

the second individual. In the case of the untreated patient for whom the iNKT cell levels were determined, one of the lowest values in the MPS II patient group was observed. Even though it was not possible to evaluate the effect of ERT on the iNKT cell frequency in MPS II patients, owing to the limited availability of untreated patients that could be included in our study, ERT was already shown to partially correct a deficiency of iNKT cells found in the Fabry disease mouse model [86]. In that report, ERT caused not only a decrease in the intralysosomal storage of macromolecular substrate in the spleen and liver of Fabry disease mice, but also an increase in the frequency of splenic iNKT cells, in particular of the iNKT CD4+ cell subset, thus preventing the reduction in iNKT cell levels that occurs with age in untreated mice [86].

Furthermore, in the present work, the percentage of iNKT cells expressing CD4, CD8, or none of the surface markers was not significantly altered in MPS II and MPS VI patients as compared with control subjects or between the two patient groups. Despite the absence of abnormalities in the frequency of total iNKT cells, a prior study conducted in Fabry disease patients demonstrated alterations in the composition of iNKT cell compartments, including an increase of iNKT double-negative cells with a concomitant reduction of iNKT CD4+ cells [41]. In agreement with the results reported herein, no differences were detected in Niemann-Pick disease type C1 patients with respect to the CD4 and CD8 status of the iNKT cell population [44].

Interestingly, both groups of MPS II and MPS VI patients presented a decrease in the expression of the NK cell marker CD161 in iNKT cells when comparing with control subjects. On the contrary, normal levels of CD161-expressing iNKT cells were documented in Niemann-Pick disease type C1 patients [44].

5.4. Longitudinal study in MPS VI patients

Ten out of sixteen MPS VI patients under ERT were analyzed twice over a period of 2–3 years with respect to the frequency of T cells and their two major subpopulations, as well as B cells and iNKT cells.

Between these two determinations, an overall slight increase of T cells was observed in eight MPS VI patients. This, however, does not appear to be associated with a specific T cell

compartment, since some patients displayed predominantly an increment of CD4+ helper T cell levels whereas others presented mostly an increased percentage of CD8+ cytotoxic T cells. Previous studies described that the relative frequency of T cells within the lymphocyte population shows certain stability from the first months of life until early adulthood, ranging between median narrow limits of 62–73% in healthy human subjects [87,88]. Similarly, the percentage of the CD4+ and CD8+ T cell subsets tends to vary slightly with age, with mean values oscillating from 35% to 55% and from 16% to 28%, respectively [87,88]. Therefore, the small increase of T cell levels identified in MPS VI patients between 2012/2013 and 2015, as well as the variations detected in CD4+ and CD8+ T cells are within the standard value ranges and can be considered as normal limited fluctuations that are typically registered over time, from neonates until young adults.

In regards to the evolution of B cell frequency, a tendency toward a decrease between the two analyses was detected in eight MPS VI patients. Interestingly, the only two cases wherein B cell levels increased over time – MPS VI patients #5 and #13 – correspond also to both individuals whose percentage of T cells was exceptionally reduced. Age-associated alterations in the B cell population were already described in healthy human subjects, in which the relative frequency of B cells generally duplicates from a median of 12% to 24% during the first months of life, then stabilizes until 5 years of age, after which a gradual decrease to approximately 13–15% occurs until early in adult life [87,88]. Although lower levels of B cells were reported in the present work, the slight reduction herein identified in this cellular compartment constitutes an expected result considering that most MPS VI patients were analyzed in the period between adolescence and young adulthood.

With respect to the percentage of iNKT cells within the total T cell population, MPS VI patients showed relatively similar values in 2012/2013 and 2015. In agreement with these findings, prior longitudinal studies carried out in MPS VI [49] and Fabry disease [89] patients under ERT also documented the absence of significant alterations in the iNKT cell frequency over time. A previous report, however, described a slight increase of iNKT cells with age in healthy young individuals [90]. Nevertheless, the interpretation of such results is hampered by the wide variability of iNKT cell levels in human peripheral blood.

The fact that all MPS VI patients included in this study were already under ERT for several years at the time that the first analysis was performed in our laboratory, together with the findings that they presented normal variations in the levels of immune cell populations that are

associated with increasing age, raises the question of whether ERT may have an influence on these results. Therefore, the longitudinal analysis of untreated MPS VI patients would be crucial to answer this question.

CHAPTER II

***PRODUCTION AND CHARACTERIZATION OF
EBV-TRANSFORMED B CELL LINES FROM
MPS II AND MPS VI PATIENTS***

6. CHAPTER II – RESULTS

In the study concerning the generation and phenotypic characterization of EBV-transformed B cell lines that was developed during the period of my thesis, I implemented the respective protocols in the laboratory, executed all the experimental activities, and performed the analysis of all the results presented hereafter in this chapter.

6.1. *MPS patients and control subject characteristics*

For the production of EBV-transformed B cell lines, five male MPS II patients with a mean age of 13 ± 3.4 years (range: 9–17 years) and five MPS VI patients with a mean age of 15.2 ± 4.7 years (range: 8–21 years), which comprised one female and four males, were analyzed.

The control group, on the other hand, was composed of nine apparently healthy adult subjects, including six females and three males, with a mean age of 32 ± 5.2 years (range: 26–41 years).

6.2. *Efficacy in the production of EBV-transformed B cell lines from MPS II and MPS VI patients*

Before the generation of EBV-transformed B cell lines from MPS II and MPS VI patients, a preliminary work was conducted to produce EBV virions and implement in our laboratory the protocol for the transformation of human B cells by EBV; this implementation was based on standard protocols [91–93]. This primary work allowed the optimization of some experimental conditions, such as the optimal amount of EBV-containing supernatant that should be used according to the stock of EBV virions that was produced, the proper concentration of cyclosporine A, and the minimum time necessary for the formation of large cell aggregates.

To induce B cell transformation *in vitro*, PBMCs isolated from peripheral blood samples were incubated with EBV virions and, after a period of 35 days of culture that enabled sufficient

cell growth, infected cells were analyzed by flow cytometry. From a total of nineteen individuals for whom this protocol was applied, the production of EBV-transformed B cell lines was successful in all but one of those cases. In the case wherein the B cell transformation failed, the number of PBMCs available for the process of EBV infection was very low (1×10^6 PBMCs); this was the case of MPS II patient #9, in which a marked decrease in cell number occurred during the first two weeks after infection, rather than the expansion of cells into actively proliferating cultures.

The development of EBV-transformed B cell lines was regularly monitored, being documented through weekly photographs, until day 35 post-infection, when cryopreservation and phenotypic characterization were performed. According to what has been described, small clusters of infected B cells in suspension are generally visible under the microscope within the first week of culture, which typically exhibit rosette morphology and are composed of cells with increased size [78,92,94], as demonstrated in Figure 6.1. Between the days 14 and 21 after infection, the growth of microscopic colonies usually starts to evolve exponentially and, as time progresses, large cell clumps become visible macroscopically [92,94].

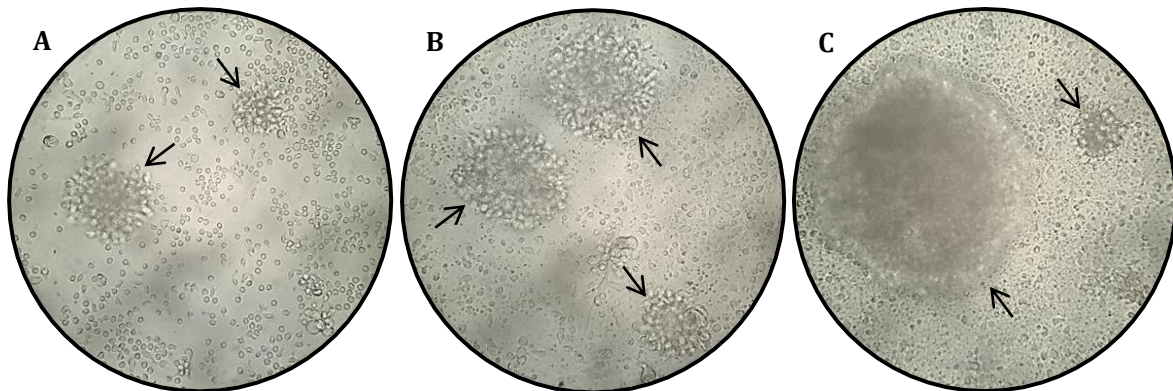


Figure 6.1. EBV-infected B cell clusters. Microscopic appearance on (A) day 7 post-infection, (B) day 21 post-infection, and (C) day 35 post-infection. EBV-transformed B cell aggregates are identified by the arrows. Magnification: 400x.

Based on the weekly microscopic observation of cell cultures from control subjects, the growth rate of infected cells revealed high variability between individuals, particularly since the third week of culture. In general, the evolution of cell clusters was similar between the various cultures until day 21 post-infection; from this moment, however, while some cultures exhibited an exponential proliferation, others were more slowly progressing. This was assessed by the size and

number of cell aggregates, as shown in Figure 6.2, and also by taking into account the frequency with which the medium needed to be changed and the culture splitting had to be performed. In three cultures whose development was less pronounced since the third week after infection, the presence of adherent cells may have slowed down the growth of cell clusters. Even though it partially increased after several changes of cell clumps in suspension into new wells of the culture plate, these cell aggregates did not reach the same proliferative capacity until day 35 post-infection as observed in the cultures wherein there were no adherent cells.

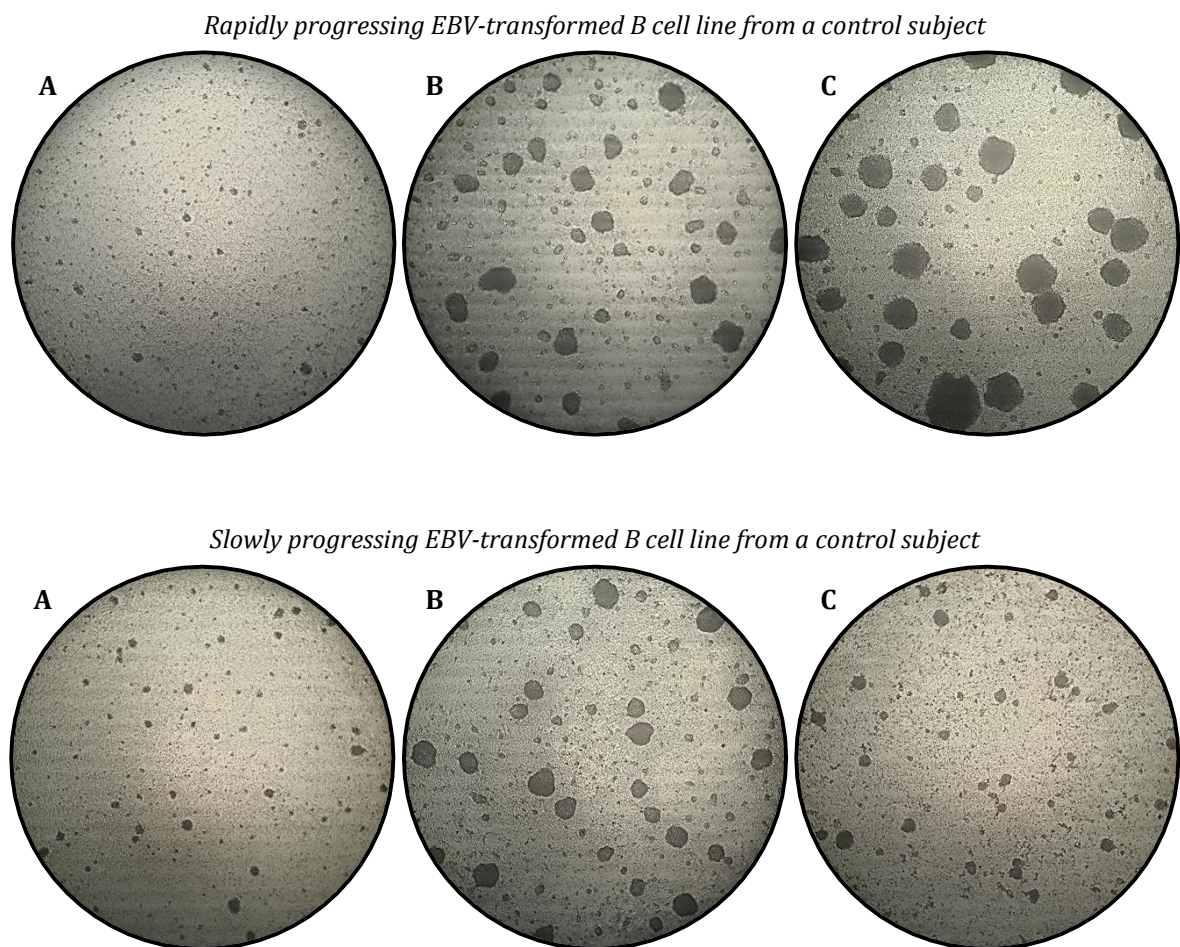


Figure 6.2. Growth progression of EBV-transformed B cell lines from two control subjects. Microscopic appearance on (A) day 7 post-infection, (B) day 21 post-infection, and (C) day 35 post-infection. Dark agglomerates represent clusters of EBV-infected B cells. Magnification: 40x.

In the case of all four MPS II patients, the development of cell clusters was initially hampered after the appearing of many adherent cells, typically during the second or third weeks upon infection. The presence of such large number of adherent cells in the culture was always

associated with a lower proliferation rate of the infected cells. Even so, the growth of cell aggregates was, in general, recovered after applying the same technique of successive changes of cells in suspension into new wells of the culture plate, although not with the same degree in all cultures. In this way, some exhibited a significant improvement of their development, as evidenced by increased splitting and changes of the medium, as well as the size and number of cell clumps; in contrast, other cultures did not follow the same positive growth evolution until day 35 post-infection, as represented in Figure 6.3. When comparing MPS II patients with control subjects, the variability registered in the global proliferation of cell cultures – in which some were slowly progressing and others actively proliferating – seems to indicate similar outcomes in these two groups in regards to the production of EBV-transformed B cell lines.

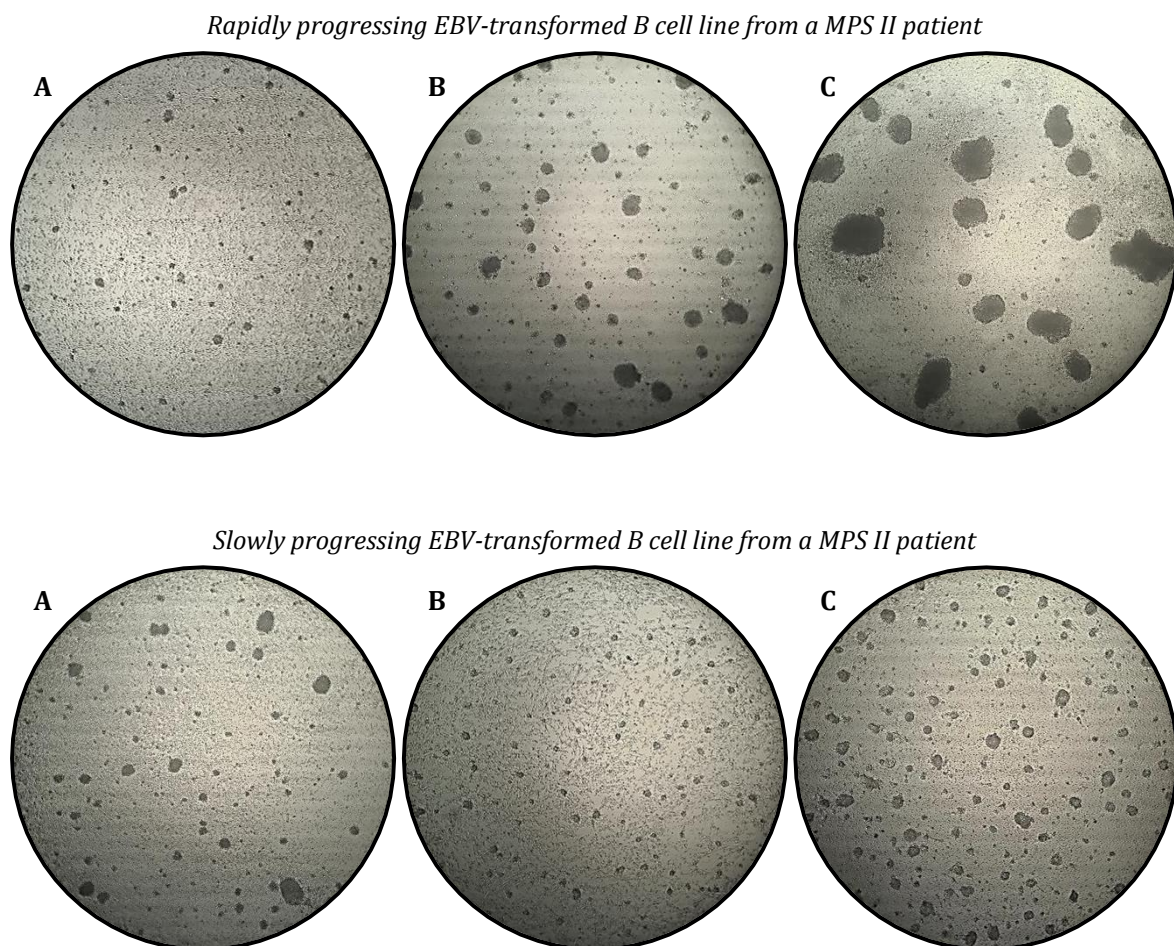


Figure 6.3. Growth progression of EBV-transformed B cell lines from two MPS II patients. Microscopic appearance on (A) day 7 post-infection, (B) day 21 post-infection, and (C) day 35 post-infection. Dark agglomerates represent clusters of EBV-infected B cells. Magnification: 40x.

In the group of MPS VI patients, a total of four out of five cell cultures presented a higher growth rate than in the overall cases of MPS II patients and control subjects, considering not only the presence of many large cell colonies clearly observed since the third week after infection, but also the number of times that the cultures had to be splitted due to increased cell density. The exceptional case was MPS VI patient #6, in which the initial development of cell clusters was significantly hindered in the presence of many adherent cells in the culture. Even though the procedure of transferring the cell aggregates in suspension into new wells of the culture plate was also applied, the growth of infected cells did not register a great improvement until day 35 post-infection, as evidenced by the reduced frequency with which the medium had to be changed. The evolution of the growth of an EBV-transformed B cell line from one of these four MPS VI patients, whose production was achieved without registering any problem, as well as of the EBV-transformed B cell line from MPS VI patient #6 is shown in Figure 6.4.

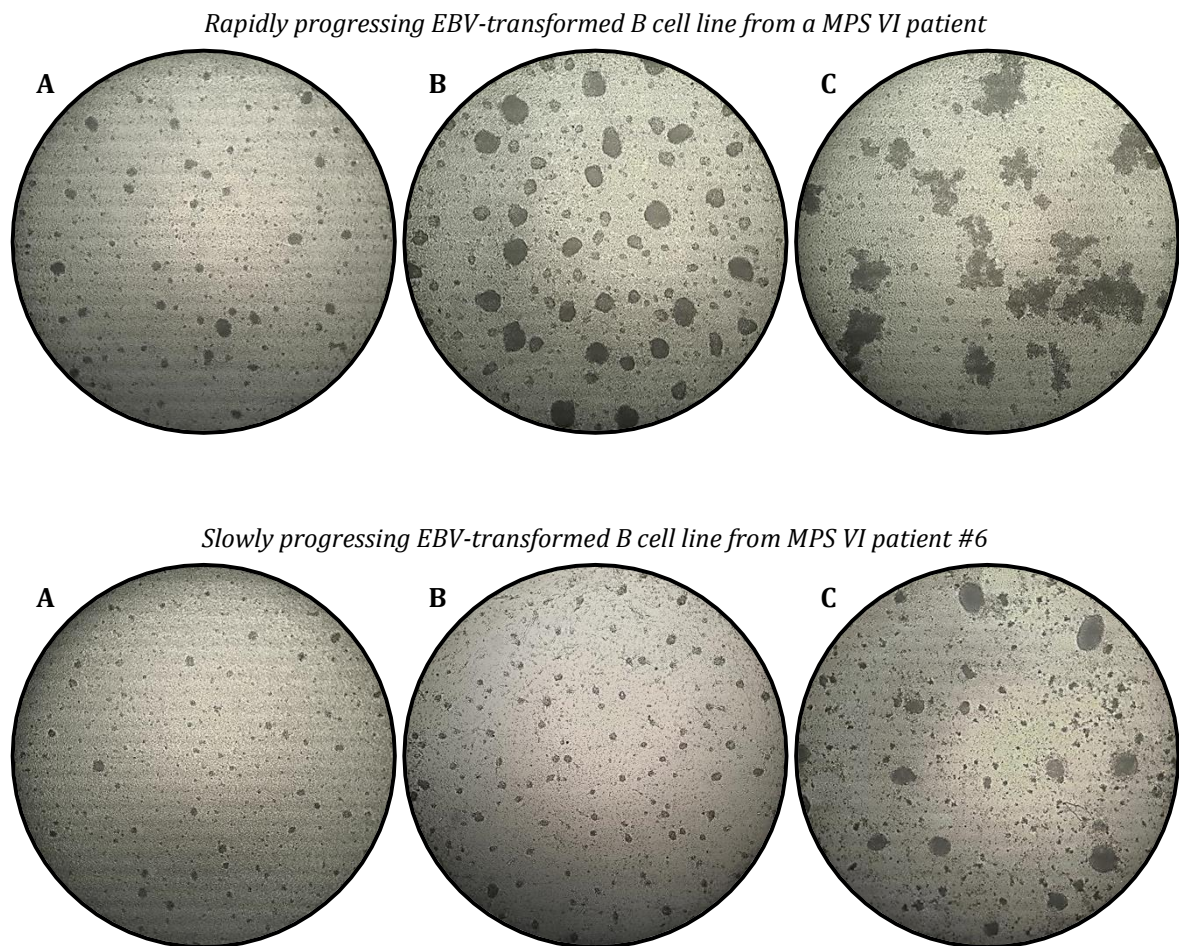


Figure 6.4. Growth progression of EBV-transformed B cell lines from two MPS VI patients. Microscopic appearance on (A) day 7 post-infection, (B) day 21 post-infection, and (C) day 35 post-infection. Dark agglomerates represent clusters of EBV-infected B cells. Magnification: 40x.

In addition to the regular monitoring of their development, the successful generation of EBV-transformed B cell lines was tested by thawing the cryopreserved cells from one MPS VI patient as well as one control subject and putting them back in culture during one week. The results confirmed the cell viability and the high proliferation rate of EBV-transformed B cell lines.

The efficacy in the production of EBV-transformed B cell lines was also evaluated by taking into consideration the B cell percentage before and after viral transformation. A first determination of the frequency of B cells, identified as CD19+ lymphocytes, was performed by flow cytometry using PBMCs prior to incubation with EBV. A second flow cytometry analysis was carried out using EBV-infected cells after 35 days of culture. Both parameters were assessed in all individuals for whom the EBV-transformed B cell lines were successfully generated. However, in the case of the first control subject analyzed in this work, the intensity of the fluorescence signal of CD19+ cells in the EBV-transformed B cell line sample, which were exceptionally stained with fluorescein isothiocyanate (FITC)-labelled anti-human CD19 antibody, was very low; thus, the data from control subject #1 will not be considered in the following analyses.

The results concerning the B cell frequency within PBMCs prior to viral transformation (day 0, D0) and in EBV-transformed B cell lines following 35 days of culture (day 35, D35) are presented in Figure 6.5. As described in Chapter I, MPS II and MPS VI patients do not show alterations in the B cell population in comparison with control subjects. In both patient groups for whom the EBV-transformed B cell lines were produced, normal B cell levels are also detected before EBV infection (Figure 6.5-A), being in accordance with the previous result.

Similarly, no differences in the frequency of B cells in EBV-transformed B cell lines are observed when MPS II and MPS VI patients are compared with control subjects or between the two patient groups (Figure 6.5-B). Surprisingly, for three control subjects, the percentage of B cells upon viral transformation is less than 50%, despite the general similar appearance, although exhibiting smaller cell clusters, of the infected cell cultures from these individuals comparing with those from the remaining control subjects.

As expected, the B cell frequency increases after EBV-induced transformation when compared with the corresponding samples of PBMCs before viral infection ($p=0.0286$, $p=0.0079$, and $p=0.0006$ in the groups of MPS II patients, MPS VI patients, and control subjects, respectively) (Figure 6.5-C), thus confirming the global successful generation of EBV-transformed B cell lines.

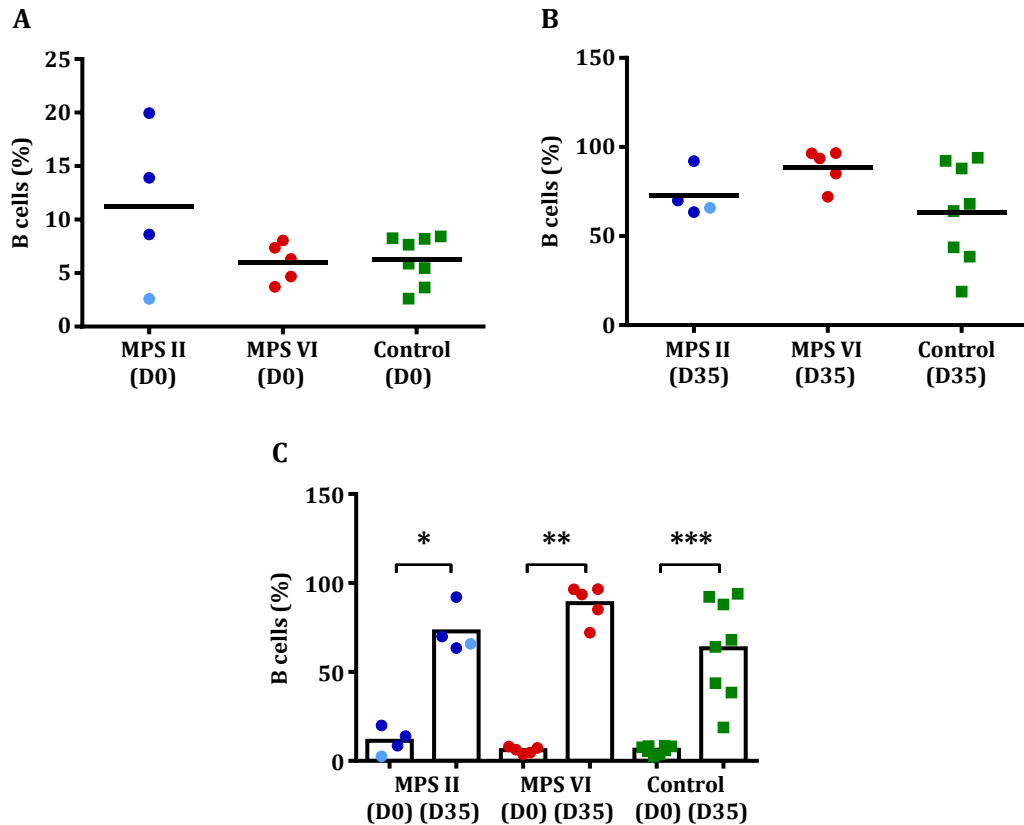


Figure 6.5. B cell frequency before and after EBV-induced transformation of B cells in MPS II and MPS VI patients. (A) B cell frequency before viral transformation; (B) B cell frequency after viral transformation; (C) Comparison between the B cell frequency before (D0) and after (D35) viral transformation. Dark blue circles represent cell frequency in MPS II patients under ERT; the light blue circle represents cell frequency in the untreated MPS II patient; red circles represent cell frequency in MPS VI patients under ERT; green squares represent cell frequency in control subjects; horizontal and vertical bars represent mean values. * $p < 0.05$; ** $p < 0.01$; *** $p < 0.001$.

To investigate whether the B cell percentage prior to the transformation process may have any influence on the levels of B cells obtained after producing the EBV-transformed B cell lines, the evolution of B cell frequency between day 0 (D0) and day 35 post-infection (D35) was analyzed for each individual.

The results shown in Figure 6.6 indicate that the efficacy in the generation of EBV-transformed B cell lines cannot be predicted based on the percentage of B cells within the PBMC samples used for viral infection. This can be demonstrated, for instance, by the cases of MPS II patient #7 (Figure 6.6–A) and control subject #7 (Figure 6.6–C), in which both individuals display similar B cell levels on day 0 (8.6% and 8.2%, respectively), but clearly present different outcomes with respect to the frequency of B cells after viral transformation (92% and 18.8%, respectively).

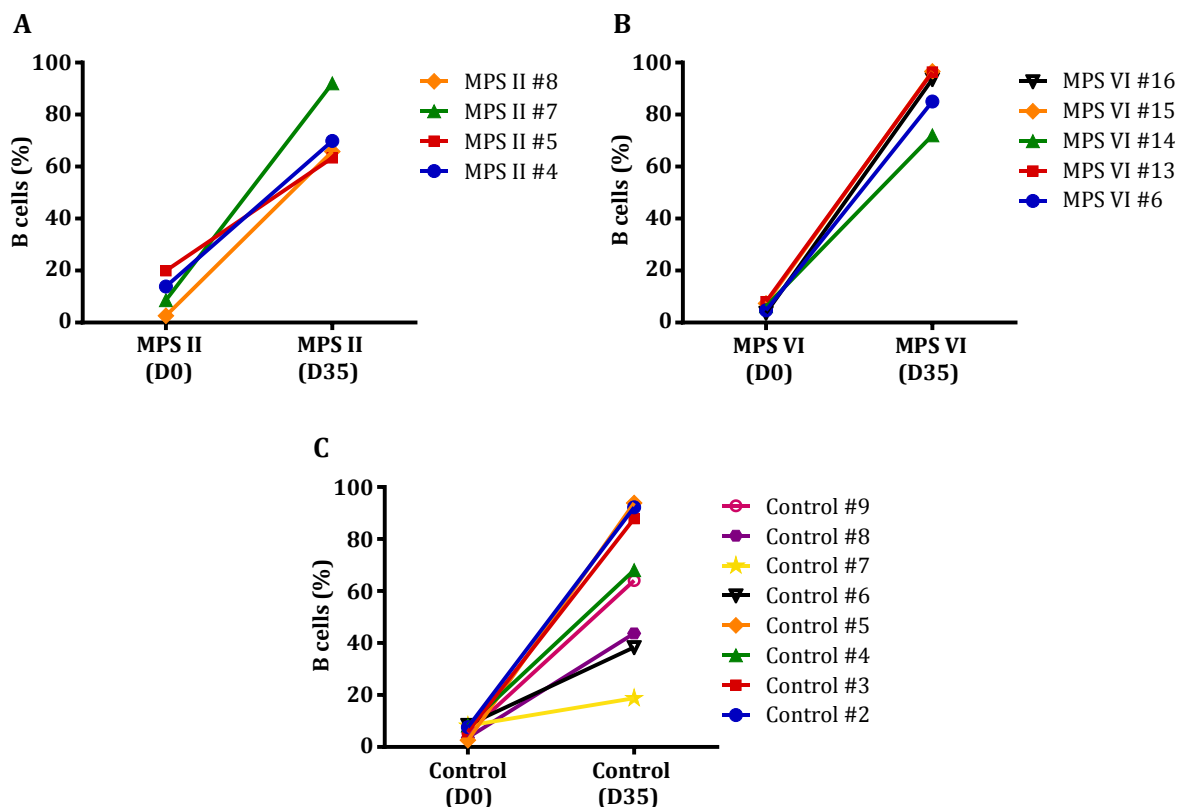


Figure 6.6. Evolution of B cell frequency before and after EBV-induced transformation of B cells in MPS II and MPS VI patients. Evolution of B cell frequency in (A) MPS II patients, (B) MPS VI patients, and (C) control subjects before (D0) and after (D35) viral transformation.

To further assess the efficacy in the production of EBV-transformed B cell lines, the ratio of B cell expansion was calculated by dividing the number of B cells in culture on day 35 after infection by the number of B cells that were initially infected by EBV.

According to the results represented in Figure 6.7, it is evident that, in the three groups, there is a considerable expansion of the original B cell population owing to the generation of EBV-transformed B cell lines. As expected taking into account the microscopic observation of the growth of cell cultures, the MPS VI patient group exhibits the greatest increase in the number of B cells acquired after the transformation process (mean ratio: 35.1 ± 27.8), while the groups of MPS II patients and control subjects register a similar, although slightly lower, progress (mean ratios: 11.2 ± 10.8 and 17.8 ± 26 , respectively). In all groups, there are one or more cases wherein the B cell expansion between day 0 and day 35 post-infection is less pronounced, which correspond to the cultures of infected cells whose proliferation was affected after the appearing of adherent cells. Of these, the cases of two control subjects, in which the ratio of B cell numbers between the two time points is lower than 1, reflect the difficulty in the development of EBV-transformed B cell lines from these individuals, related with the presence of adherent cells in the culture. Despite the

low number of B cells that was obtained, the cultures from these two control subjects showed signs of B cell transformation, although there were clearly less and smaller cell clusters on day 35 upon infection when compared with the cultures wherein no adherent cells emerged.

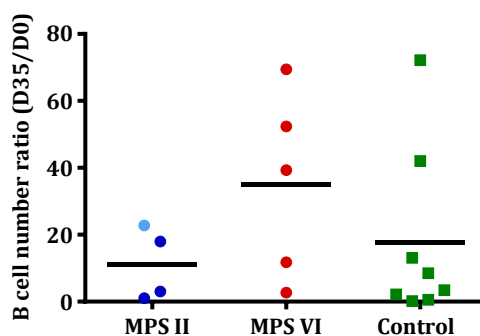


Figure 6.7. B cell expansion after EBV-induced transformation of B cells in MPS II and MPS VI patients. Dark blue circles represent B cell number ratio in MPS II patients under ERT; the light blue circle represents B cell number ratio in the untreated MPS II patient; red circles represent B cell number ratio in MPS VI patients under ERT; green squares represent B cell number ratio in control subjects; horizontal bars represent mean values.

The frequency of B cells before EBV-mediated transformation was correlated with the ratio of B cell expansion between day 0 and day 35 post-infection. In all groups, no significant correlations were found between the two parameters (Spearman correlation coefficients: $r=-1$, $r=0.6$, and $r=-0.64$ in MPS II patients, MPS VI patients, and control subjects, respectively). These results confirm that the B cell percentage in PBMC samples used in EBV infection does not predict and is not a determinant factor of the growth evolution of EBV-transformed B cell lines.

6.3. Phenotype of EBV-transformed B cell lines from MPS II and MPS VI patients

Following 35 days of culture of the infected B cells, the phenotypic characterization of EBV-transformed B cell lines was performed by flow cytometry. For this purpose, four phenotypes were defined based on the differential expression of IgM and CD27 surface markers in CD19+ B cells: naïve (IgM+CD27-), IgM memory (IgM+CD27+), double-negative memory (IgM-CD27-), and switched memory (IgM-CD27+) B cells. This analysis was carried out in two MPS II patients, three MPS VI patients, and four control subjects. The gating strategy used to identify the B cell subsets by flow cytometry is represented in Figure 6.8.

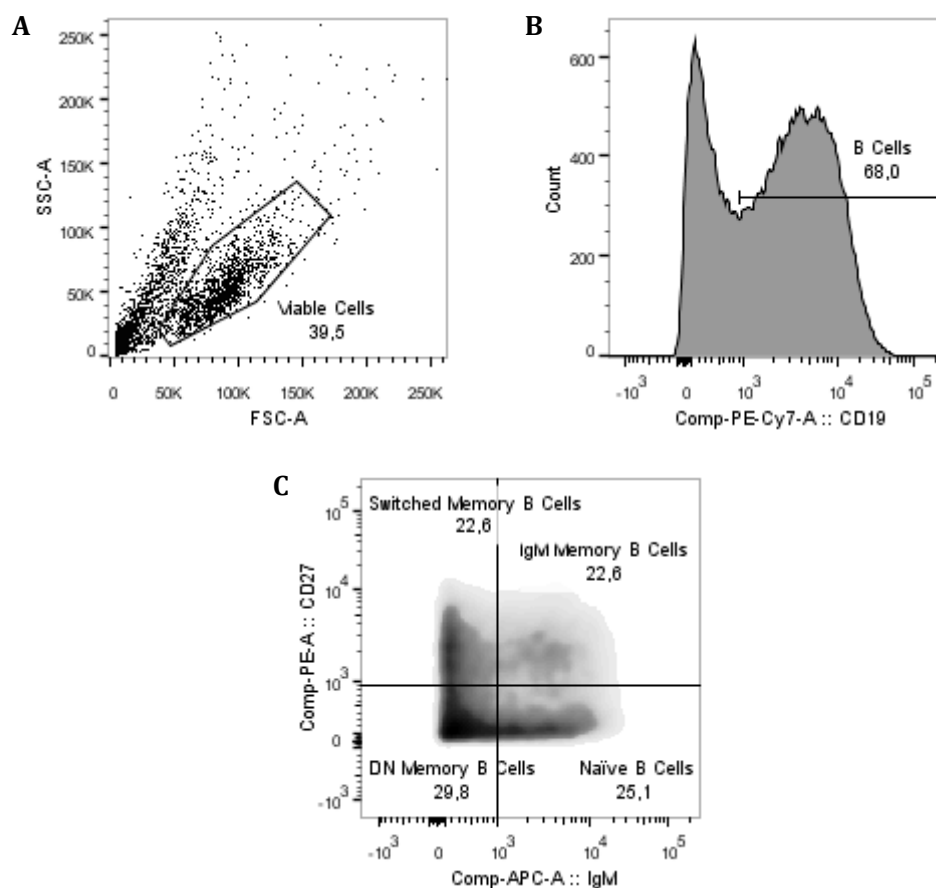


Figure 6.8. Flow cytometry analysis of B cell subsets. A gate comprising viable cells is firstly defined in a forward scatter and side scatter cytogram (A), after which B cells are recognized as CD19+ cells (B). B cell subsets are then distinguished according to IgM and CD27 differential expression within the B cell gate (C).

The results regarding the relative frequency of each B cell subpopulation in the EBV-transformed B cell lines are displayed in Figure 6.9. In all groups, the predominant phenotype of EBV-transformed B cells is that corresponding to double-negative (DN) memory B cells, whose percentage is especially high in MPS VI patients (mean value: $63.6 \pm 10.1\%$), followed by MPS II patients (mean value: $55.4 \pm 7.8\%$) and control subjects (mean value: $44 \pm 23.1\%$) (Figure 6.9-C). With respect to the other phenotypes that characterize the EBV-transformed B cell lines, naïve B cells constitute the second subset more frequent in the three groups (Figure 6.9-A), with IgM memory B cells (Figure 6.9-B) and switched memory B cells (Figure 6.9-D) presenting lower levels. As expected, no alterations are identified in the EBV-transformed B cell lines between the two patient groups or when comparing MPS II and MPS VI patients with control subjects, in relation to the percentage of the various B cell subpopulations.

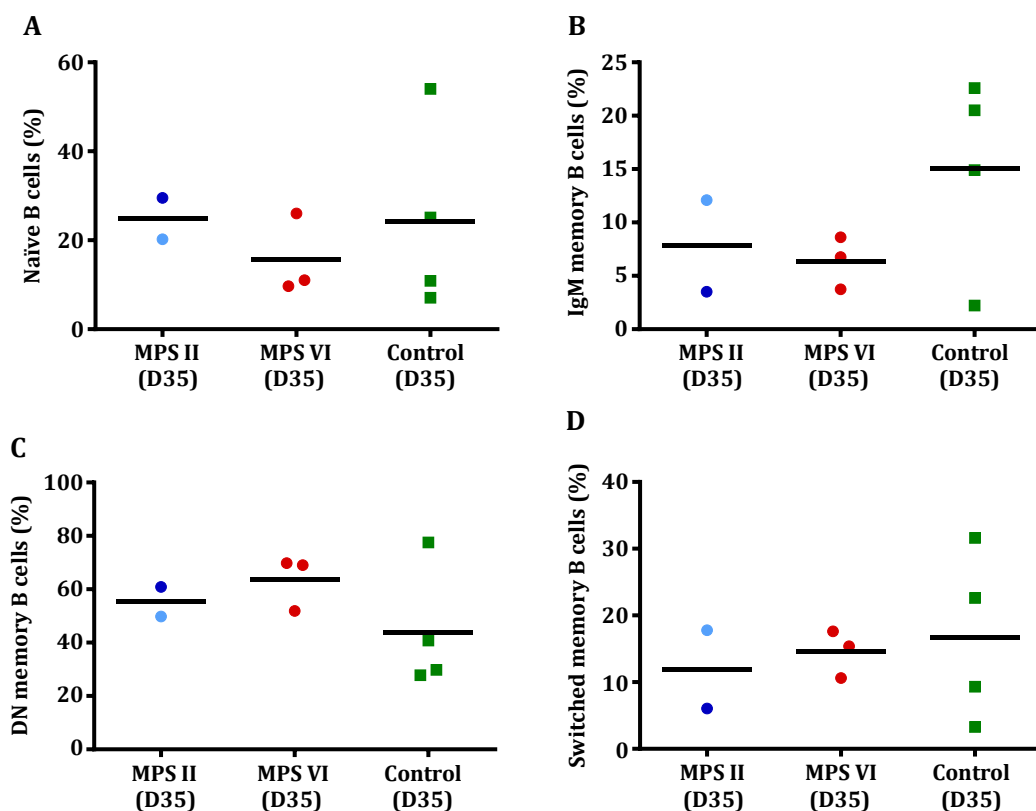


Figure 6.9. B cell subset frequency in EBV-transformed B cell lines from MPS II and MPS VI patients. Frequency of (A) naïve B cells, (B) IgM memory B cells, (C) double-negative memory B cells, and (D) switched memory B cells after viral transformation. The dark blue circle represents cell frequency in the MPS II patient under ERT; the light blue circle represents cell frequency in the untreated MPS II patient; red circles represent cell frequency in MPS VI patients under ERT; green squares represent cell frequency in control subjects; horizontal bars represent mean values.

The B cell subsets within PBMCs were evaluated by flow cytometry prior to EBV infection. In addition to the four B cell compartments distinguished according to IgM and CD27 differential expression, plasma B cells were also identified as CD138-expressing B cells. These parameters were studied in four MPS II patients, all MPS VI patients, and eight control subjects.

The results concerning the relative frequency of each B cell phenotype in the samples of PBMCs before viral transformation are described in Figure 6.10. In the three groups, naïve B cells present the highest percentage in the B cell population, showing similar levels between MPS II patients (mean value: $62.4 \pm 23.3\%$) and MPS VI patients (mean value: $60.6 \pm 12.7\%$), with control subjects displaying slightly lower numbers (mean value: $47.3 \pm 19.3\%$) (Figure 6.10-A). In terms of the other B cell subsets, IgM memory B cells (Figure 6.10-B) and switched memory B cells (Figure 6.10-D) present intermediary frequencies in all groups, whereas double-negative (DN) memory B cells (Figure 6.10-C) and plasma B cells (Figure 6.10-E) are the rarest B cell subpopulations, especially the latter which is almost undetectable. As these findings anticipated,

there are no significant differences in the various B cell compartments prior to EBV infection when comparing each patient group with control subjects or between MPS II and MPS VI patients.

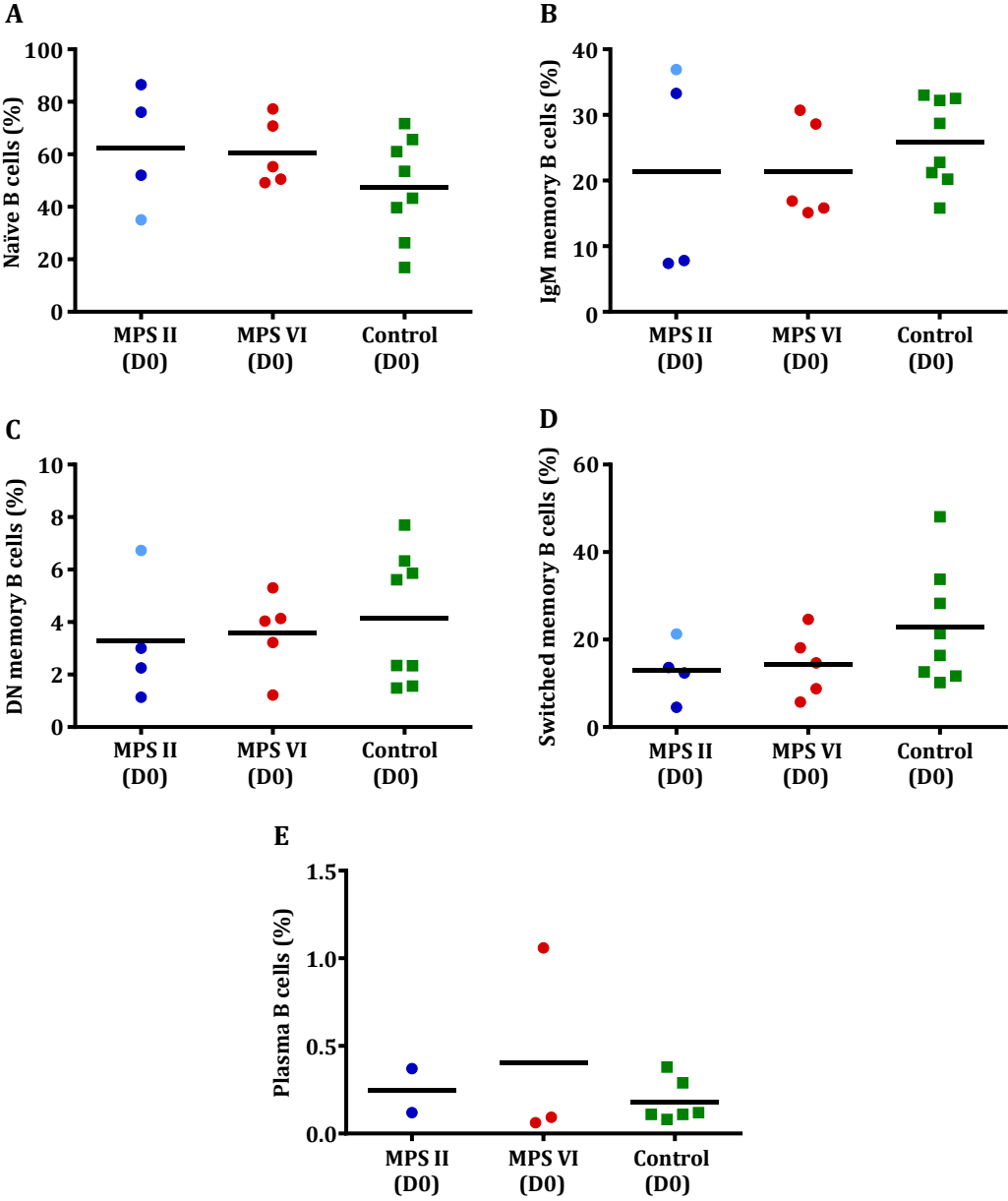


Figure 6.10. B cell subset frequency before EBV-induced transformation of B cells in MPS II and MPS VI patients. Frequency of (A) naïve B cells, (B) IgM memory B cells, (C) double-negative memory B cells, (D) switched memory B cells, and (E) plasma B cells before viral transformation. Dark blue circles represent cell frequency in MPS II patients under ERT; the light blue circle represents cell frequency in the untreated MPS II patient; red circles represent cell frequency in MPS VI patients under ERT; green squares represent cell frequency in control subjects; horizontal bars represent mean values.

Finally, to assess if the percentage of each B cell subset could be altered between the two

time points due to EBV infection, both analyses were compared within each group. For this purpose, only the individuals for whom the two determinations were available were considered: two MPS II patients, three MPS VI patients, and four control subjects.

The results relative to the frequency of B cell subpopulations before (day 0, D0) and after (day 35, D35) transformation of B cells are represented in Figure 6.11. A tendency to a decrease of naïve B cells (Figure 6.11–A) and IgM memory B cells (Figure 6.11–B) is seen in all groups when comparing PBMC samples prior to viral infection with EBV-transformed B cell lines. Also, there is clearly a trend toward an increase of double-negative (DN) memory B cells (Figure 6.11–C) after B cell transformation, reaching statistical significance in the control group ($p=0.0286$) which has more individuals analyzed. In contrast, no alterations in the levels of switched memory B cells (Figure 6.11–D) are observed within each group between the two time points.

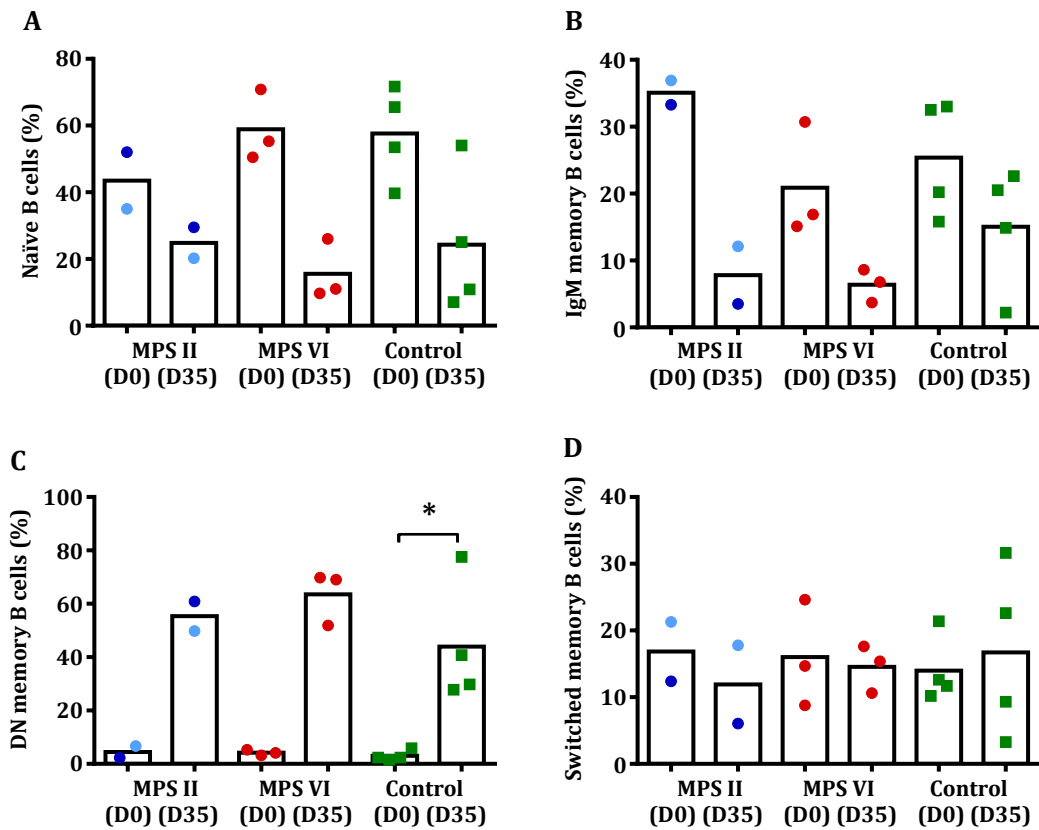


Figure 6.11. B cell subset frequency before and after EBV-induced transformation of B cells in MPS II and MPS VI patients. Comparison of the frequency of (A) naïve B cells, (B) IgM memory B cells, (C) double-negative memory B cells, and (D) switched memory B cells before (D0) and after (D35) viral transformation. The dark blue circle represents cell frequency in the MPS II patient under ERT; the light blue circle represents cell frequency in the untreated MPS II patient; red circles represent cell frequency in MPS VI patients under ERT; green squares represent cell frequency in control subjects; vertical bars represent mean values. $*p<0.05$.

7. CHAPTER II – DISCUSSION

In this study, the main aim was to produce EBV-transformed B cell lines from MPS II and MPS VI patients. The repeated collection of blood samples from these pediatric patients is not only an invasive procedure, but also especially hampered by their disease. Therefore, circulating B cells were employed in the generation of EBV-transformed B cell lines with the purpose of providing a continuous *in vitro* source of cells from these MPS patients, which can be applied in future immunological, biochemical, and genetic analyses. In this way, this work contributed to the preservation of the genetic material from Portuguese MPS II and MPS VI patients, which is now available in our laboratory to be used by the national and international scientific communities.

More specifically, this study was also designed to evaluate the efficacy in the production of EBV-transformed B cell lines from the two MPS patient groups. In order to assess this, the EBV-transformed B cell lines from MPS II and MPS VI patients were compared with those from control subjects in terms of the growth progression of infected cells over 35 days of culture, as well as the estimated number of B cells that were obtained after the transformation process.

Furthermore, another specific objective of this work was to characterize phenotypically the EBV-transformed B cell lines from both groups of MPS patients and compare with the phenotypes of the B cell population prior to viral infection.

Of note, the mean age of MPS II and MPS VI patients (13 ± 3.4 years and 15.2 ± 4.7 years, respectively) was substantially different from the mean age of control subjects (32 ± 5.2 years). It was not possible to include age-matched controls in this study because no approval was obtained from the ethical committee of *Centro Hospitalar de São João* regarding the use of blood donor samples to produce EBV-transformed B cell lines. Such consent was given by the ethics commission of IBMC, but it was restricted to adult subjects.

7.1. Production of EBV-transformed B cell lines from MPS II and MPS VI patients

Eighteen EBV-transformed B cell lines were successfully generated *in vitro* from a total of nineteen individuals included in this study: four were from MPS II patients, five from MPS VI patients, and nine from control subjects. The only exception was the MPS II patient #9, in which it

was not possible to obtain an exponentially proliferating cell culture from EBV-infected cells. The most likely explanation for the failure in the production of an EBV-transformed B cell line in this case is related to the fact that the volume of peripheral blood received from this patient was very low, thus limiting the number of PBMCs that were isolated and employed in B cell transformation (1×10^6 PBMCs). It should be noted that, for all the other MPS patients, a minimal amount of 2×10^6 PBMCs was used to generate EBV-transformed B cell lines.

According to the weekly observation of the growth progression of EBV-transformed B cell lines during 35 days of culture, similar outcomes were achieved when comparing MPS II patients with control subjects. In both groups, there were some cultures that expanded more actively over time, whereas others were relatively more slowly progressing. Also, the appearing of adherent cells in the cultures with concomitant slowdown in cell aggregate expansion was a recurrent problem in the group of MPS II patients and did also occur in one-third of control subjects.

On the other hand, the proliferation of the EBV-infected cell cultures from MPS VI patients evolved exponentially until day 35 post-infection in the majority of cases, thus registering a higher growth rate than that observed in the groups of control subjects and MPS II patients. The exceptional case wherein the development of cell clusters did not follow the same exponential evolution corresponded to the only case within MPS VI patients in which adherent cells arose in the culture.

In this way, the differences identified between the two patient groups concerning the efficacy in the production of EBV-transformed B cell lines appear to be related with the presence of adherent cells typically in the cultures from MPS II patients. This hypothesis is supported by the fact that the global expansion of the respective cell aggregates was significantly attenuated following the emergence of adherent cells and also because an increase of their proliferation rate, although with variable degrees among MPS II patients, was seen after the removal of adherent cells from the virally infected cell cultures. To accomplish this, a technique commonly applied to T cell cultures was performed, which consisted in the transference of cell clusters in suspension into new wells of the culture plate, while maintaining the adherent cells in the original well.

Given that the arising of adherent cells occurred not only in the cultures from all four MPS II patients, but also in those from one MPS VI patient and three control subjects, this event does not seem to be disease-specific or correlated with the health status of individuals. Instead, it may be associated with the transformation process, in which the adherent cells could be DCs or macrophages activated upon viral infection. It was described that DCs play a role in the priming of

both innate and adaptive EBV-specific immune responses [95]. The innate control can be mediated through the secretion of IFN- α , IFN- β , and IFN- γ , which prevents the outgrowth of infected B cells [96,97]. Moreover, the EBV-encoded small RNAs released from these cells can be detected by DCs via the toll-like receptor 3 [97], which respond through the release of IL-12; the subsequent NK cell activation results in IFN- γ production and limits EBV-induced B cell transformation by delaying viral LMP-1 expression [98]. In turn, DCs were also shown to phagocytize dying infected B cells and prime both adaptive CD4+ and CD8+ T cells by presenting viral latency antigens via MHC class I and II molecules; consequently, activated EBV-specific T cells promote the growth regression of transformed B cells through perforin-granzyme-mediated lysis, IFN- γ secretion, and Fas-FasL-induced lysis [99].

The actions of DCs during EBV infection may possibly explain the impaired development of cell clusters that was observed when adherent cells were present in the cultures produced *in vitro*. Although the immune control primed by DCs is, in general, ultimately executed by NK cells and T cells, any protective responses of these cells against EBV were most likely inhibited by the immunosuppressive effect of cyclosporine A and, thus, were not responsible for such reversion of cell growth. Instead, given that the removal of adherent cells from the cultures conducted, at least partially, to an improvement in the expansion of cell aggregates, it is reasonable to think that their proliferation was mostly affected by direct actions of DCs, namely the secretion of IFN cytokines. Even so, it remains to be elucidated the reason why the appearing of adherent cells did only occur in some EBV-infected cell cultures. One hypothesis is that the frequency of DCs or their activity in the PBMC samples was higher in those particular cases comparing with the remaining individuals. Hence, it would be important to analyze, in the future, the percentage of DCs prior to EBV-induced B cell transformation to test this theory.

To evaluate whether EBV-transformed B cells were still viable after they have been frozen on day 35 post-infection, as well as if their growth could be negatively affected by the thawing process, two cryopreserved EBV-transformed B cell lines from a MPS VI patient and a control subject were put back in culture during one week. The results confirmed not only the cell viability, but also the maintenance of the high proliferative capacity of EBV-transformed B cell lines, thus constituting an important indicator of their successful production *in vitro*.

Other methods used to assess the efficacy in the generation of EBV-transformed B cell lines from MPS II and MPS VI patients consisted in the determination of (i) the B cell frequency in PBMC samples before viral infection (day 0) and in EBV-transformed B cell lines after 35 days of culture (day 35), as well as (ii) the ratio of B cell expansion between the two time points. When

comparing each patient group with control subjects or MPS II with MPS VI patients, no differences were found in the levels of B cells before and after EBV-mediated transformation. In contrast, the comparative analysis within each group of the B cell percentage between day 0 and day 35 showed, as expected, a significant increase following viral infection. The successful production of EBV-transformed B cell lines was further confirmed by the demonstration that the original B cell population was expanded as a result of the transformation process. The greater rise in B cell frequency and in variation of B cell numbers between the two time points was observed in MPS VI patients, with identical outcomes registered in the two other groups, which is in agreement with the microscopic observation that the virally infected cell cultures from MPS VI patients presented, in general, a higher proliferation rate than those from control subjects and MPS II patients.

Surprisingly, both methods revealed that, in all groups, there were one or more cultures wherein the B cell expansion was less prominent, which were the ones whose development was significantly hampered after the arising of adherent cells. Despite the low number of B cells obtained on day 35 post-infection, especially in the case of two control subjects, these cultures exhibited signs of B cell transformation upon microscopic observation, including the presence of cell clusters with typical rosette morphology. Therefore, it is reasonable to think that, if such EBV-transformed B cell lines had been maintained in culture beyond day 35 after infection, the growth of cell aggregates might have been fully recovered and the final results would have been similar to those obtained for the cultures wherein no adherent cells emerged.

The finding that the percentage of B cells recognized by CD19 expression in the samples of EBV-transformed B cell lines was below 100% in all groups raises uncertainties on the identity of the cells that did not express this surface marker. Likely explanations for the origin of such CD19⁻ cells are that the gate created to select viable cells within the EBV-transformed B cell lines might also have included (i) cellular debris (e.g. from NK cells and T cells suppressed by cyclosporine A), or (ii) PBMCs other than B cells (e.g. monocytes, DCs) that survived until day 35 post-infection. Characteristically, EBV-transformed B cell lines are negative for the expression of T cell (CD3), NK cell (CD56), granulocyte (CD66b), and monocyte (CD14) surface markers, as previously reported [100,101]. Thereby, it would be important to use a cell viability marker to exclude dead cells, as well as additional surface markers specific to other leukocyte populations to confirm the purity of EBV-transformed B cell lines in future studies.

In turn, another hypothesis is that those CD19⁻ cells are transformed B cells that lost CD19 expression in the course of EBV-induced transformation. This seems to be supported by the fact that, during the phenotyping of the EBV-transformed B cell line from control subject #1 using fluorescein isothiocyanate (FITC)-labelled anti-human CD19 antibody, no fluorescence signal was

detected in spite of the successful transformation of B cells based on regular observations of the culture; this problem did not occur in subsequent analyses of the remaining EBV-transformed B cell lines wherein phycoerythrin conjugated with cyanin-7 (PE-Cy7)-labeled anti-human CD19 antibody was used. Since the first fluorochrome is comparatively less sensitive than this latest, the absence of the fluorescein isothiocyanate (FITC) signal may have been potentiated by a reduced expression of CD19 in transformed B cells from control subject #1. In a previous report, the CD19 expression did also appear to be down-regulated in EBV-transformed B cells in comparison with non-infected B cells, as evidenced by a decrease in the mean fluorescence of CD19 [102]. Another study concerning the phenotype of EBV-transformed B cell lines described that, although the majority expressed CD19, some were negative for this B cell marker, as assessed by a level of cell staining lower than 10% [101]. Together, these data suggest that EBV-mediated B cell transformation may induce an alteration of surface marker expression, namely of CD19. Thereby, it would be important to perform, in the future, the characterization of EBV-transformed B cell lines using additional B cell-specific markers to assess if their expression is more homogeneous than that of CD19, thus allowing the identification of all B cells within the cultures after viral transformation, or whether the combined expression of two surface markers (e.g. CD19 and CD20) would allow the recognition of a higher percentage of EBV-transformed B cells.

In terms of the factors that could have conditioned the efficacy in the generation of EBV-transformed B cell lines, herein it was demonstrated that the frequency of B cells within PBMCs used in the transformation process does not influence the B cell levels in the samples of EBV-transformed B cell lines and, therefore, is not an indicator of the growth progression of virally infected cell clusters. Surprisingly, in this study, it was observed that the emergence of adherent cells in the culture was a major limiting factor of the development of EBV-transformed B cell lines.

7.2. Phenotype of EBV-transformed B cell lines from MPS II and MPS VI patients

The phenotyping of EBV-transformed B cell lines from MPS II and MPS VI patients upon 35 days of culture revealed a predominance of double-negative memory B cells in both groups as well as in control subjects. When considering the frequency of each B cell phenotype in the EBV-transformed B cell lines, no differences concerning the levels of naïve, double-negative memory, IgM memory, and switched memory B cells were found in MPS II and MPS VI patients as compared with control subjects or between both patient groups.

Prior to EBV-induced transformation, the predominant B cell subpopulation in the PBMC samples from the three groups corresponded to naïve B cells. Interestingly, in contrast to the EBV-transformed B cell lines, the percentage of double-negative memory B cells within PBMCs was quite reduced in all groups. The determination of the B cell subset frequency before viral infection showed no alterations in peripheral blood naïve, double-negative memory, IgM memory, switched memory, and plasma B cells between MPS II and MPS VI patients or when comparing each patient group with control subjects. As expected, circulating plasma B cells were almost undetectable in the three groups, indicating that all individuals included in this study were at steady-state conditions.

In the comparative analysis within each group of the percentage of B cell compartments before infection with EBV virions (day 0) and following viral transformation (day 35), a significant increase of double-negative memory B cells was identified in the EBV-transformed B cell lines from control subjects. Furthermore, a tendency toward increased levels of the double-negative memory B cell subpopulation after EBV-mediated transformation was clearly observed in MPS II and MPS VI patients. Given the large variation in the frequency of double-negative memory B cells in these two groups between day 0 and day 35 post-infection, the most likely explanation for the lacking of statistical significance is the reduced number of MPS II and MPS VI patients that were analyzed for these parameters. Similarly, a trend to a decrease of naïve and IgM memory B cells was detected in the three groups when comparing the respective percentage within PBMCs prior to viral infection with the samples of EBV-transformed B cell lines. On the contrary, in all groups, no differences were found in the switched memory B cell levels between the two time points.

Taking into account that the predominant phenotype of EBV-transformed B cell lines was the one corresponding to the double-negative memory B cell subset, three hypotheses can be proposed regarding the origin of such phenotype: (i) the double-negative memory B cells, whose frequency on day 0 was considerably reduced, were selectively infected by EBV; (ii) IgM memory B cells, which presented intermediary levels before viral infection, were mostly transformed by EBV and, in the course of this process, lost the expression of IgM and CD27 surface markers; or (iii) naïve B cells, which constituted the major compartment within the B cell population on day 0, were preferentially infected by the virus and, as a consequence, differentiated into memory B cells with double-negative phenotype.

A previous study on the susceptibility of B cell subsets to EBV-induced transformation *in vitro* reported that circulating naïve B cells were significantly more prone to infection than their memory counterparts [103]. However, this finding contrasts with the fact that, in latently infected human carriers, EBV was found exclusively in the peripheral blood compartment of memory B

cells, whose phenotype was characterized as IgD-Ig+CD27+ [104,105]. Some authors proposed that, although EBV is capable of directly infecting resting memory B cells, it specially shows the capacity to target naïve B cells and establish a latent infection in them, possibly owing to their inherently higher proliferation rate [103,104]. Subsequently, the activated naïve B cells are driven by the virus through a maturation stage that mimics the GC reaction and, as a consequence, the newly infected cells are induced to proliferate; however, they are also able to exit the cell cycle and become resting memory B cells, rather than terminally differentiate into antibody-secreting plasma B cells [103,104]. For this purpose, after infecting naïve B cells, the resulting activated, proliferating B blasts initially express EBNA-2 [104,106], which promotes the transcriptional activation of viral (e.g. LMP-1, LMP-2) and cellular genes (e.g. CD21, CD23), leading to EBV-infected cell expansion [77,81]. Due to their ability to switch off EBNA-2 transcription, they can become GC cells which, instead of expressing such growth program, downregulate the latent genes and only produce EBNA-1 [104,106], a protein essential for EBV genome replication and its maintenance as viral episomes [77,81]; consequently, these B blasts can transit from a proliferating to a resting state [104,106]. Then, in order to escape from apoptosis due to absence of antigen-stimulatory signals and T cell-mediated positive selection, infected B cells express LMP-1 and LMP-2 by an EBNA-2-independent pathway [104,106]: the first mimics the function of CD40, a cellular B cell-activating surface molecule that interacts with CD40 ligand in helper T cells, which induces B cell proliferation, affinity maturation, and Ig class switching during GC reaction; the second acts like the genuine BCR, blocking the normal signal transduction via this cellular receptor to prevent EBV lytic infection [81]. As a result, both viral proteins supply the required rescue signals that replace antigen- and T cell-dependent activation, thus promoting the survival of GC cells and their differentiation into memory B cells that express solely LMP-2, which provides the frequent signaling through a functional BCR that is essential for prolonged survival [104,106].

Summing up, EBV has evolved to exploit the normal cellular mechanisms by which antigen-responsive, proliferating naïve B cells develop *in vivo* into resting memory B cells, allowing this human herpesvirus to ensure its lifetime persistency in this long-lived B cell pool [104,106]. Therefore, this may potentially be the pathway through which the EBV-transformed B cell lines produced *in vitro* in our work acquired a predominant phenotype of double-negative memory B cells. This hypothesis is in accordance with the findings that the frequency of the naïve B cell subpopulation considerably decreased in the course of EBV-induced transformation, at the same time that the percentage of the double-negative memory B cell subset substantially increased during the 35 days of culture of the virally infected cells.

8. CONCLUSION AND FUTURE PERSPECTIVES

This thesis aimed to characterize the immune system in MPS II and MPS VI diseases by studying the frequency of the major peripheral blood leukocyte populations – T cells and their compartments, NK cells, B cells and their subsets, as well as monocytes. Other main purposes of this work were to generate EBV-transformed B cell lines from MPS II and MPS VI patients, evaluate the efficacy in their production, and perform their phenotyping.

In the study of the various immune cell populations in MPS II and MPS VI diseases, a statistically significant decrease in the levels of NK cells and monocytes was uncovered in MPS VI patients, but not in MPS II patients, as compared with the control group. On the contrary, no alterations were detected in the percentage of total T cells, helper and cytotoxic T cell subsets, iNKT cells, iNKT cell CD4/CD8 compartments, and B cells in the two patient groups when comparing with control subjects. On the other hand, the analysis of the memory state of T cells revealed significant differences in the naïve and memory phenotypes of both helper and cytotoxic T cells between MPS VI patients, but not MPS II patients, and age-matched control subjects.

In the case of other human LSDs, identical imbalances in the frequency of NK cells were reported in Gaucher disease [84] and Niemann-Pick disease type C1 [45], as well as a deficiency of monocytes in Fabry disease [40] and Gaucher disease [85] patients. Normal levels of NK cells were already documented in MPS II [31]. In terms of the percentage of total T cells, no alterations were found in Niemann-Pick disease type C1 [45] and Fabry disease [36]. Similar findings concerning the helper and cytotoxic T cell subpopulations were demonstrated in MPS II [31]. The frequency of iNKT cells was unaltered in Niemann-Pick disease type C1 [44], Fabry disease [36,40,41], and Gaucher disease [43]. The CD4 and CD8 status of iNKT cells was described as normal in Niemann-Pick disease type C1 patients [44]. In regards to the levels of B cells, no differences were observed in Gaucher disease [84] and Niemann-Pick disease type C1 [45]. Finally, alterations in the memory state of helper T cells were reported in Gaucher disease [84].

Altogether, the disease-specific abnormalities in some leukocyte populations that were identified in our work, along with similar results demonstrated in other LSDs, suggest that the type of macromolecular substance stored inside the lysosome or the specific causative mutation(s), rather than the abnormal substrate accumulation *per se*, play a major role in the triggering of particular cellular damages that potentially cause such alterations. This underlines the importance to assess the potential negative effects of the different storage materials and enzymatic defects on the normal cellular composition of the immune system in LSD patients.

With respect to the production of EBV-transformed B cell lines, this process was successfully accomplished in the two groups of MPS patients. Comparing with control subjects, the efficacy in the generation of EBV-transformed B cell lines from MPS II patients did not show substantial differences. On the other hand, a considerably higher efficacy in the production of EBV-transformed B cell lines was registered in the case of MPS VI patients when compared with control subjects and MPS II patients, as demonstrated by the larger ratio of expansion of the B cell population subsequent to viral transformation. The main difference observed between the two patient groups regarding the development of EBV-transformed B cell lines was related with the appearing of adherent cells, which occurred in all virally infected cell cultures from MPS II patients, but only in one of the MPS VI patients. Such regression of the global expansion of cell aggregates in the presence of adherent cells is proposed to be associated with the actions of DCs in the priming of both innate and adaptive EBV-specific immune responses. Either by directly secreting IFN cytokines [96], through activation of innate NK cells [98], or via stimulation of adaptive T cells [99], DCs may have been an important factor that conditioned the proliferation of cell clusters in the cultures from MPS II patients. On the other hand, the frequency of B cells within the original PBMC samples was shown herein not to be a determinant factor of the growth progression of EBV-infected cells and their expansion into actively proliferating EBV-transformed B cell lines.

The analysis of the frequency of B cell subpopulations revealed no alterations in MPS II and MPS VI patients in comparison with control subjects, either before or after EBV-mediated transformation of B cells. The phenotypic characterization of EBV-transformed B cell lines demonstrated a predominance of double-negative memory B cells in both patient groups and similar results were observed for control subjects. However, in the samples of PBMCs used in viral infection, naïve B cells represented the more prevalent B cell subset in MPS II and MPS VI patients as well as in the control group. This discrepancy led to the hypothesis that naïve B cells were preferentially infected by EBV *in vitro* and that, during the transformation process, they differentiated into memory B cells with double-negative phenotype. In agreement with this theory is the fact that peripheral blood naïve B cells were already described to be significantly more susceptible to EBV infection than their memory counterparts [103], as well as the observation that this virus was found exclusively in the circulating memory B cell compartment in latently infected human carriers [104,105]. Accordingly, some authors proposed that EBV produces a latent infection in naïve B cells, which are driven by the virus to differentiate into resting memory B cells so that EBV is able to ensure its lifetime persistency in this long-lived B cell pool *in vivo* [104,106]. Hence, this may also be the mechanism exploited by EBV to establish transformed B cell lines *in vitro*.

Given that this work involved immunological analyses performed in human patients, several limitations emerged in the course of our studies. To cite a few, since MPS II and MPS VI are rare disorders – with an estimated prevalence in Portugal of 1.09 and 0.42 per 100,000 live births [13], respectively – and few Portuguese subjects are affected by these diseases, it was only possible to recruit a small number of patients for this work; there were also some contretemps regarding the reception of blood samples from these patients that delayed the overall experimental activities; in various cases, a small amount of peripheral blood was received from patients, owing to the fact that most of them were children and also because of their general poor health status, which limited the number of PBMCs that were isolated and used for B cell transformation as well as for PBMCs flow cytometry; some alterations may have not been identified as statistically significant comparing with control subjects due to the reduced number of individuals that composed each MPS patient group, especially in the study related to EBV-transformed B cell lines. This problem was complicated by the fact that it is always more difficult to perform studies using blood samples from children and, although we have had the collaboration of one hospital to receive blood from pediatric MPS patients and control subjects, the respective ethical committee did not approve their use in the process of B cell transformation. Consequently, another limitation was the impossibility to include age-matched controls for the production and phenotyping of EBV-transformed B cell lines, as only adult volunteers from IBMC could participate in this work.

To conclude, since the pathophysiology of LSDs remains largely unknown, we expect to continue analyzing MPS II and MPS VI patients in the future, including untreated affected individuals, to improve our understanding on the effect of ERT in the correction and/or alteration of the immune status in these disorders. With our study, we hope to have contributed for the better comprehension of these two rare diseases, namely the effects of their metabolic deficiencies in the normal cellular composition of the immune system. Moreover, the production of EBV-transformed B cell lines, which were obtained by a less invasive method compared to fibroblast cell lines, allowed not only to perpetuate the genetic material of these rare Portuguese patients, but also their potential use by the national and international scientific communities. As a result of this work, we have nowadays available in our laboratory four EBV-transformed B cell lines from MPS II patients and five from MPS VI patients, which can be used in future immunological, biochemical, and genetic analyses.

9. LITERATURE

1. Xu, H., and D. Ren, *Lysosomal Physiology*. Annual Review of Physiology (2015), 77, p. 57–80.
2. Parkinson-Lawrence, E.J., et al., *Lysosomal Storage Disease: Revealing Lysosomal Function and Physiology*. Physiology (2010), 25(2), p. 102–115.
3. Schultz, M.L., et al., *Clarifying lysosomal storage diseases*. Trends in Neurosciences (2011), 34(8), p. 401–410.
4. Coutinho, M.F., L. Matos, and S. Alves, *From bedside to cell biology: A century of history on lysosomal dysfunction*. Gene (2015), 555(1), p. 50–58.
5. Vellodi, A., *Lysosomal storage disorders*. British Journal of Haematology (2005), 128(4), p. 413–431.
6. Platt, F.M., B. Boland, and A.C. van der Spoel, *Lysosomal storage disorders: The cellular impact of lysosomal dysfunction*. Journal of Cell Biology (2012), 199(5), p. 723–734.
7. Lampe, C., et al., *Mucopolysaccharidoses and Other Lysosomal Storage Diseases*. Rheumatic Disease Clinics of North America (2013), 39(2), p. 431–455.
8. Applegarth, D.A., J.R. Toone, and R.B. Lowry, *Incidence of Inborn Errors of Metabolism in British Columbia, 1969–1996*. Pediatrics (2000), 105(1), p. 1–6.
9. Dionisi-Vici, C., et al., *Inborn errors of metabolism in the Italian pediatric population: A national retrospective survey*. Journal of Pediatrics (2002), 140(3), p. 321–327.
10. Poupětová, H., et al., *The birth prevalence of lysosomal storage disorders in the Czech Republic: comparison with data in different populations*. Journal of Inherited Metabolic Disease (2010), 33(4), p. 387–396.
11. Meikle, P.J., et al., *Prevalence of Lysosomal Storage Disorders*. Journal of the American Medical Association (1999), 281(3), p. 249–254.
12. Poorthuis, B., et al., *The frequency of lysosomal storage diseases in The Netherlands*. Human Genetics (1999), 105, p. 151–156.
13. Pinto, R., et al., *Prevalence of lysosomal storage diseases in Portugal*. European Journal of Human Genetics (2004), 12(2), p. 87–92.

14. Neufeld, E.F., and J. Muenzer, *The Mucopolysaccharidoses*. In *The Online Metabolic & Molecular Bases of Inherited Disease*, D. Valle, et al., (editors). McGraw-Hill Medical (2001): www.ommbid.com, p. 3421–3452.
15. Coutinho, M.F., L. Lacerda, and S. Alves, *Glycosaminoglycan Storage Disorders: A Review*. *Biochemistry Research International* (2012), 2012, p. 1–16.
16. Muenzer, J., *Overview of the mucopolysaccharidoses*. *Rheumatology* (2011), 50 (Suppl. 5), p. v4–v12.
17. Tomatsu, S., et al., *Newborn screening and diagnosis of mucopolysaccharidoses*. *Molecular Genetics and Metabolism* (2013), 110, p. 42–53.
18. Noh, H., and J.I. Lee, *Current and potential therapeutic strategies for mucopolysaccharidoses*. *Journal of Clinical Pharmacy and Therapeutics* (2014), 39(3), p. 215–224.
19. Valayannopoulos, V., and F.A. Wijburg, *Therapy for the mucopolysaccharidoses*. *Rheumatology* (2011), 50 (Suppl. 5), p. v49–v59.
20. Lodish, H., et al., *Integrating Cells Into Tissues*. In *Molecular Cell Biology*, H. Lodish, et al., (editors). W. H. Freeman and Company (2013): New York, 7th edition, p. 925–976.
21. Giugliani, R., et al., *Mucopolysaccharidosis I, II, and VI: Brief review and guidelines for treatment*. *Genetics and Molecular Biology* (2010), 33(4), p. 589–604.
22. Muenzer, J., et al., *The role of enzyme replacement therapy in severe Hunter syndrome – an expert panel consensus*. *European Journal of Pediatrics* (2012), 171(1), p. 181–188.
23. Wraith, J.E., et al., *Mucopolysaccharidosis type II (Hunter syndrome): a clinical review and recommendations for treatment in the era of enzyme replacement therapy*. *European Journal of Pediatrics* (2008), 167(3), p. 267–277.
24. Scarpa, M., et al., *Mucopolysaccharidosis type II: European recommendations for the diagnosis and multidisciplinary management of a rare disease*. *Orphanet Journal of Rare Diseases* (2011), 6, p. 72–89.
25. Li, P., A.B. Bellows, and J.N. Thompson, *Molecular basis of iduronate-2-sulphatase gene mutations in patients with mucopolysaccharidosis type II (Hunter syndrome)*. *Journal of Medical Genetics* (1999), 36(1), p. 21–27.
26. Valayannopoulos, V., et al., *Mucopolysaccharidosis VI*. *Orphanet Journal of Rare Diseases* (2010), 5, p. 5–24.

27. Karageorgos, L., et al., *Mutational Analysis of 105 Mucopolysaccharidosis Type VI Patients*. Human Mutation (2007), 28(9), p. 897–903.
28. Giugliani, R., P. Harmatz, and J.E. Wraith, *Management Guidelines for Mucopolysaccharidosis VI*. Pediatrics (2007), 120(2), p. 405–418.
29. Castaneda, J.A., et al., *Immune system irregularities in lysosomal storage disorders*. Acta Neuropathologica (2008), 115(2), p. 159–174.
30. Archer, L.D., et al., *Characterisation of the T cell and dendritic cell repertoire in a murine model of mucopolysaccharidosis I (MPS I)*. Journal of Inherited Metabolic Disease (2013), 36(2), p. 257–262.
31. Torres, L.C., et al., *NK and B cell deficiency in a MPS type II family with novel mutation in the IDS gene*. Clinical Immunology (2014), 154, p. 100–104.
32. Brück, W., H.H. Goebel, and P. Dienes, *B and T lymphocytes are affected in lysosomal disorders – an immunoelectron microscopic study*. Neuropathology and Applied Neurobiology (1991), 17(3), p. 219–222.
33. Kieseier, B.C., and H.H. Goebel, *Characterization of T-cell subclasses and NK-cells in lysosomal disorders by immune-electron microscopy*. Neuropathology and Applied Neurobiology (1994), 20(6), p. 604–608.
34. Kieseier, B.C., K.E. Wisniewski, and H.H. Goebel, *The monocyte-macrophage system is affected in lysosomal storage diseases: an immunoelectron microscopic study*. Acta Neuropathologica (1997), 94(4), p. 359–362.
35. Gadola, S.D., et al., *Impaired selection of invariant natural killer T cells in diverse mouse models of glycosphingolipid lysosomal storage diseases*. Journal of Experimental Medicine (2006), 203(10), p. 2293–2303.
36. Balreira, A., et al., *Anomalies in conventional T and invariant natural killer T-cell populations in Fabry mice but not in Fabry patients*. British Journal of Haematology (2008), 143(4), p. 601–604.
37. Plati, T., et al., *Development and maturation of invariant NKT cells in the presence of lysosomal engulfment*. European Journal of Immunology (2009), 39(10), p. 2748–2754.
38. Sagiv, Y., et al., *Cutting Edge: Impaired Glycosphingolipid Trafficking and NKT Cell Development in Mice Lacking Niemann-Pick Type C1 Protein*. Journal of Immunology (2006), 177(1), p. 26–30.

39. Schümann, J., et al., *Differential alteration of lipid antigen presentation to NKT cells due to imbalances in lipid metabolism*. *European Journal of Immunology* (2007), 37(6), p. 1431–1441.
40. Rozenfeld, P., et al., *Leukocyte perturbation associated with Fabry disease*. *Journal of Inherited Metabolic Disease* (2009), 32 (Suppl. 1), p. S67–S77.
41. Pereira, C.S., et al., *Invariant natural killer T cells are phenotypically and functionally altered in Fabry disease*. *Molecular Genetics and Metabolism* (2013), 108(4), p. 241–248.
42. Micheva, I., et al., *Dendritic cells in patients with type I Gaucher disease are decreased in number but functionally normal*. *Blood Cells, Molecules, and Diseases* (2006), 36(2), p. 298–307.
43. Balreira, A., et al., *Evidence for a link between sphingolipid metabolism and expression of CD1d and MHC-class II: monocytes from Gaucher disease patients as a model*. *British Journal of Haematology* (2005), 129(5), p. 667–676.
44. Speak, A.O., et al., *Invariant natural killer T cells are not affected by lysosomal storage in patients with Niemann-Pick disease type C*. *European Journal of Immunology* (2012), 42(7), p. 1886–1892.
45. Speak, A.O., et al., *Altered distribution and function of natural killer cells in murine and human Niemann-Pick disease type C1*. *Blood* (2014), 123(1), p. 51–60.
46. Daly, T.M., R.G. Lorenz, and M.S. Sands, *Abnormal Immune Function In Vivo in a Murine Model of Lysosomal Storage Disease*. *Pediatric Research* (2000), 47(6), p. 757–762.
47. DiRosario, J., et al., *Innate and Adaptive Immune Activation in the Brain of MPS IIIB Mouse Model*. *Journal of Neuroscience Research* (2009), 87(4), p. 978–990.
48. Lopes, N., *iNKT cells in Mucopolysaccharidosis type II patients* (Masters Thesis). Aveiro: University of Aveiro (2013).
49. Maia, M., *Lipid specific T cells in Mucopolysaccharidosis VI patients* (Masters Thesis). Aveiro: University of Aveiro (2012).
50. Cianferoni, A., *Invariant Natural Killer T Cells*. *Antibodies* (2014), 3, p. 16–36.
51. Gottschalk, C., E. Mettke, and C. Kurts, *The role of invariant natural killer T cells in dendritic cell licensing, cross-priming, and memory CD8+ T cell generation*. *Frontiers in Immunology* (2015), 6(379), p. 1–8.
52. Macho-Fernandez, E., and M. Brigl, *The extended family of CD1d-restricted NKT cells: sifting through a mixed bag of TCRs, antigens, and functions*. *Frontiers in Immunology* (2015), 6(362), p. 1–19.

53. Brennan, P.J., M. Brigl, and M.B. Brenner, *Invariant natural killer T cells: an innate activation scheme linked to diverse effector functions*. *Nature Reviews – Immunology* (2013), 13(2), p. 101–117.
54. Van Kaer, L., V.V. Parekh, and L. Wu, *Invariant natural killer T cells: bridging innate and adaptive immunity*. *Cell and Tissue Research* (2011), 343(1), p. 43–55.
55. Berzins, S.P., M.J. Smyth, and A.G. Baxter, *Presumed guilty: natural killer T cell defects and human disease*. *Nature Reviews – Immunology* (2007), 11(2), p. 131–142.
56. Pieper, K., B. Grimbacher, and H. Eibel, *B-cell biology and development*. *Journal of Allergy and Clinical Immunology* (2013), 131(4), p. 959–971.
57. Fettke, F., et al., *B cells: the old new players in reproductive immunology*. *Frontiers in Immunology* (2014), 5(285), p. 1–10.
58. LeBien, T.W., and T.F. Tedder, *B lymphocytes: how they develop and function*. *Blood* (2008), 112(5), p. 1570–1580.
59. Abbas, A.K., A.H. Lichtman, and S. Pillai, *Antibodies and Antigens*. In *Cellular and Molecular Immunology*, A.K. Abbas, A.H. Lichtman, and S. Pillai, (editors). Elsevier Saunders (2012): Philadelphia, 7th edition, p. 89–108.
60. Goldsby, R.A., et al., *Antibodies: Structure and Function*. In *Immunology*, R.A. Goldsby, et al., (editors). W. H. Freeman (2003): New York, 5th edition, p. 76–104.
61. Perez-Andres, M., et al., *Human Peripheral Blood B-Cell Compartments: A Crossroad in B-Cell Traffic*. *Cytometry Part B – Clinical Cytometry* (2010), 78B (Suppl. 1), p. S47–S60.
62. Abbas, A.K., A.H. Lichtman, and S. Pillai, *Lymphocyte Development and Antigen Receptor Gene Rearrangement*. In *Cellular and Molecular Immunology*, A.K. Abbas, A.H. Lichtman, and S. Pillai, (editors). Elsevier Saunders (2012): Philadelphia, 7th edition, p. 173–202.
63. Goldsby, R.A., et al., *B-Cell Generation, Activation, and Differentiation*. In *Immunology*, R.A. Goldsby, et al., (editors). W. H. Freeman (2003): New York, 5th edition, p. 247–275.
64. Kaminski, D.A., et al., *Advances in human B cell phenotypic profiling*. *Frontiers in Immunology* (2012), 3(302), p. 1–15.
65. Griffin, D.O., and T.L. Rothstein, *Human B1 cell frequency: isolation and analysis of human B1 cells*. *Frontiers in Immunology* (2012), 3(122), p. 1–10.
66. Cunningham, A.F., et al., *B1b cells recognize protective antigens after natural infection and vaccination*. *Frontiers in Immunology* (2014), 5(535), p. 1–11.

67. Covens, K., et al., *Characterization of proposed human B-1 cells reveals pre-plasmablast phenotype*. *Blood* (2013), 121(26), p. 5176–5183.
68. Sims, G.P., et al., *Identification and characterization of circulating human transitional B cells*. *Blood* (2005), 105(11), p. 4390–4398.
69. Bella, S.D., et al., *Human Herpesvirus-8 Infection Leads to Expansion of the Preimmune/Natural Effector B Cell Compartment*. *PLoS ONE* (2010), 5(11), p. 1–10.
70. Benson, M.J., et al., *Affinity of antigen encounter and other early B-cell signals determine B-cell fate*. *Current Opinion in Immunology* (2007), 19(3), p. 275–280.
71. Abbas, A.K., A.H. Lichtman, and S. Pillai, *B Cell Activation and Antibody Production*. In *Cellular and Molecular Immunology*, A.K. Abbas, A.H. Lichtman, and S. Pillai, (editors). Elsevier Saunders (2012): Philadelphia, 7th edition, p. 243–268.
72. Good-Jacobson, K.L., and D.M. Tarlinton, *Multiple routes to B-cell memory*. *International Immunology* (2012), 24(7), p. 403–408.
73. Wu, Y.-C.B., D. Kipling, and D.K. Dunn-Walters, *The relationship between CD27 negative and positive B cell populations in human peripheral blood*. *Frontiers in Immunology* (2011), 2(81), p. 1–12.
74. Allman, D., and S. Pillai, *Peripheral B cell subsets*. *Current Opinion in Immunology* (2008), 20(2), p. 149–157.
75. Longnecker, R., and F. Neipel, *Introduction to the human γ -herpesviruses*. In *Human Herpesviruses: Biology, Therapy, and Immunoprophylaxis*, A. Arvin, et al., (editors). Cambridge University Press (2007): Cambridge, p. 341–359.
76. Chandran, B., and L. Hutt-Fletcher, *Gammaherpesviruses entry and early events during infection*. In *Human Herpesviruses: Biology, Therapy, and Immunoprophylaxis*, A. Arvin, et al., (editors). Cambridge University Press (2007): Cambridge, p. 360–378.
77. Klein, G., E. Klein, and E. Kashuba, *Interaction of Epstein–Barr virus (EBV) with human B-lymphocytes*. *Biochemical and Biophysical Research Communications* (2010), 396(1), p. 67–73.
78. Hussain, T., and R. Mulherkar, *Lymphoblastoid cell lines: a continuous in vitro source of cells to study carcinogen sensitivity and DNA repair*. *International Journal of Molecular and Cellular Medicine* (2012), 1(2), p. 75–87.

79. Shannon-Lowe, C., et al., *Epstein–Barr virus-induced B-cell transformation: quantitating events from virus binding to cell outgrowth*. *Journal of General Virology* (2005), 86, p. 3009–3019.
80. Kalla, M., and W. Hammerschmidt, *Human B cells on their route to latent infection – Early but transient expression of lytic genes of Epstein–Barr virus*. *European Journal of Cell Biology* (2012), 91(1), p. 65–69.
81. Bishop, G.A., and L.K. Busch, *Molecular mechanisms of B-lymphocyte transformation by Epstein–Barr virus*. *Microbes and Infection* (2002), 4(8), p. 853–857.
82. Lieberman, P.M., J. Hu, and R. Renne, *Gammaherpesvirus maintenance and replication during latency*. In *Human Herpesviruses: Biology, Therapy, and Immunoprophylaxis*, A. Arvin, et al., (editors). Cambridge University Press (2007): Cambridge, p. 379–402.
83. Young, L.S., J.R. Arrand, and P.G. Murray, *EBV gene expression and regulation*. In *Human Herpesviruses: Biology, Therapy, and Immunoprophylaxis*, A. Arvin, et al., (editors). Cambridge University Press (2007): Cambridge, p. 461–489.
84. Braudeau, C., et al., *Altered innate function of plasmacytoid dendritic cells restored by enzyme replacement therapy in Gaucher disease*. *Blood Cells, Molecules and Diseases* (2013), 50(4), p. 281–288.
85. Bettman, N., et al., *Impaired migration capacity in monocytes derived from patients with Gaucher disease*. *Blood Cells, Molecules and Diseases* (2015), 55(2), p. 180–186.
86. Macedo, M.F., et al., *Enzyme replacement therapy partially prevents invariant Natural Killer T cell deficiency in the Fabry disease mouse model*. *Molecular Genetics and Metabolism* (2012), 106(1), p. 83–91.
87. Comans-Bitter, W.M., et al., *Immunophenotyping of blood lymphocytes in childhood. Reference values for lymphocyte subpopulations*. *Journal of Pediatrics* (1997), 130(3), p. 388–393.
88. Tosato, F., et al., *Lymphocytes Subsets Reference Values in Childhood*. *Cytometry Part A* (2015), 87(1), p. 81–85.
89. Pereira, C., *Lipid antigen presentation in Fabry disease patients* (Masters Thesis). Aveiro: University of Aveiro (2011).
90. Bienemann, K., et al., *iNKT Cell Frequency in Peripheral Blood of Caucasian Children and Adolescent: The Absolute iNKT Cell Count is Stable from Birth to Adulthood*. *Scandinavian Journal of Immunology* (2011), 74(4), p. 406–411.

91. Lan, K., et al., *Epstein–Barr Virus (EBV): Infection, Propagation, Quantitation, and Storage*. *Current Protocols in Microbiology* (2007), 6(14E.2), p. 14E.2.1–14E.2.21.
92. Ling, P.D., and H.M. Huls, *Isolation and immortalization of lymphocytes*. *Current Protocols in Molecular Biology* (2005), 70(28.2), p. 28.2.1–28.2.5.
93. Tosato, G., *Generation of Epstein–Barr Virus (EBV)-Immortalized B Cell Lines*. *Current Protocols in Immunology* (2001), 7(7.22), p. 7.22.1–7.22.3.
94. Hui-Yuen, J., et al., *Establishment of Epstein–Barr Virus Growth-transformed Lymphoblastoid Cell Lines*. *Journal of Visualized Experiments* (2011), 57(e3321), p. 1–6.
95. Münz, C., *Dendritic cells during Epstein Barr virus infection*. *Frontiers in Microbiology* (2014), 5(308), p. 1–5.
96. Lotz, M., et al., *Regulation of Epstein–Barr virus infection by recombinant interferons. Selected sensitivity to interferon- γ^** . *European Journal of Immunology* (1985), 15(5), p. 520–525.
97. Iwakiri, D., et al., *Epstein–Barr virus (EBV)-encoded small RNA is released from EBV-infected cells and activates signaling from toll-like receptor 3*. *Journal of Experimental Medicine* (2009), 206(10), p. 2091–2099.
98. Strowig, T., et al., *Tonsillar NK Cells Restrict B Cell Transformation by the Epstein–Barr Virus via IFN- γ* . *PLoS Pathogens* (2008), 4(2), p. 1–13.
99. Bickham, K., et al., *Dendritic Cells Initiate Immune Control of Epstein–Barr Virus Transformation of B Lymphocytes In Vitro*. *Journal of Experimental Medicine* (2003), 198(11), p. 1653–1663.
100. Hussain, T., et al., *Establishment & characterization of lymphoblastoid cell lines from patients with multiple primary neoplasms in the upper aero-digestive tract & healthy individuals*. *Indian Journal of Medical Research* (2012), 135(6), p. 820–829.
101. Wroblewski, J.M., et al., *Cell surface phenotyping and cytokine production of Epstein–Barr Virus (EBV)-transformed lymphoblastoid cell lines (LCLs)*. *Journal of Immunological Methods* (2002), 264, p. 19–28.
102. O’Nions, J., and M.J. Allday, *Proliferation and differentiation in isogenic populations of peripheral B cells activated by Epstein–Barr virus or T cell-derived mitogens*. *Journal of General Virology* (2004), 85, p. 881–895.

103. Dorner, M., et al., *Distinct Ex Vivo Susceptibility of B-Cell Subsets to Epstein–Barr Virus Infection According to Differentiation Status and Tissue Origin*. *Journal of Virology* (2008), 82(9), p. 4400–4412.

104. Babcock, G.J., et al., *EBV Persistence in Memory B Cells In Vivo*. *Immunity* (1998), 9(3), p. 395–404.

105. Joseph, A.M., G.J. Babcock, and D.A. Thorley-Lawson, *EBV Persistence Involves Strict Selection of Latently Infected B Cells*. *Journal of Immunology* (2000), 165(6), p. 2975–2981.

106. Babcock, G.J., D. Hochberg, and D.A. Thorley-Lawson, *The Expression Pattern of Epstein–Barr Virus Latent Genes In Vivo Is Dependent upon the Differentiation Stage of the Infected B Cell*. *Immunity* (2000), 13(4), p. 497–506.

APPENDIX

Composition of the solutions employed in the experimental activities

PBS 10x

For a final volume of 1000mL:

- 80g of NaCl
- 2g of KCl
- 6.09g of Na₂HPO₄
- 2g of KH₂PO₄
- 1000mL of H₂O

Adjust pH to 7.3

PBS 1x

For a final volume of 500mL:

- 50mL of PBS 10x
- 450mL of H₂O

ACK lysing solution

For a final volume of 500mL:

- 4.15g of NH₄Cl
- 0.5g of KCO₃
- 500mL of H₂O

Adjust pH to 7.2

Flow cytometry solution (PBS 0.2% BSA 0.1% NaN₃)

For a final volume of 100mL:

- 0.2g of bovine serum albumin (BSA)
- 0.1g of NaN₃
- 100mL of PBS 1x

Cell fixing solution (PBS 1% formaldehyde)

For a final volume of 10mL:

- 0.625mL of 16% formaldehyde
- 9.375mL of PBS 1x

Culture media

- RPMI 10% iFBS

- 50mL of iFBS (Invitrogen)
- 5mL of non-essential amino acids (Invitrogen)
- 5mL of kanamycin (Invitrogen)
- 5mL of sodium pyruvate (Invitrogen)
- 500mL of RPMI-1640 medium, GlutaMAX™-I supplement (Gibco®)

- RPMI 20% iFBS

- 100mL of iFBS (Invitrogen)
- 500mL of RPMI 1640 medium, GlutaMAX™-I supplement (Gibco®)

Freezing medium (iFBS 10% DMSO)

For a final volume of 55mL:

- 5mL of dimethyl sulfoxide (DMSO)
- 50mL of iFBS